Diagnosis of a base metal mine tailings capping failure

Drilling operations underway on the rehabilitated upper tailings at Conrad mine

Gyan Connor BEnv., Macquarie University

This 9 month thesis was submitted in accordance with the requirements of the Master of Research

Department of Environmental Sciences

Macquarie University, Sydney, Australia

November 2018

Declaration of originality

This work has not been previously submitted for a degree or diploma in any university. To the best of my knowledge and belief, this thesis contains no material previously published or written by another person except where due reference is made in the thesis itself.

Signed: 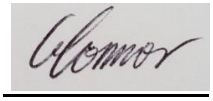 **Date:** 23/11/2018

Gyan Connor

Acknowledgements

I thank my supervisor Professor Damian Gore for accepting me, guiding me, assisting me, and supporting me through this thesis. This project challenged me greatly, with its never-ending twists, turns, and dead ends. Without his streams of "Progress update please" emails, late night editing, phone calls, home visits, and weeks of fieldwork assistance, this thesis would have looked very different indeed. The Inverell rain gods may not have favored us, but we got there in the end without them.

I would also like to thank my co-supervisor, Dr Scott Wilson. While ecotoxicology ended up not playing as large a roll as expected in this thesis, the skills he helped me develop and time he invested in the project is greatly appreciated. Thank you to other Macquarie academics who helped shape and guide my academic experience over the past six years: Dr Tim Ralph, Associate Professor Kira Westaway, Dr Paul Hesse, and Dr Kerrie Tomkins. Laboratory analyses were completed with great help from Professor Damian Gore and Russell Field in the MQ Environmental Quality Laboratory.

Thank you to personnel from the NSW Legacy Mines Program, who provided access to the site, hired the drilling crew and rig, and provided information wherever possible. Thank you also to the NSW OEH Science Division, particularly Anneke Coomans, who generously gave her time, algae, and *Daphnia* to help with my failed acute toxicity tests.

Thank you Professor Damian Gore, Dr Scott Wilson, Peter Johnston, and Mike Ashelford for assisting with fieldwork. Particularly Damian and Mike, who spent two days helping dig pits through compacted clay and cobbles in the summer sun with no cover. Fieldwork is never as easy as when you planned it back in airconditioned comfort. An honorable mention goes to Ruth at the Bundarra Commercial Hotel, who kept us well fed, watered, and rested during our time in the field. Another thanks to Mike Ashelford for generously sharing his time while completing his own thesis to help me with any sticky spots in my research, particularly in GIS mapping.

A great thank you to my family, Phil, Christine, and Bodhi, who have helped keep me motivated and well fed over the past year. To my friends, Alex, Marlan, Andy, Tasman, and Issy, thank you for keeping me sane and reminding me that there is more to life than university alone. A final and most appreciative thank you to my partner Amrit for supporting me, encouraging me, and putting up with me over the duration of this work.

Abstract

Conrad, in northern NSW, is a derelict base metal mine that has undergone extensive rehabilitation. In 2002, the upper tailings (UT) was hydraulically isolated through clay capping; however this was unsuccessful as As, Pb, Cu, and Zn enriched water is exiting the containment structure into Borah and Maids creeks, then Copeton Reservoir, the local drinking water supply, 3 km downstream of the mine. This thesis identifies UT as the highest priority for further rehabilitation. The UT is characterised through elemental and mineralogical analysis of solid samples taken from 0-10 m depth, and leachate extraction from tailings. Metal(loid) concentrations of sediment and water exceed NEPM and ANZECC guidelines onsite and downstream of the mine. Aquatic macroinvertebrate edge sampling along the creeks shows decreased family richness and diversity onsite and downstream from the mine. These results show that capping of the UT has been ineffective, and improvements are suggested to properly rehabilitate the area to stop further offsite spread of contamination. These include a replacement capping design incorporating geofabric, and investigating the possibility that water is infiltrating through the fractured granite in the valley wall on which the UT rests.

1. Introduction

Mining has been an integral part of Australia's economic growth since the first mining boom in the 1840s, and has contributed significantly to Australia's evolution as a modern nation (Pearson & McGowan, 2000). However, lax environmental regulations at the time resulted in hundreds of mines across NSW being abandoned and left derelict, with no rehabilitation undertaken. In this thesis, 'legacy mine' will refer to sites where responsibility cannot be allocated to any individual or company, leaving the social and environmental liability to the state (Grant et al. 2002). There are approximately 550 legacy mines in NSW today, with the onus of rehabilitation falling on the state government (Legacy Mines Program 2018). These legacy and therefore un-rehabilitated mines can pose significant threats to the environment, as they can contain waste materials with a wide variety of chemistries. These materials include waste rock, tailings, slag and mill waste, which are susceptible to leaching, and erosion and transport offsite through fluvial and aeolian processes (Lottermoser 2010) to the receiving environment. Fluvial transport is particularly problematic, with mine wastes transported kilometers downstream, or acid rock drainage (ARD) enabling metal(loid) mobilisation leading to contamination extending further downstream and into groundwater (Lottermoser 2010).

Of the mine wastes described above, tailings are probably the cause of most environmental pollution from legacy mines (Ledin & Pedersen 1996, Williams 2001, Rashed 2010). Their large volume, surface area, and fine grain size allows for rapid acid generation, oxidation, and dissolution of metal(loids) (Johnson & Hallberg 2005). Tailings, being the leftovers of the benefaction process, has chemistry representative of the ore, and while most of the economic minerals have been removed, significant metal(loid) bearing minerals remain (Cato & Mahmud 2003). Tailings are produced as slurries or sands and are stored onsite in dams or compounds which often fail at legacy mines (Cato & Mahmud 2003). Often other wastes, including highly concentrated flue and smelter fines, were also stored in these structures (Lottermoser 2010). Options for geochemical stabilisation include hydraulic isolation, total solidification, mixing tailings with a neutralising material, or microencapsulation (Johnson & Hallberg 2005). These options aim to inhibit the generation and discharge of metal(loid) rich ARD through halting water and/or oxygen interacting with the tailings (Johnson & Hallberg 2005).

Conrad Mine (hereafter "Conrad") is a legacy base metal mine with two tailings storage compounds that have undergone rehabilitation, using hydraulic isolation. Conrad is the largest of six derelict mines at Howell, which includes Conrad, King Conrad, Moore, Davis and Queen shafts along strike of a sulfide vein hosted in granite in Borah Creek valley. This thesis focusses on the former Conrad and King Conrad operations, associated waste material and environmental impacts. The mines primarily extracted silver (Ag) with by-product ore rich in zinc (Zn), copper (Cu), arsenic (As), tin (Sn) and lead

(Pb) (Gore et al. 2007, Pietrass-Wong et al. 2012). Mineralisation was discovered in 1878 and the site intermittently operated from 1891 – 1958. It sprawls over 17.5 ha with numerous shafts and industrial ruins lying amongst waste rock, tailings piles, slag heaps and processing fines (Burke 2000, Kolkert 2015).

1.1 Thesis aims and approach

This thesis investigates the spread of metal(loid) contamination offsite from Conrad, and aims to identify onsite sources in need of rehabilitation. I hypothesise that amongst the multitude of mine wastes and unrehabilitated contaminant sources present at Conrad, the capped UT is the most important area in need of further investigation and rehabilitation to stop the spread of metal(loid) contamination offsite through Borah and Maids Creeks.

2. Regional setting

The mine lies on Crown Land, 21 km southwest of Inverell, northeastern New South Wales (NSW) (**Fig 1**). The mine follows Borah Valley parallel to Conrad Lode and was worked for 1.4 km along strike and to 267 m depth (Pietrass-Wong et al. 2012). The base of the mine on Borah Creek is 2.7 km upstream of Copeton Reservoir and 300 m upstream of the confluence with Maids Creek (Kolkert 2015). Channelisation and sedimentation occurs downstream to the reservoir (Gore et al. 2007, Kolkert 2015). Borah Creek valley (**Fig 2**) maintains steep topography with a relief of 85 m and an average longitudinal gradient of 0.0625. Borah Creek is ephemeral with a 7 km^2 catchment while the Maids Creek catchment is 45 km^2 (Brooks & McIlveen 1988) and flows most of the time except in severe drought. Channel incision has stranded the floodplain (Gore et al. 2007) and undisturbed areas are forested with shallow soil/granitic outcrops, contrasting with the cleared and eroded site (Brooks & McIlveen 1988, Kolkert 2015).

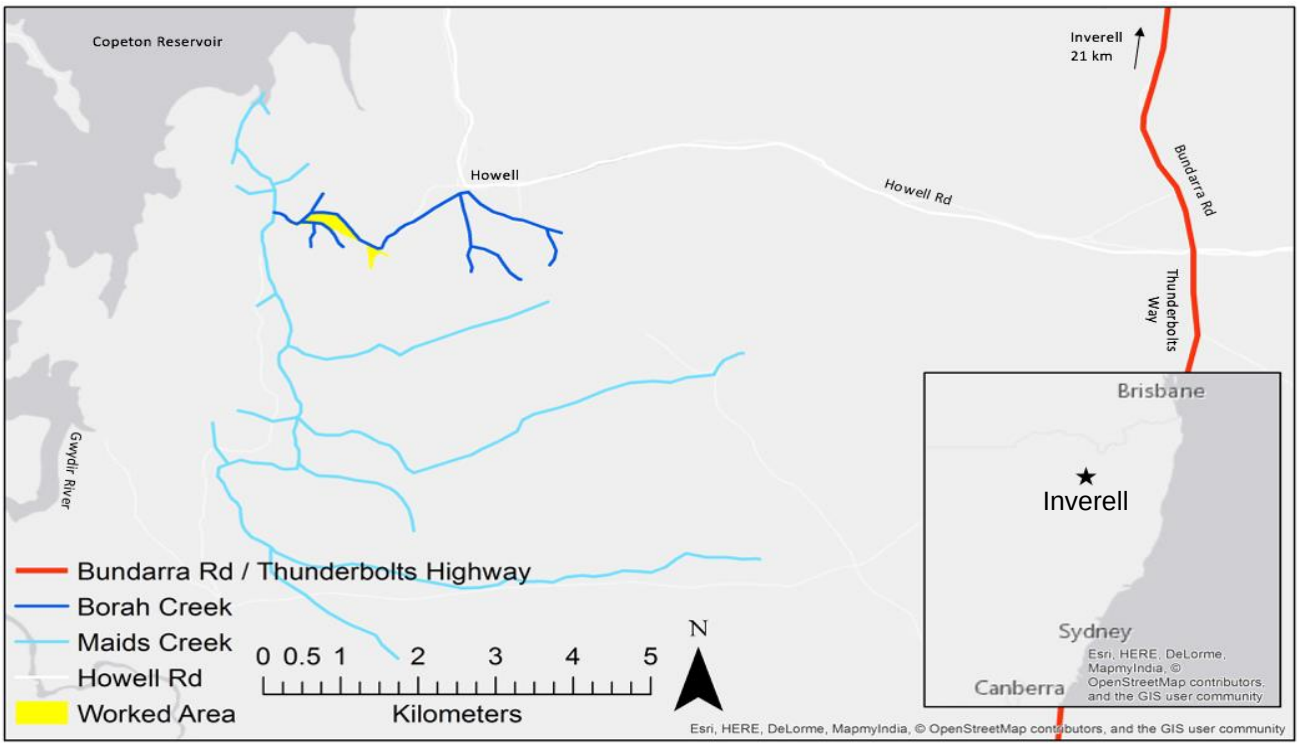

Fig 1: The study area in northeastern NSW. Borah Creek flows into Maids Creek which contributes to Lake Copeton, the drinking and irrigation reservoir for Inverell and areas downstream.

2.1 Geology

Conrad Lode is a large polymetallic sulfide vein, sustained along strike and with depth (Brown & Stroud 1997). The lode is confined within the western edge of the highly mineralised I-type granite pluton responsible for the New England region's numerous vein and disseminated ore deposits (Pietrass-Wong et al. 2012). These deposits have supported several other, now derelict and Arsenic contaminated, mines in the region, such as Webbs Consols, Ottery, and Mole River mines. (Ashley et al. 2004). Catchments atop this pluton have elevated sulfide and base metal geochemistry, in addition to the New England Fold Belt's widespread mineralisation (Pietrass-Wong et al. 2012). Mineralisation is represented by galena (PbS), sphalerite (ZnS), arsenopyrite (FeAsS), stannite (Cu_2FeSnS_4) and chalcopyrite ($CuFeS_2$), with minor tetrahedrite ($Cu_6[Cu_4(Fe,Zn)_2]Sb_4S_{13}$) and cassiterite ($SnO_2$) that host the elements zinc (Zn), copper (Cu), arsenic (As), molybdenum (Mo), silver (Ag), tin (Sn) and lead (Pb) (Brown & Stroud 1997, Brooks & McIlveen 1988).

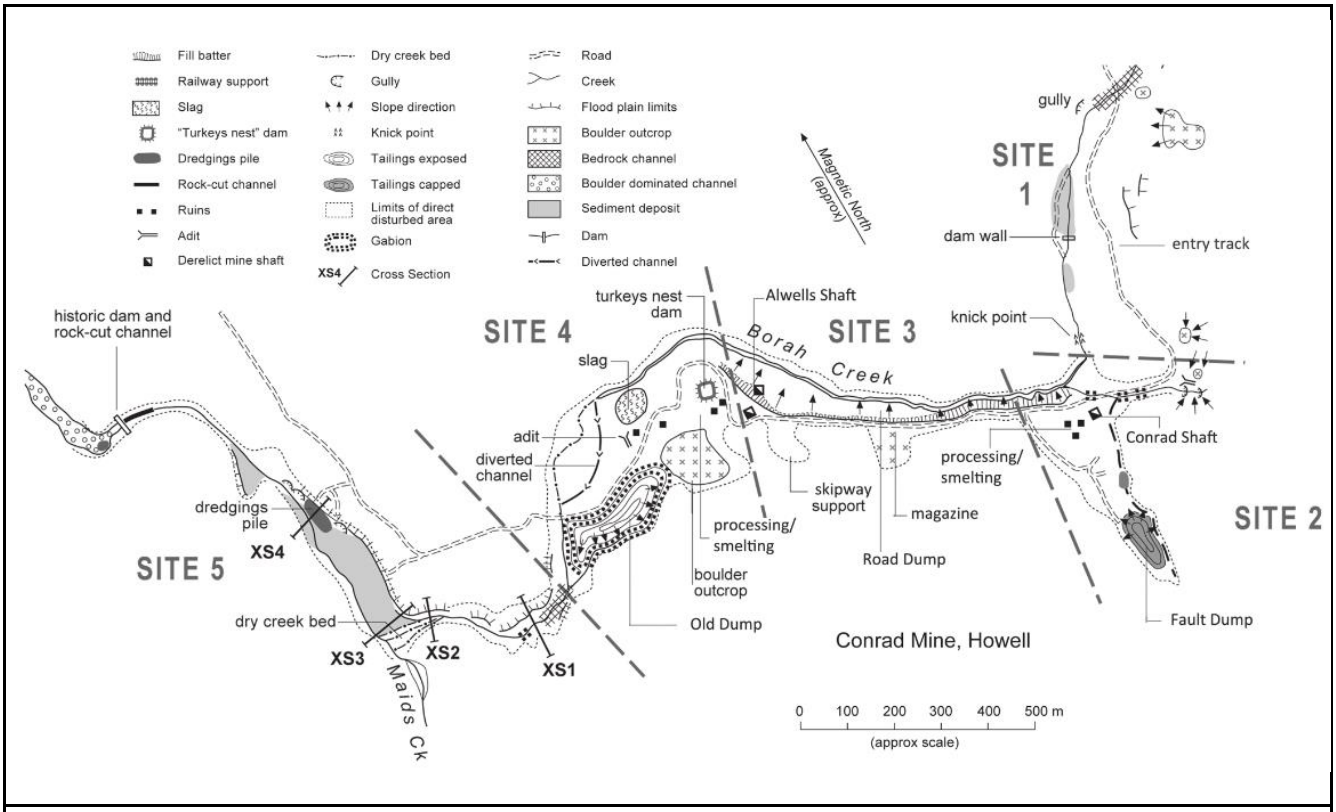

Fig 2: Sites within, upstream and downstream of the worked area (from Gore et al. 2007). Site 1 – Slightly disturbed/upstream of workings. Site 2 – Conrad shaft workings. Site 3 – Road Dump, Allwell and King Conrad shafts. Site 4 – King Conrad workings and LT (Old Dump). Site 5 – Downstream of workings. Upper Tailings (UT; aka Fault Dump) is the dark ellipse in Site 2.

2.2 Biology

Native vegetation is predominantly Northern Tablelands Dry Sclerophyll Woodland, however the worked site contains Howell Shrublands (Northern Montane Heaths), an endangered ecological community (EEC) (Kolkert 2015). Key vegetation species include *Eucalyptus prava*, *Angophora floribunda*, *Eucalyptus caleyi*, *Callitris endlicheri*, *Leptospermum*, and *Aristida ramosa* (Hawes & Eade 1998). Soils are poor and can be characterised as thin and sandy (Hawes & Eade 1998). Feral animals and weeds are key threatening processes (Donnelly 2011). The majority of the site is denuded of vegetation, with limited regrowth.

2.3 History of working

The grade of the polymetallic ore recovered between 1891 and 1958 was on average 0.06 wt% Ag as well as 8 wt% Pb, 4 wt% Zn, 1.5 wt% Cu and 1.5 wt% Sn (Pietrass-Wong et al. 2012). The two major mining periods 1891 - 1913 and 1950 - 1957 involved progressive extraction and recovery to treat

the complex ore that reduced the concentration of contaminants in tailings, slag and waste rock (Menzies 1967, Brooks & McIlveen 1988, Gore et al. 2007).

During 1898-1913, Conrad and King Conrad shafts were established and operated before liquidating in 1913-1914 (Menzies 1967). During this period, concentrating infrastructure was constructed south of Conrad shaft and west of King Conrad shaft. Ore was inefficiently milled, concentrated and sent offsite with waste remaining on-site. An experimental furnace successful in smelting Cu-Sn-Pb concentrates instigated the construction of smelters south of Conrad shaft to produce more refined concentrates (Menzies 1967). Smelter ash, tailings, and poorly recovered slag mixture was deposited below the smelters and remains in situ (Burke 2000). Tailings from King Conrad were transported to the Lower Tailings (LT) (also known as Old Dump) and Road dumps (**Fig 2**) (Brooks & McIlveen 1988). Cu-Pb and Ag-Pb concentrates were produced, however the ore complexity limited the effectiveness of smelting and the Cu-Pb concentrate was retained for further processing while the Ag-Pb concentrate was sold (Menzies 1967, Brown & Stroud 1997). In 1906 a magnetic separator was added and later a blast furnace for pre-treatment as roasting removed excess sulfur and arsenic. Arsenic was initially atmospherically discharged from roasting but was later captured for sale, while tin was left in the slag due to inefficient removal (Burke 2000).

In 1955 a concentration plant at the upper workings, including ball mills and froth flotation, was erected and the site was powered by overland electricity transmission (Burke 2000). This allowed a pump to de-water the mine into Borah Creek and a processing capacity up to 200 t of ore a day, with slag and tailings deposited at the UT (**Fig 2**) south of Conrad shaft (Burke 2000, Brooks & McIlveen 1988). The mine was abandoned in 1958 and no rehabilitation was attempted. Recent exploration in 2003 and 2009, predominantly through drilling, has been conducted by Malachite Resources (Pearson & McGowan 2000).

2.4 Rehabilitation works

From closure until 2003 the site had been relatively untouched with waste material extensively eroding from stockpiles into Borah Creek (Burke 2000). Tailings, predominantly the upper tailings, generated large quantities of Acid Rock Drainage (ARD), mobilising residual metal(loid)s from the complex ore waste, with contaminant rich leachate draining into Borah Creek (Gore et al. 2007). Adits, including Allwell shaft (**Fig 2**), expelled ARD due to collapsed stopes increasing groundwater recharge (Brooks & McIlveen 1988). In 2003, the then NSW Department of Primary Industries, Derelict Mines Program (now NSW Department of Planning and Environment, Legacy Mines Program) partly rehabilitated the upper tailings and implemented bedload control strategies, including gravel and clay

capping and revegetation of the UT, gabion containment of the LT, stream realignment, infilling/smoothing of drainage lines with waste rock, bank battering and head-cut control with basalt gabions (Gore et al. 2007, Donnelly 2011). However, treated and untreated sources continued to exceed ANZECC (2018) water and sediment guidelines (Gore et al. 2007). In 2003 and 2009, Malachite Resources implemented trial rehabilitation plots to determine the effectiveness of natural regrowth and tube stock in the skeletal soils around the mine, continuing the work of Grant et al. (2002) on the effectiveness of mulch and impact of tailings on natural biotic regeneration (Donnelly 2011). In 2018 the LT was capped using a gravel capillary break, overlain by geofabric, and 1 m of clay, and topsoil.

3. Current site condition

The study area at Conrad and King Conrad workings has been divided into five sites (**Fig 2**). Site 1 is considered a reference site as it is upstream of mine workings; sites 2, 3, and 4 are worked sites containing waste materials and residual infrastructure, and site 5 continues from the lowest workings downstream to Copeton Reservoir.

3.1 Overview - Site 1

The reference site has had limited disturbance relative to the rest of the study area and remains mostly in a natural condition. However it does contain the entry/haul road and existing infrastructure of the former Howell township. A former water supply dam on Borah Creek (**Figs 3, 4**), that has three residential properties in its catchment, forms the upstream extent of this report. The haul road crosses Borah Creek downstream of the dam and immediately downhill of a locked gate (29°57’5.47’’ S 151°1’42.25’’ E). Borah Creek is in a mostly natural state throughout Site 1 (**Fig 5**).

Fig 3: Water supply dam above the worked site at Howell (29°56’53.15’’ S 151°1’56.35’’ E).

Fig 4: Borah Creek within Site 1 with extensive in-channel and riparian vegetation (29°57’10.62’’ S 51°1’32.95’’ E).

3.2 Overview - Site 2

Conrad Mine workings contain the most upstream disturbances from ore extraction and processing. Inputs of leachate from Moore, Davis and Queen shafts occur along strike to the east, entering Borah Creek at Site 2, as well as UT leachate, Conrad processing/smelting runoff and the adjacent tributary south of Site 2 (**Fig 2**).

Existing Infrastructure

The dominant feature is the headframe (poppet head) over Conrad shaft (**Fig 5**) and the surrounding processing and smelting infrastructure to the south of the haul road. North of the haul road there are two concrete slabs, one at ground level west of the headframe and another supported by pillars north of the headframe, which supported massive winding engines for trucks hauling ore up the shaft. A small intact dam west of the UT (**Fig 6**) spills northward to the processing area.

Fig 5: Ore processing and smelting infrastructure at the Conrad shaft (29°57'16.66'' S 151°1'26.21'' E).

Fig 6: The small dam immediately west of the UT (29°57'21.15'' S 151°1'26.67'' E).

Waste Material

South of the haul road, multiple slag heaps (**Fig 7**) contain different textures, indicating successive generations of smelting. These slag heaps are top dressed with waste rock, as is the haul road (**Fig 8**), processing area, and creek bed (**Fig 9**). Waste rock heaps are piled against the hillslope east - southeast of the headframe and on the southern bank of Borah Creek. Fines from processing and smelting remain around remaining infrastructure at the processing area where the ground is protected from rainfall.

Fig 7: Multiple generations of slag and waste rock (29°57’16.45’’ S 151°1’27.85’’ E)

Fig 8: Haul road top dressed with waste rock (29°57’17.98’’ S 151°1’33.16’’ E).

Fig 9: Creek bed lined with waste rock. All fine material has been transported downstream (29°57’17.32’’ S 151°1’31.62’’ E).

Rehabilitation infrastructure

Rehabilitation work at Site 2 included tailing capping and drainage line modification. At the time of works in March 2017, January 2018, and October 2018, the UT capping was well vegetated (**Fig 10),** however the thick iron precipitate in the overflowing sediment trap below the structure indicates that the tailings capping is ineffective (**Fig 11**). This ARD precipitate continues down the drainage line (**Fig 12)** until level with the haul road. Extensive drainage lines and contour banks have been formed to redirect flow around the processing area and these are still intact, however they are formed from waste rock and most of the fine materials have been transported downstream (**Figs 9, 13**). The basalt gabions inhibit any potential knickpoint retreat (**Figs 2, 14**).

Fig 10: The western side of the capped and vegetated UT. (29°57’20.69’’ S 151°1’28.04’’ E).

Fig 11: Precipitates in the sediment trap below the UT (29°57’20.69’’ S 151°1’28.04’’ E).

Fig 12: Looking north from the UT, down the drainage line to Conrad shaft (29°57’18.08’’ S 151°1’28.63’’ E).

Fig 13: Acid mine drainage and extensive precipitation from the UT (29°57’18.08’’ S 151°1’28.63’’ E).

Fig 14: Basalt gabions preventing potential knickpoint retreat (29°57’18.08’’ S 151°1’28.63’’ E).

3.3 Overview - Site 3

Site 3 is predominantly a narrow road south of Borah Creek which contains a roadside waste rock dump along its length as well as King Conrad and Allwell shafts at its downstream end. The majority of the waste rock dump is sparsely vegetated, with denser vegetation towards King Conrad. Within the channel are the remains of a former dam (29°57'11.72'' S 151°1'23.72'' E) and downstream of this point the channel is incised to bedrock, with some overlying precipitates forming at the edges of base flow. The portal to Allwell shaft (**Fig 2**) has been collapsed to prevent entry, however mine water is discharging at this point and causing a large increase in As-rich channel bed precipitation at and immediately below its junction with Borah Creek (**Fig 15**). The only heritage items in Site 3 are the intact skipway support next to the capped King Conrad shaft and the explosives magazine halfway along the haul road. On the hillslope south of King Conrad is a large waste rock dump which surrounds the southern skipway support.

Fig 15: As-rich precipitate forming terracettes in the channel below Allwell shaft (29°7'1.82'' S 151°1'14.65'' E). Image is ~1 m across.

3.4 Overview - Site 4

The King Conrad smelter/processing infrastructure and mining wastes are predominantly contained in Site 4, however additional ore from Conrad shaft was transported to King Conrad via the skipway.

Existing Infrastructure

A Turkeys Nest dam, a large concrete lined square dam used for electrowinning Cu, located at the top of Site 4, contains a fine sediment covered with white efflorescence on the upper concrete and the soil downslope of the dam where leachates surface. Surrounding the dam and towards the former smelter works to the south are capped drill holes from exploration by Malachite Resources. The remains of the smelter stack lies amongst rubble of previously demolished infrastructure, including processing plants and skipway supports (**Fig 16**). Numerous salt efflorescences are present among the mixed processing wastes.

Fig 16: King Conrad processing and smelting ruins (29°57'1.39'' S 151°1'9.09'' E).

Waste Material

The LT (**Figs 2, 17**) is the most recent tailings, which contains fines from processing as well as recent material from rehabilitation works in 2003. Multiple generations of material from different processes and locations are present in the LT and the drainage line contains significant efflorescence on rocks and a thick algal mat (**Fig 18**). Similar efflorescence and algal coverings occur in the drainage line of the large slag dump at the northern end of Site 4 (**Fig 2**). The large slag dump is physically stable as a consolidated mass, however smaller crushed slag dumps, coke, flue dust and waste rock distributed throughout the processing/smelting area are physically mobile (**Figs 2, 16**).

Fig 17: The recently capped LT (soil covered mound to the left of photograph) (29°57’0.32’’ S 4151°1’4.36’’ E).

Fig 18: Efflorescence and algae amongst the discharge of the LT compound (29°57’1.99’’ S 151°0’59.78’’ E).

Rehabilitation infrastructure

The LT (**Figs 2, 17, 19**) had been previously contained with basalt gabions to limit physical transport of tailings material, however deposition at the downslope end infilled against, and was overflowing the edge of the gabion (**Fig 19**). Fine grained material eroding from the LT, as well as the contour banks and exposed space north of the LT (**Fig 17)**, has infilled the channel behind the lower gabions, limiting the base flow of Borah Creek to beneath the sediment (**Fig 20**). During 2018 the LT was contoured and capped (**Fig 17**), reducing the transport of mine waste offsite. The section of Borah Creek between the slag dump and LT which was realigned in the 2003 rehabilitation has incised the channel to bedrock and is actively widening.

Fig 19: Transported tailings overtopping the containment of the LT before capping (29°57’2.82’’ S 151°0’59.9’’ E).

Fig 20: Water in Borah Creek enters subsurface flow due to the backfilling of fine grained permeable sediment in the channel upstream of the basalt gabions (29°57’3.32’’ S 151°0’54.3’’ E).

3.5 Overview - Site 5

The downstream site includes all solid and aqueous phase materials below the outlet of the lower tailings. The channel is over widened and incised to bedrock for 200 m below the lower gabions, where extensive in-channel sediment deposition again causes subsurface base flow until the downstream confluence with Maids Creek (**Fig 21**). Maids Creek is well vegetated and has a shallower and narrower channel than Borah Creek, despite its increased catchment area. The splay of sediment at the confluence has partially truncated Maids Creek, forcing flow to the left bank (**Fig 21**). Fine sediment is deposited at knickpoints, however the majority of the channel downstream to Copeton Reservoir is either incised to bedrock or consists of large clasts with no fine sediment. There is no in channel vegetation established in Maids Creek below the confluence with Borah Creek.

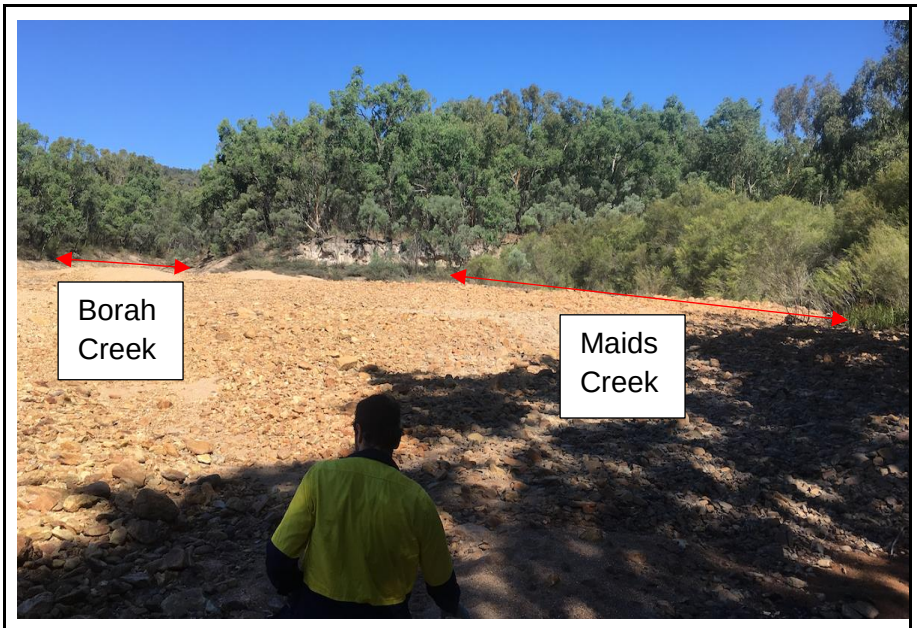

Fig 21: Increased sediment load from Borah Creek (left) has partially infilled Maids Creek (right). (29°56'57.3'' S 151°0'46.99'' E).

4. Methods

4.1 Mine waste analyses

Mine waste from the upper tailings and across Conrad mine were analysed for their metal(loid) concentrations and mineralogy. Sampling focussed on the upper tailings, but measurements and samples were also taken from across the mine to characterise the site. Sampling from the upper tailings was facilitated by the use of a site investigation rig operating a power auger, able to extract tailings from 10 m depth. Nine holes were augered into the upper tailings in three rows, spaced to map the tailings comprehensively with as few holes as possible. (**Fig 22**). 500 g of sample was taken approximately every 1 m of depth at each auger location (n = 80), collected directly from the

auger flight. All mine wastes were collected using a plastic trowel, ethanol wiped between uses, and deposited into polyethylene zip lock bags.

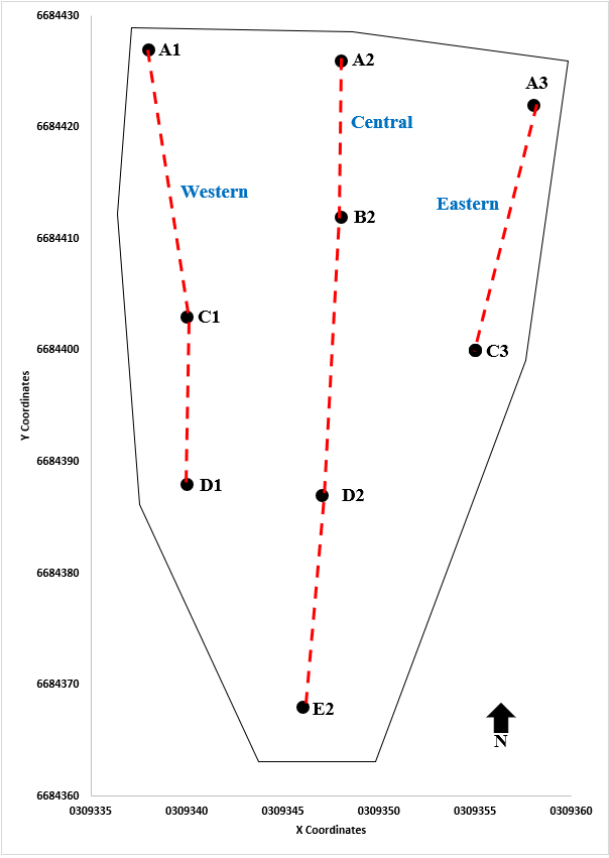

Fig 22: Map of the UT showing auger hole placement. Holes are laid out from A – E in a north – south direction, and from 1 – 3 in a west to east direction. The X and Y axes are in UTM eastings and northings.

Sediments were assessed against ANZECC (2018) ISQG Low and High criteria (Table 1). Material exceeding ISQG High classification is deemed contaminated and can pose a threat to freshwater ecosystems (ANZECC, 2018). Soils were assessed against NEPM (2013) Health Investigation Levels (HIL) – D for commercial/industrial sites (**Table 1**).

Table 1: Sediment and soil quality guidelines for selected metal(loid)s.

	Sediment *		**Soil ****
Analyte	**ISQG Low (mg/kg)**	**ISQG High (mg/kg)**	**HIL – D (mg/kg)**
Cu	65	270	240,000
Zn	200	410	400,000
As	20	70	3000
Pb	50	220	1500

** ISQG (Interim Sediment Quality Guidelines) Low and High trigger values for sediment contamination in freshwater ecosystems (ANZECC, 2018).*
*** HIL (Health Investigation Levels) – D for soil at commercial and industrial sites (NEPM, 2013).*

Nineteen sediment samples were collected along Borah Creek, Maids Creek, and the bank of Copeton Reservoir (**Fig 23**). Sampling begun immediately downstream of the LT, and continued to Copeton Reservoir. One reference sample was taken in Maids Creek, ~1 km upstream of the confluence with Borah Creek.

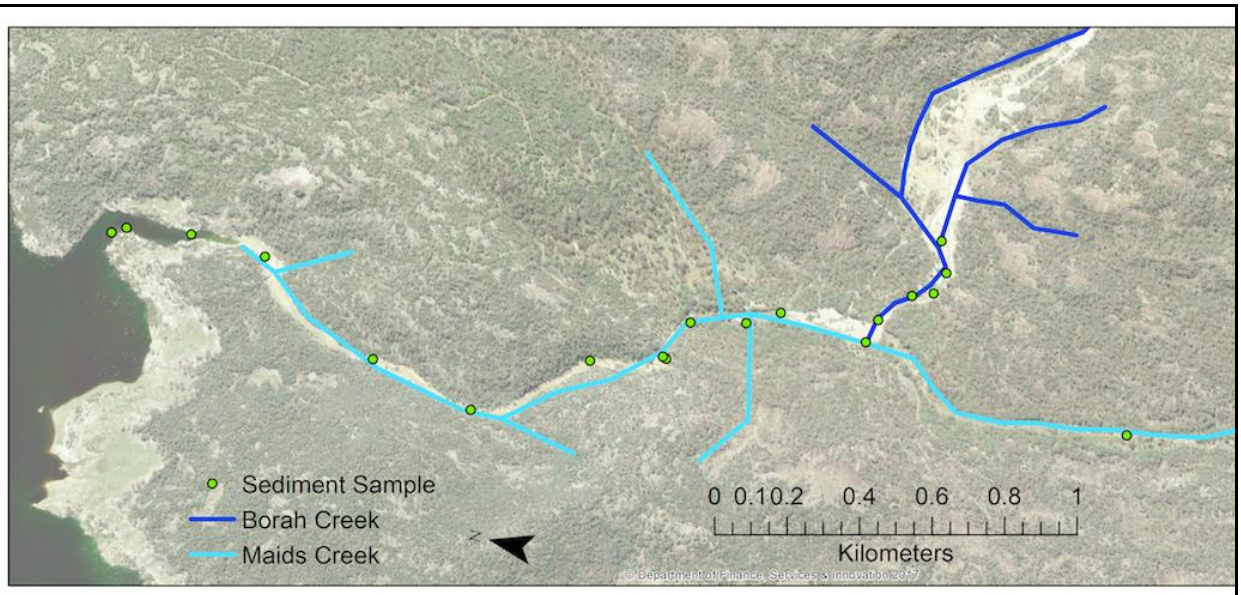

Fig 23: Location of sediment samples on Borah Creek and Maids Creek downstream of the worked area.

4.1.1 Elemental composition

Solid samples were oven dried at 105 °C for 24 h, sieved to remove the >2 mm fraction, before being disaggregated with a tungsten-carbide mortar and agate pestle. Terminal grain size was estimated at ~50-60 µm after this process, but was not measured. Disaggregation was required as wet samples hardened into consolidated balls when dried. The resulting material was then mixed, and a representative sample lightly packed into plastic cups with a 3.6 µm Mylar® X-ray film base. Cupped samples underwent elemental analysis using an Olympus Delta Pro X-ray fluorescence (XRF) spectrometer with 50 kV tantalum anode tube in a desktop stand, using measurement conditions of 50 kV, 40 kV and 15 kV for 60 s each in soil calibration mode. All equipment was cleaned with a Kim-Wipe wetted with ethanol after use, and cups were washed using warm soapy water, dried, and ethanol wiped before re-use.

An experiment was undertaken to establish the number of cumulative sample aliquot measurements required to create a stable geometric mean of elemental concentration. The aim of the experiment was to understand whether or not it was possible to reduce sample preparation time

by using un-milled mine waste while remaining within the data quality objectives of the research. Ten samples were each divided into 10 sub-samples; these were then prepared and measured using the methods described above. Note that this method does not involve milling the sample, only disaggregation in a mortar and pestle. The cumulative geometric mean of these results was plotted, which showed that measuring four aliquots of a sample produced a relatively stable geometric mean (**Fig 24**). Given these results, all subsequent elemental concentrations of tailings reported in this research were the geometric mean of four dried, un-milled aliquots of sample. This experiment justified the decision to not mill all samples, saving valuable time and effort while remaining within the study's data quality objectives of <20% inaccuracy (USEPA 2007, 6200-16).

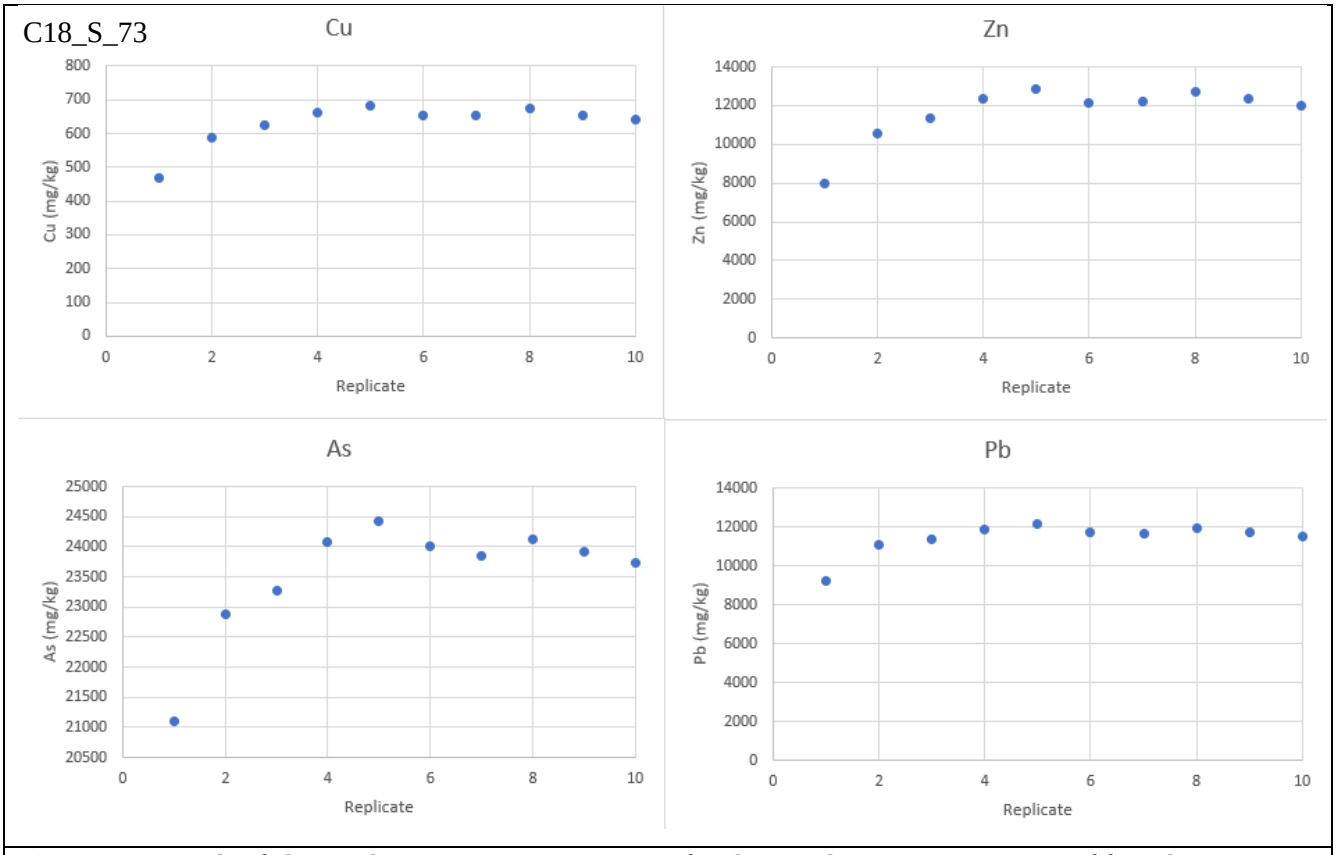

Fig 24: An example of elemental concentration evening out after the cumulative geometric mean of four aliquots is measured. A full explanation of these data can be found in **Appendix 1**.

In-situ (in the field) elemental analyses were conducted using an Olympus Delta Pro X-ray fluorescence spectrometer with 40 kV rhodium anode tube, using measurement conditions of 40 kV, 15 kV and 5 kV for 20 s each in soil calibration mode. These measurements (n = 207) were performed in the field to quickly characterise other mine wastes present at the site, and to establish elemental background concentrations of the surrounding area. Inaccuracy, constrained by

measuring NIST standards 2710a and 2711a, and a blank material (SiO_2) at the start and end of each day's measurements, was better than 10 % where the analytes were > 0.1 wt%.

4.1.2 Mineralogy

Samples were collected from mine waste, salt efflorescences and tailings from the auger holes. Samples undergoing mineralogical analysis (n = 19) underwent the same drying and disaggregation process described above. Visible quartz grains were removed with forceps, and the remaining material crushed thoroughly in an agate mortar and pestle. Preparation equipment was cleaned after each use with an ethanol wipe. Crushed tailings samples were backloaded into a sample ring and analysed. Diffractograms were collected from 5° to 95° 2θ using a Panalytical Aeris X-ray diffractometer (XRD) with CuK_α radiation at 5° $2\theta.min^{-1}$, operated at 40 kV and 15 mA. Salt efflorescences from mine wastes were analysed on silicon crystal low background holders, with diffractograms collected from 5° to 95° 2θ using a Panalytical X'Pert Pro MPD diffractometer, with CuK_α radiation at 5° $2\theta.min^{-1}$, operated at 45 kV and 40 mA. The use of two instruments was due to availability, not experimental design and the data are equivalent. Mineral identification was undertaken using Panalytical High Score Plus v2.2.4 software with PAN-ICSD and ICDD PDF2 databases. Detection limits depend on crystallinity but are typically around 0.1-0.5 wt%.

High quartz levels in samples made identifying metal(loid) bearing minerals more difficult and less accurate, so a scoring matrix was used to rank the likelihood that a mineral suggested by the software is truly present in the sample. **Table 2** gives an example of this matrix, for the sample shown in **Fig 41**.

Table 2: Example of the scoring matrix used to calculate the certainty that an identified mineral is present in the measured sample. Meaning of each column;
HS+ %: what is the measure of certainty according to the HighScore+ software (% confidence in identification)
Geology: is the mineral geologically consistent with the granite, sulfide and their secondary minerals at the field site?
Elements: is the mineral composition consistent with the bulk elemental composition of the tailings sample?
Optical: can the minerals be seen in the raw sample with a hand lens?
Strong Unmatched Lines: are there Strong Unmatched Lines in the diffractogram which might indicate a misidentification?
Certainty: classification according to the certainty of identification based on all available information.

Mineral	HS+ score (%)	Geologically reasonable?	Chemistry consistent?	Optically endorsed?	Strong Unmatched Lines	Certainty
Quartz	70	Y	Y	NA	0	Almost certain
Phengite	16	Y	Y	NA	0	Possible
Arsenopyrite	28	Y	Y	Y	0	Highly probable
Anglesite	17	Y	Y	NA	0	Possible

4.2 Water analyses

Water quality was measured in-situ and sampled for elemental analysis. pH and conductivity were compared with ANZECC (2018) water quality guidelines for slightly disturbed ecosystems

in southeastern Australia (**Table 3**). Water chemistry results are compared to ANZECC (2018) Freshwater contaminant trigger values for 80 % and 95 % species survival (**Table 3**).

Table 3: Australian water quality and chemistry guidelines for freshwater ecosystems.

Water chemistry *			**Water quality ****		
Analyte	**80% (mg/L)**	**95% (mg/L)**	**Property**	**Low**	**High**
Cu	0.0025	0.0014	**pH**	6.5	7.5
Zn	0.031	0.008	**EC (µS/cm)**	30	350
As	0.36	0.024			
Pb	0.0094	0.0034			

** ANZECC (2018) freshwater contaminant trigger values for 80 % and 95 % species survival.*
*** ANZECC (2018) low and high water quality thresholds for slightly disturbed ecosystems in south-eastern Australia.*

4.2.1 Water quality

Measurements of pH, oxidation-reduction potential (ORP), conductivity and total dissolved solids (TDS) were taken in the field using a multi-parameter probe (n = 32 measurements). The probe was rinsed with Type II reagent water (ASTM, 2018) after each use. **Figure 25** shows water quality measurement locations.

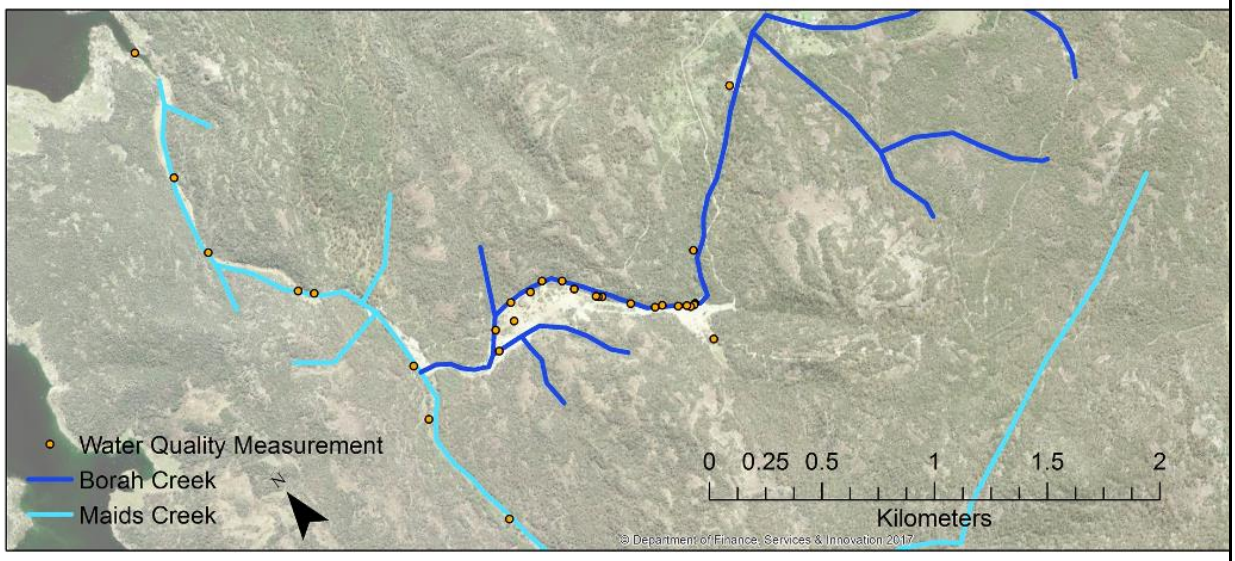

Fig 25: Locations of onsite standing water and surface water measurements of Borah Creek and Maids Creek.

4.2.2 Water chemistry

Water samples (n = 24) were collected in the field using a syringe and filtered through a 0.45 µm Sartorius MiniSart cellulose acetate filter into 50 mL HDPE bottles pre-acidified at 2

mL/L with reagent grade concentrated nitric acid to achieve a pH of <2 in storage. Two blanks of Type II reagent water were taken into the field: one field blank (exposed to air during the duration of one sample collection in the field) and one trip blank (closed until analysis).

In the laboratory, water samples had 50 µL of 20 mg/L gallium spike added to 450 µL of sample, and leachates had 10 µL of 500 mg/L gallium spike added to 490 µL of sample. These were vortex mixed for 15 s. 10 µL of this mixture was then pipetted onto a siliconized quartz disc and dried for 15 min at 60 °C on a hot plate. The resulting evaporite on the disc was measured for elemental composition in a Bruker Picofox total reflection X-ray fluorescence spectrometer (TXRF) with molybdenum anode tube, using a measurement time of 600 s and measurement conditions of 50 kV, 600 µA with no filter. Limits of quantification, defined as three times the detection limit, depend on the matrix of each sample, but were typically ~5 µg/L for Cu, Zn, As and Pb. Inaccuracy, constrained using a Merck XVI multi-element standard, was better than 20 % where concentrations exceeded 0.1 mg/L.

4.3 Leachate extraction

Leachates were extracted from nine bulk samples from the upper tailings, using a modified DIN 38 414-S4 (1984) technique. In the field, ~3 kg of tailings was collected from each auger hole, representative of the entire hole. Material was oven dried at 105 °C for 24 hours before being homogenised following US EPA SESDPROC-300-R3 (2014). This involved quartering the sample, mixing each quarter, combining and mixing two quarters to form halves, and combining and mixing the two halves to form a homogenous mix. Randomly picked spoonfuls of the homogenised sample were combined with Type 1 (ASTM, 2018) deionised water at a 1:10 ratio in a capped HDPE bottle. These bottles were shaken at 150 rpm on an orbital shaker for 24 h, then filtered at 0.45 µm using a Millipore Durapore Vacuum filtration system. Orbital shaking at 150 rpm prevented settlement of solids and abrasion (which leads to enhanced leaching) (Lewin (1996). A sample of filtered leachate was taken for TXRF analysis as described above.

4.4 Hydraulic conductivity

Hydraulic conductivity measurements were taken of three stratigraphic layers present in the upper tailings: the topsoil, clay capping, and tailings. A constant head well permeameter was used to measure the saturated hydraulic conductivity (K_{sat}) of these materials. Well permeameter measurements (n = 15) were taken using the methods and apparatus in Talsma and Hallam (1980). A deep and skinny hole, where the wetted depth is ≥10 times the hole radius (Talsma & Hallam

1980) was first augered into the material to be measured, and wetted thoroughly with local potable water to reduce sorptivity. Care was taken while augering to minimise smearing of clays over pore openings, and a wire brush was used to roughen the inside of the hole before measurement. Once saturation occurred after wetting, a water-filled well permeameter was inserted into the hole and the timing and amount of head drop was recorded until a steady state reached. With these data, K_{sat} (m/s) was calculated using the formula $K_{sat} = Q/\pi H^2$, where Q = steady state infiltration rate (m^3/s), π = the constant 3.1415926 and H = wetted depth of the hole (m).

4.5 Topographical survey

Six topographical transects were completed across the upper tailings to capture its morphology and allow tailings volume to be estimated. One transect was taken along the north-south axis, with the remaining five perpendicular in an east-west direction. These were spaced at approximately 20 m intervals. Topographic surveys were conducted using tape and clinometer, and the auger holes/piezometer collars (**Fig. 22**) were surveyed in with an automatic level.

4.6 Macroinvertebrate sampling

Macroinvertebrates were collected in the field (**Fig. 26**) using an edge sampling method, ideal for low flow conditions on small creeks (Chessman, 2003). A 10 m section of channel bank from the edge to 1 m into the channel was disturbed and the material collected with a 1 mm net. Material was screened through 10 mm and 3 mm sieves prior to 30 min of macroinvertebrate extraction from the collected material. Extraction of macroinvertebrates was completed using plastic pipettes and tweezers. Macroinvertebrates were preserved in the field in a 10 % ethanol and water solution. Identification to a family level for each macroinvertebrate was conducted in the laboratory under a microscope. A Habitat Assessment Score (HAS) was determined at each macroinvertebrate sampling location to constrain the effect of natural physical channel attributes on the results. This was undertaken in accordance with the AusRivAS Sampling and Processing Manual (Queensland Department of Natural Resources and Mines, 2001).

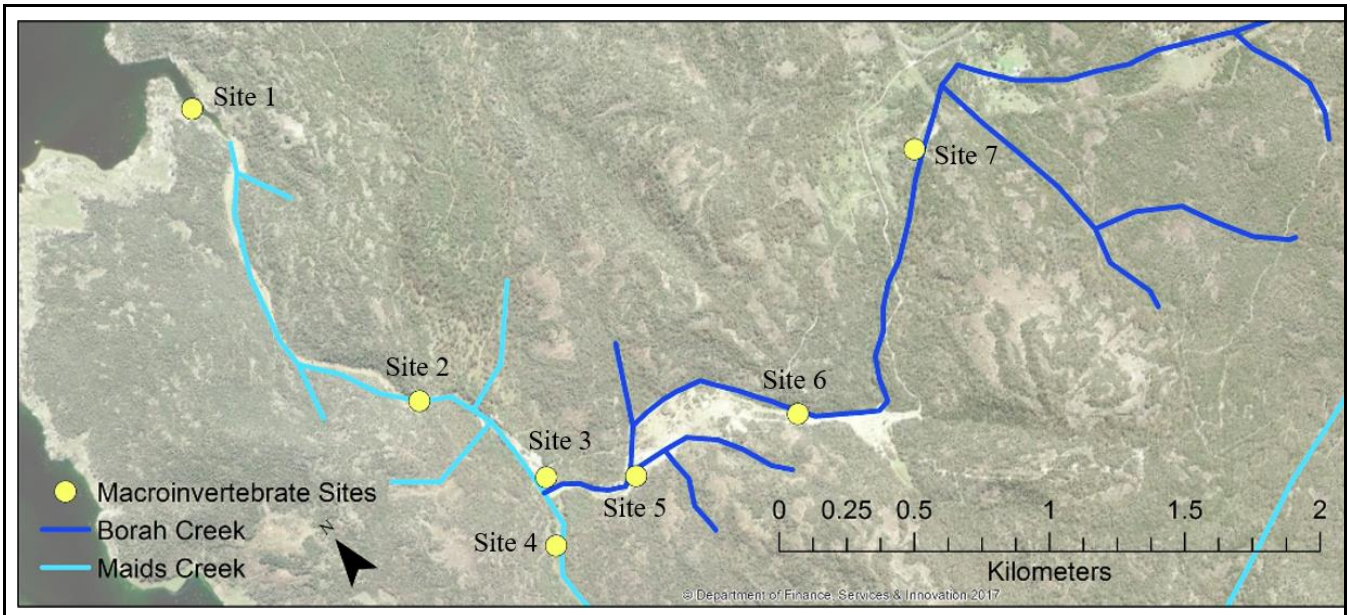

Fig 26: Macroinvertebrate sampling locations.

4.7 Rudimentary flow-rate measurements

Return flow from joints in granite bedrock was observed while water sampling in the field. Measuring its rate of flow was important, so a rudimentary method was devised using the tools at hand. A 50 mL syringe was used to draw in the flow at a narrow point where the syringe uptake would capture all exfiltrating water. This uptake was timed until a full 50 mL was collected, which was then converted into a flow rate (mL/s).

5. Results

This chapter presents the results of the sampling described in Chapter 4.

5.1 Soil chemistry

Of the soil measurement locations (n = 207), 91 (44 %) exceeded the NEPM HIL-D values (**Table 3**) for As and 136 (66 %) for Pb. Elevated levels of Cu and Zn were also recorded across the site. Background concentrations from soils above the worked site in Borah and Maids creek valleys were elevated with mean concentrations of 58 mg/kg As and 177 mg/kg Pb, indicating the large impact on local soils surrounding the mine from mining, processing and smelting. Across Conrad Mine, Cu and Zn concentrations were relatively low (**Figs 28, 30, 32, 34**) with an area of elevated Zn around the processing area in Site 4 (**Fig 34**). The worked sites (**Fig 2, sites 2, 3, 4**) contained the highest concentrations, with all analytes having the highest values around the Conrad and King Conrad processing areas.

Concentrations of As and Pb consistently exceeded HIL-D values at the majority of exposed waste and infrastructure sites (**Figs 27, 29, 31, 33**), including material that has been reworked to cover or remove waste and line drainage systems in the 2003 rehabilitation works. Despite Site 5 being unworked and considered offsite, concentrations of As (**Fig 31**) and Pb (**Fig 33**) exceed HIL-D values at numerous locations.

SITES 1-3

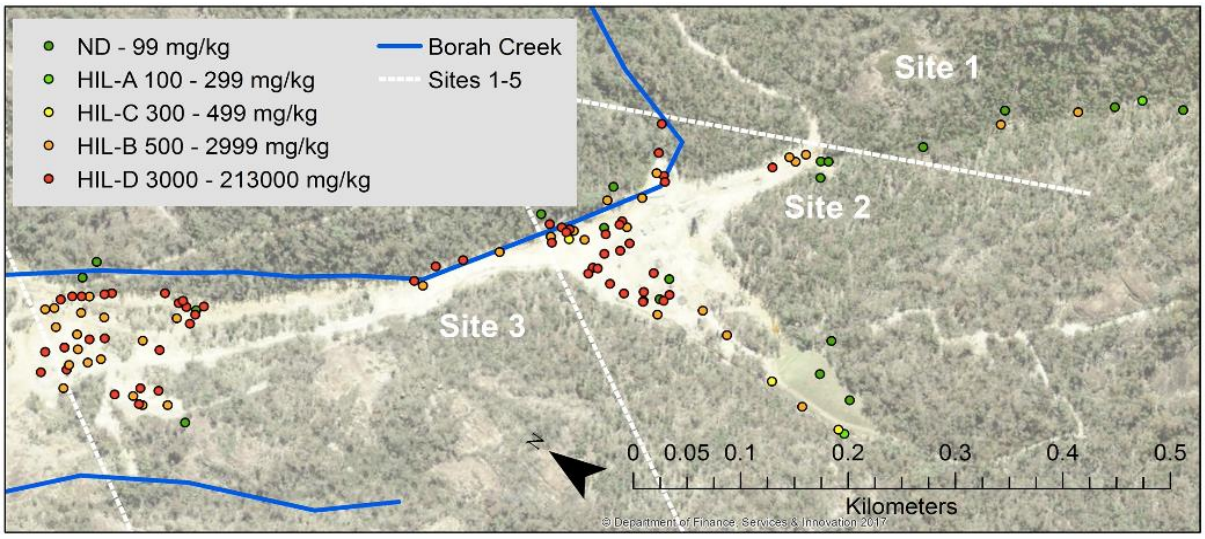

Fig 27: Site 1-3 representing As concentrations relative to NEPM guidelines for soil. Mean concentrations ± 1 standard deviation for each site; Site 1 = 82 ± 93, Site 2 = 6500 ± 9610, Site 3 = 5560 ± 6040. ND = not detected (below limits of detection).

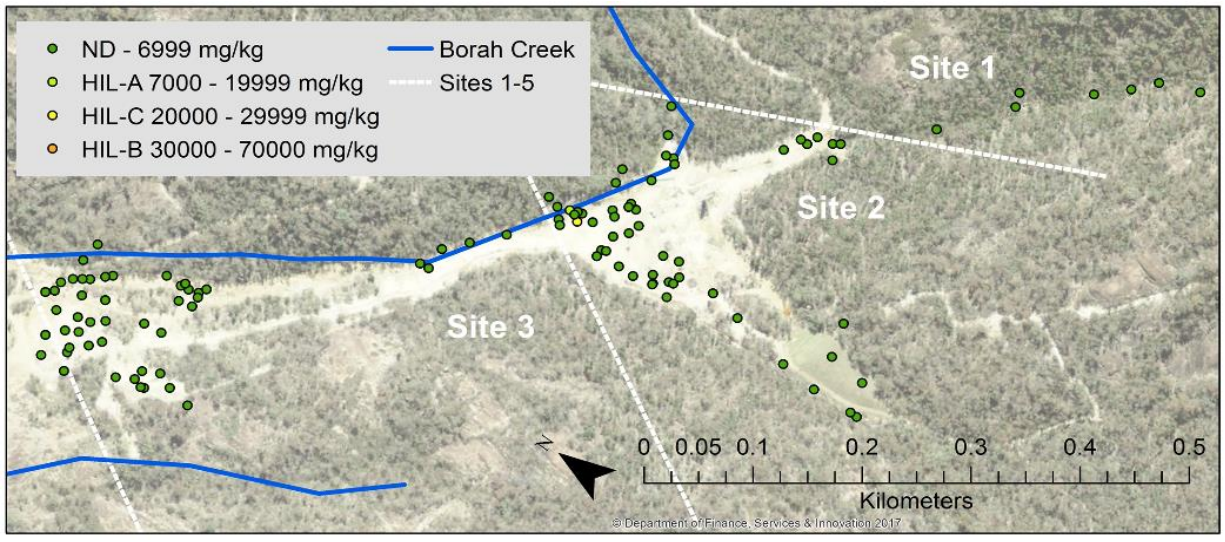

Fig 28: Site 1-3 representing Cu concentrations relative to NEPM guidelines for soil. Mean concentrations ± 1 standard deviation for each site; Site 1 = 29 ± 25, Site 2 = 524 ± 1025, Site 3 = 567 ± 880. ND = not detected (below limits of detection).

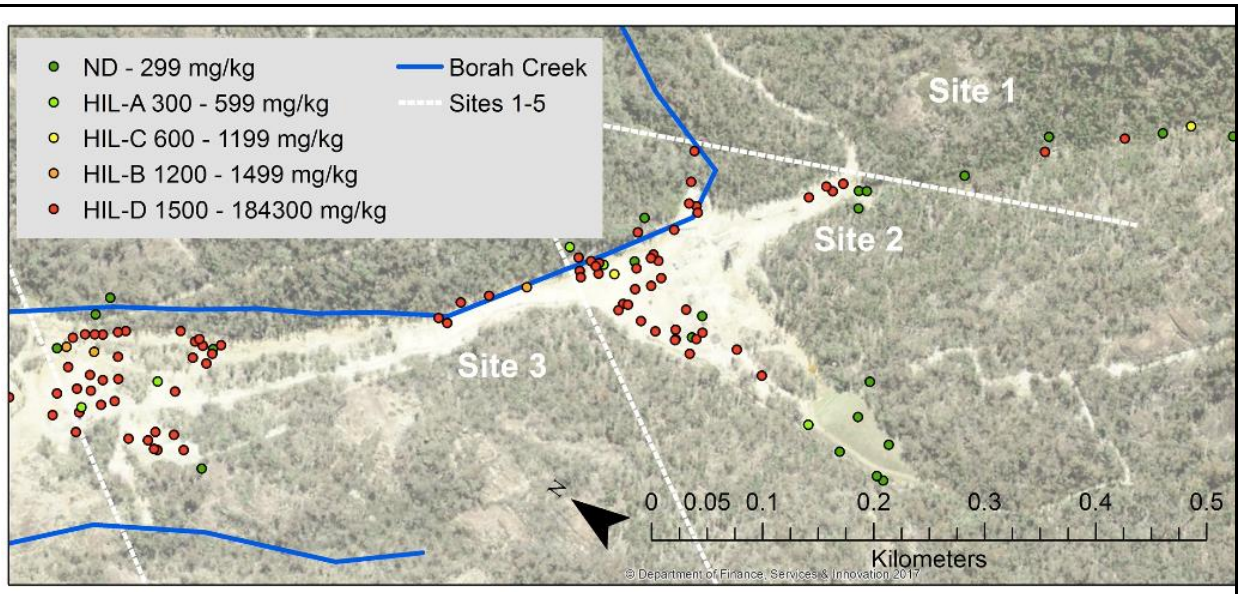

Fig 29: Site 1-3 representing Pb concentrations relative to NEPM guidelines for soil. Mean concentrations ± 1 standard deviation for each site; Site 1 = 101 ± 253, Site 2 = 5480 ± 9150, Site 3 = 6500 ± 7800. ND = not detected (below limits of detection).

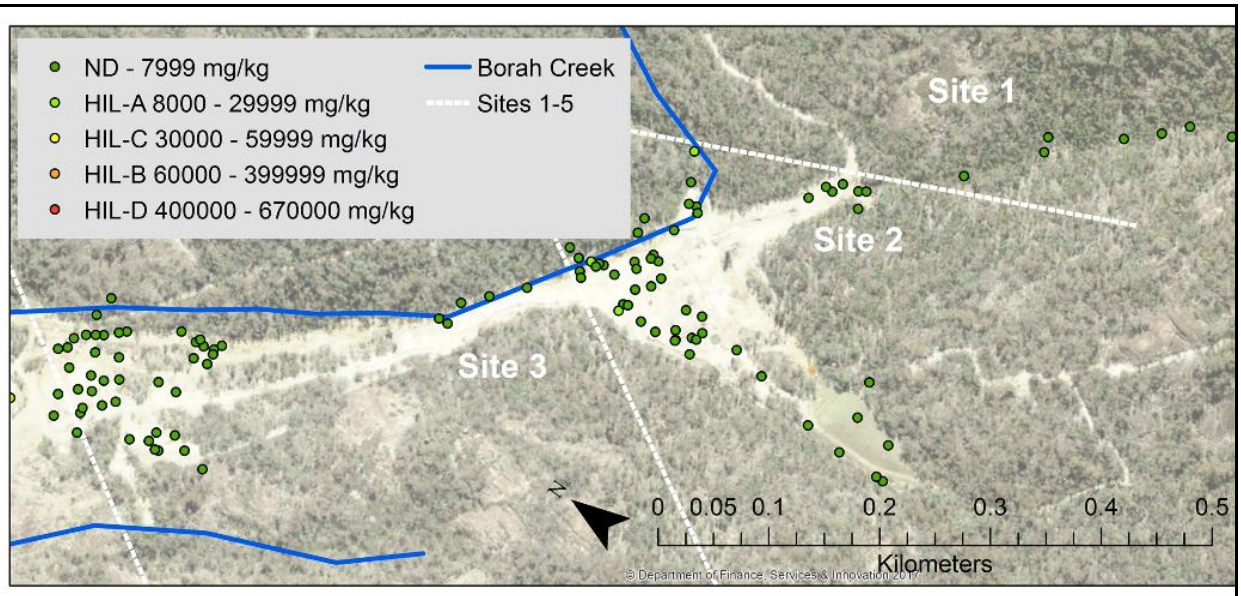

Fig 30: Site 1-3 representing Zn concentrations relative to NEPM guidelines for soil. Mean concentrations ± 1 standard deviation for each site; Site 1 = 78 ± 29, Site 2 = 2930 ± 14800, Site 3 = 802 ± 2724. ND = not detected (below limits of detection).

SITES 4-5

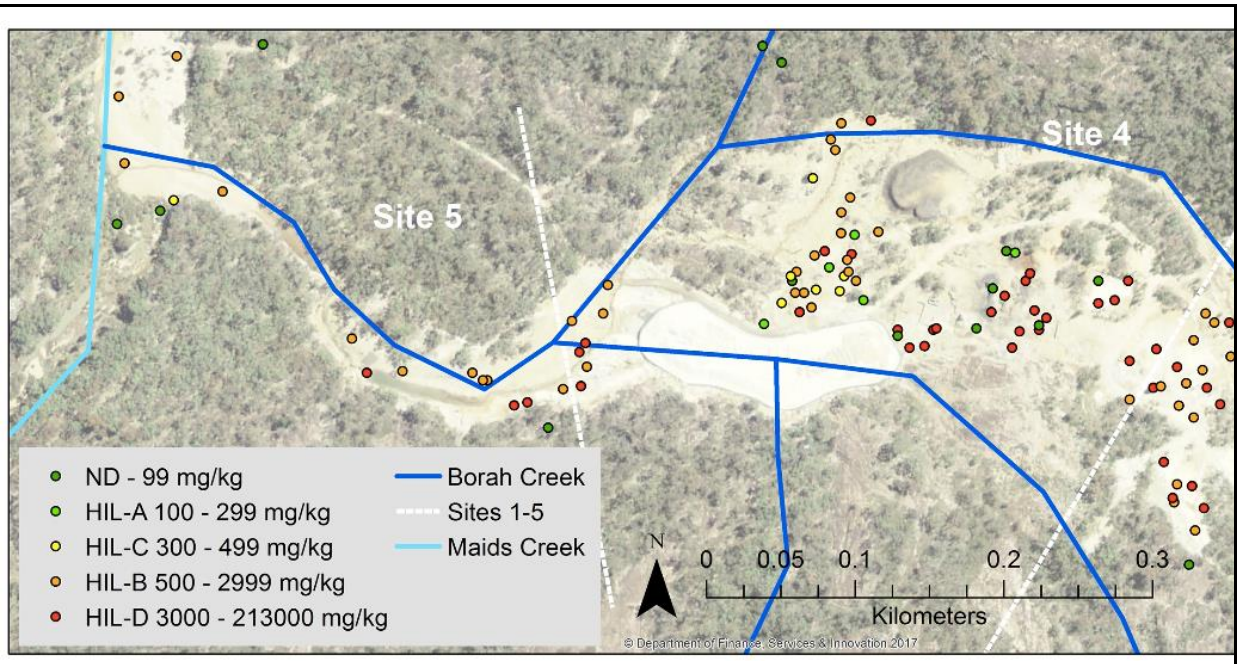

Fig 31: Site 4-5 representing As concentrations relative to NEPM guidelines for soil. Mean concentrations ± 1 standard deviation for each site; Site 4 = 4465 ± 7110, Site 5 = 1860 ± 2130. ND = not detected (below limits of detection).

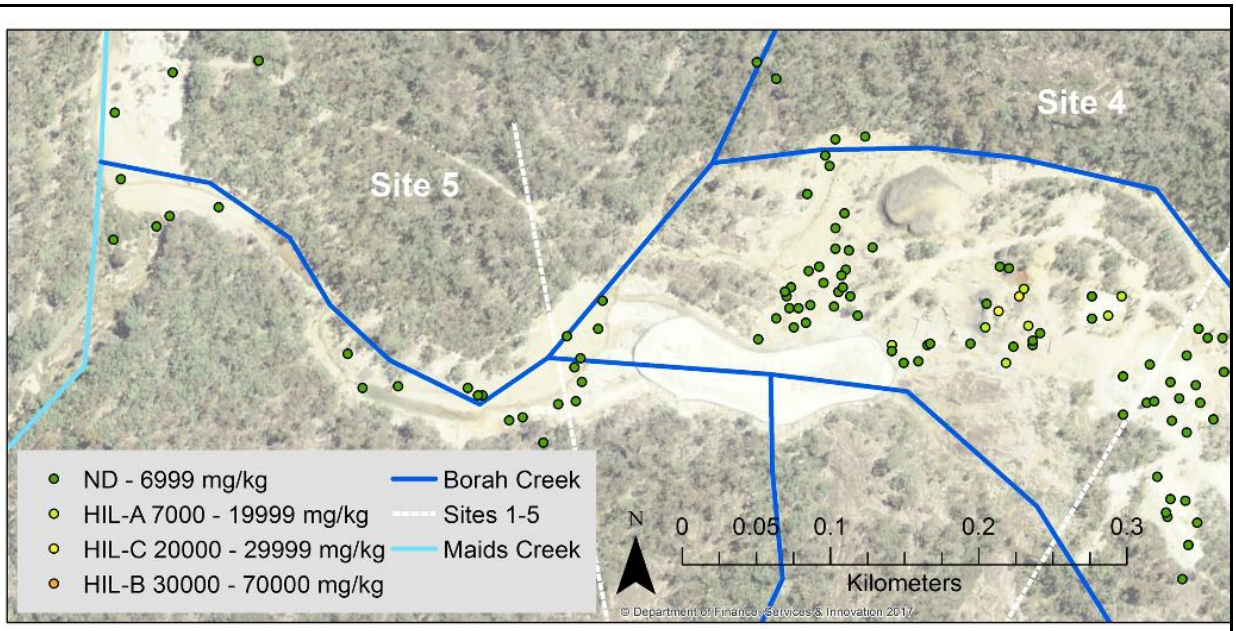

Fig 32: Site 4-5 representing Cu concentrations relative to NEPM guidelines for soil. Mean concentrations ± 1 standard deviation for each site; Site 4 = 578 ± 702, Site 5 = 541 ± 1220. ND = not detected (below limits of detection).

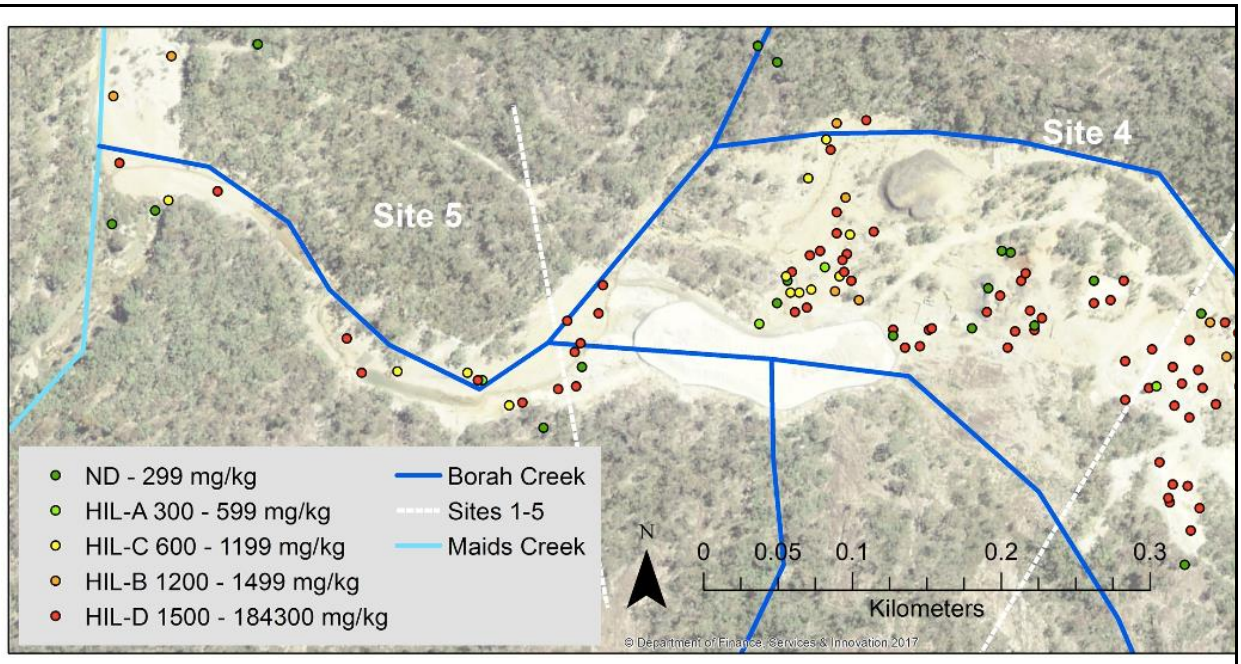

Fig 33: Site 4-5 representing Pb concentrations relative to NEPM guidelines for soil. Mean concentrations ± 1 standard deviation for each site; Site 4 = 5570 ± 6930, Site 5 = 2030 ± 2140. ND = not detected (below limits of detection).

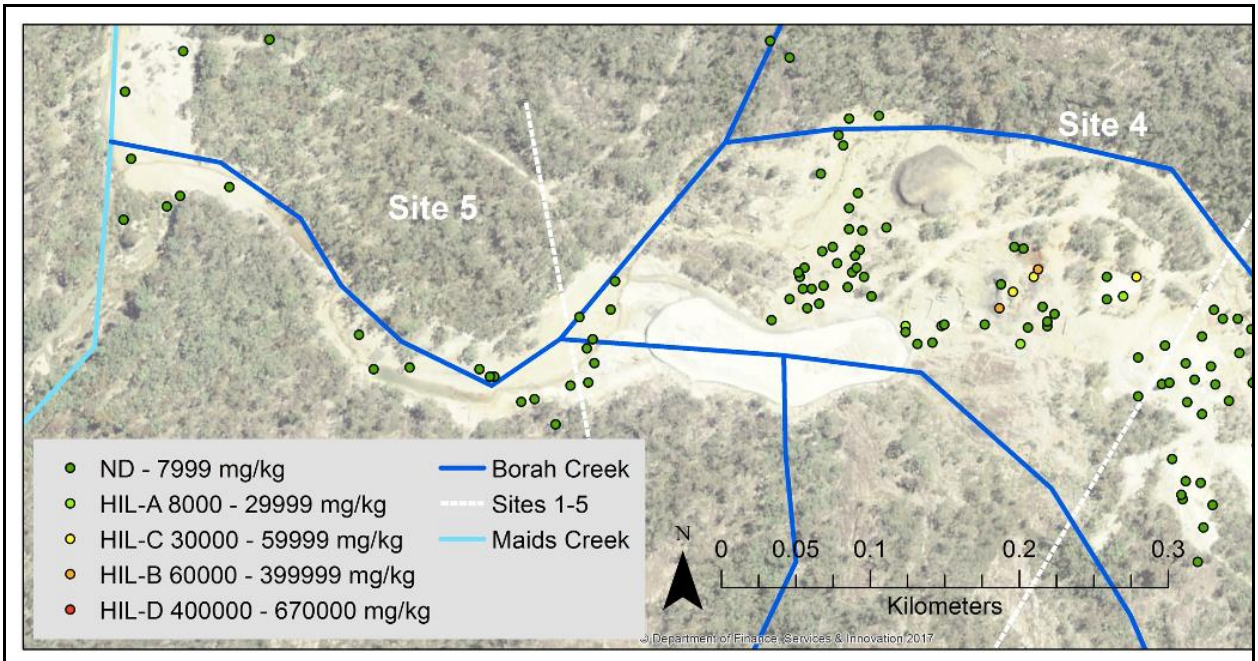

Fig 34: Site 4-5 representing Zn concentrations relative to NEPM guidelines for soil. Mean concentrations ± 1 standard deviation for each site; Site 4 = 1656 ± 5940, Site 5 = 339 ± 494. ND = not detected (below limits of detection).

5.2 Sediment chemistry

Figure 35 shows the downstream trend of metal(loid) concentration in sediment and their relevance to the ANZECC (2018) ISQG Low and ISQG High guidelines (**Table 1**). All Zn levels (n = 18) recorded concentrations below ISQG High, and most (n = 13) were below ISQG Low guidelines for non-reference locations. Cu concentrations were above the ISQG High limit near to the LT, but lowered with distance downstream. Pb and As levels trend near identically downstream, showing much greater concentrations than Cu or Zn. The highest Pb and As measurements were 3710 mg/kg, and 3780 mg/kg, respectively. This is 17 times the ISQG High limit for Pb and 54 times for As. All four metal(loid)s decrease sharply ~450 m downstream from the LT, where Borah Creek enters Maids Creek. This influx of clean sediment is contaminated within ~800 m, and metal(loid) concentrations remain high in the sediment downstream to Copeton Reservoir. While analyte concentrations were lower than locations closer to the LT, sediment metal(loid) concentration exceeded guidelines in reservoir sediments. Pb levels remain above the ISQG High limits for two of three sampling locations at Copeton Reservoir, with the third above the ISQG Low limit. All three locations at Copeton Reservoir had As and Zn levels above ISQG Low limits.

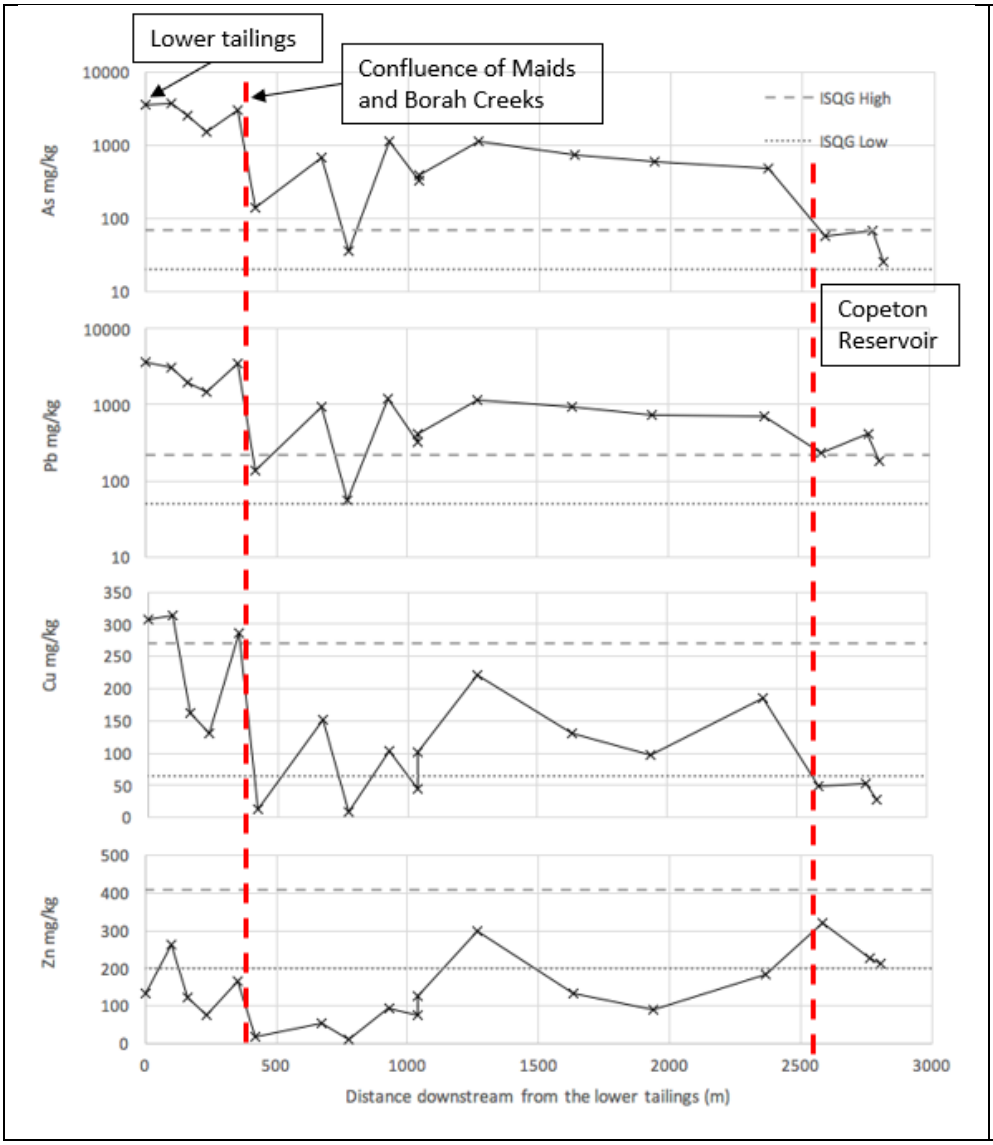

Fig 35: Analyte concentrations of sediments with distance downstream. ISQG Low and ISQG high are from the ANZECC (2018) guidelines (**Table 1**).

5.3 Elemental analysis of mine wastes

Eighty samples were taken from the UT auger holes to characterise the waste and determine if any layering or distinct features are present. **Table 4** summarises the elemental composition of the UT, showing very high metal(loid) concentrations, particularly As at 1.58 wt%.

Table 4: Summary of the elemental analysis of samples (n = 80) from the UT.

	Cu (wt%)	**Zn (wt%)**	**As (wt%)**	**Pb (wt%)**
Min	0.056	0.016	0.32	0.144
Max	0.157	1.98	3.53	1.57
Geomean	0.048	0.40	1.58	0.544

Figures 36, 37, 38 and 39 break these data down further, showing individual sample concentrations with depth. There are two distinct zones within the UT, the margin between the two being ~7 m above basement depth. The upper zone has lower Cu, Zn, and Pb concentrations, but higher As. The lower zone has more variability, but is generally higher in Cu, Zn, and Pb while lower in As. There are also physical differences between the layers, with the upper layer being white in colour and dry, while the lower layer is moist and greyer (**Fig 40**).

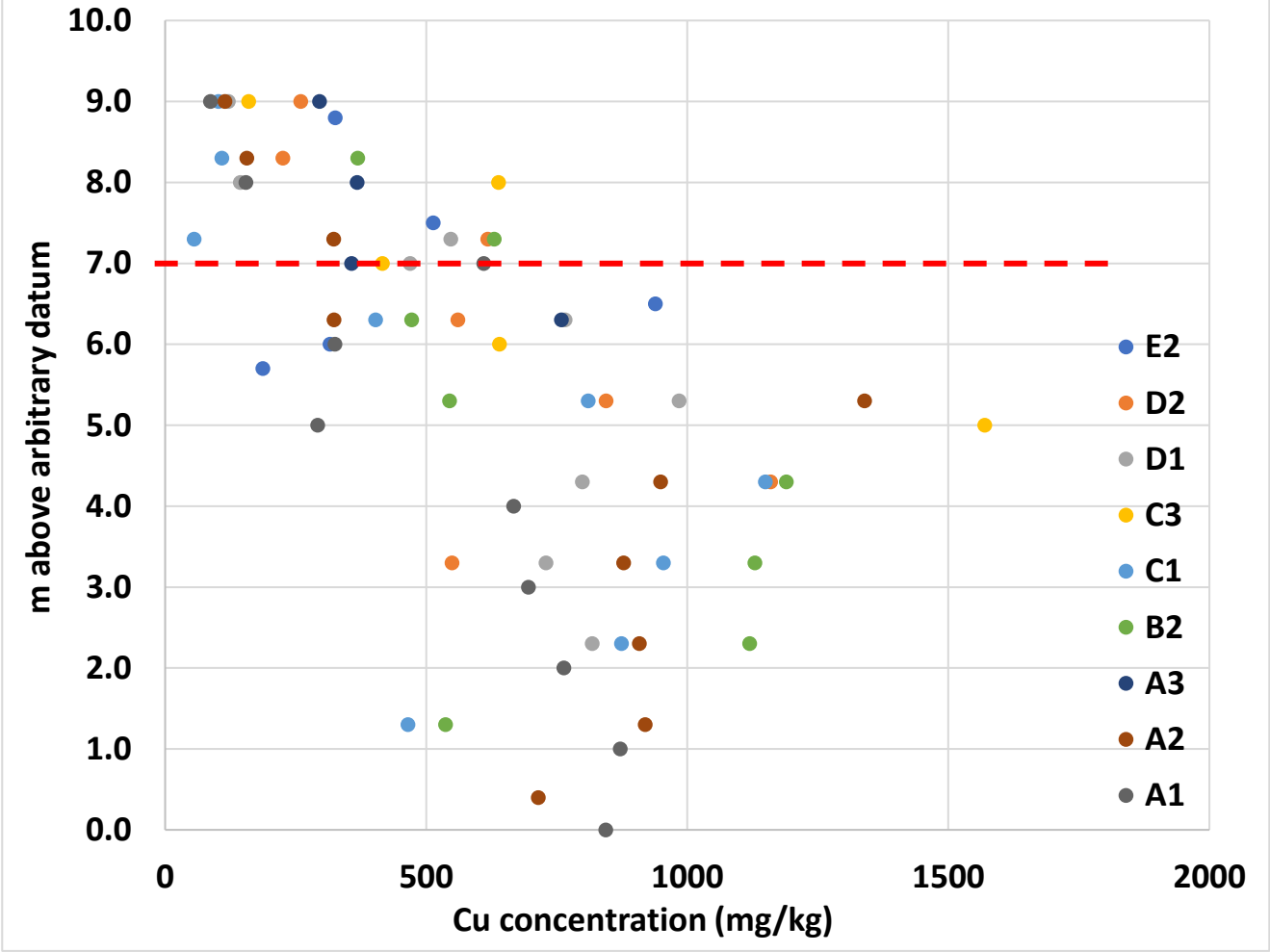

Fig 36: Scatterplot showing Cu concentration at depth in the UT. Red dotted line highlights zone of change at 7 m above basement. See **Fig 22** for auger hole locations on the UT.

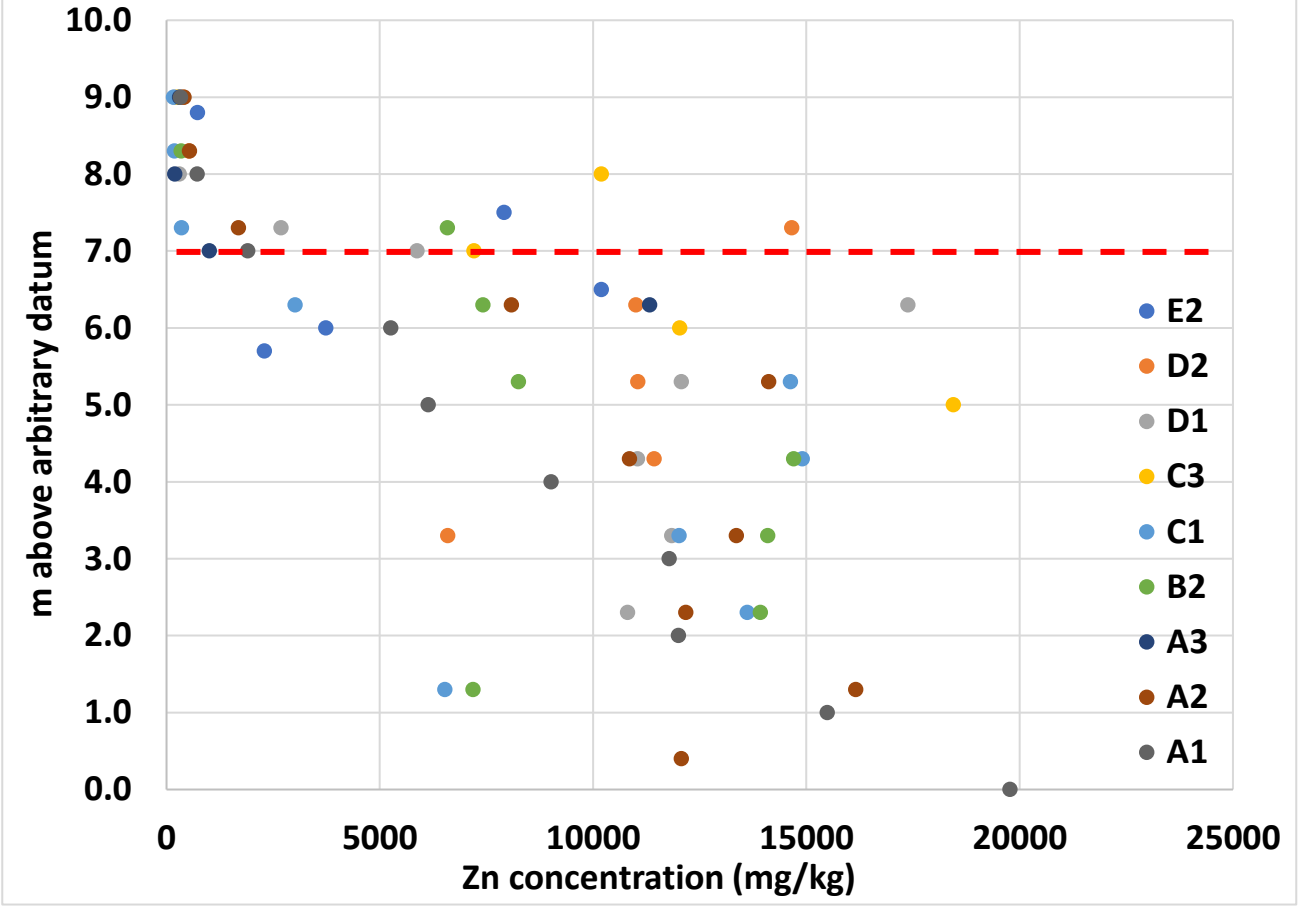

Fig 37: Scatterplot showing Zn concentration at depth in the UT. Red dotted line highlights zone of change at 7 m above basement. See **Fig 22** for auger hole locations on the UT.

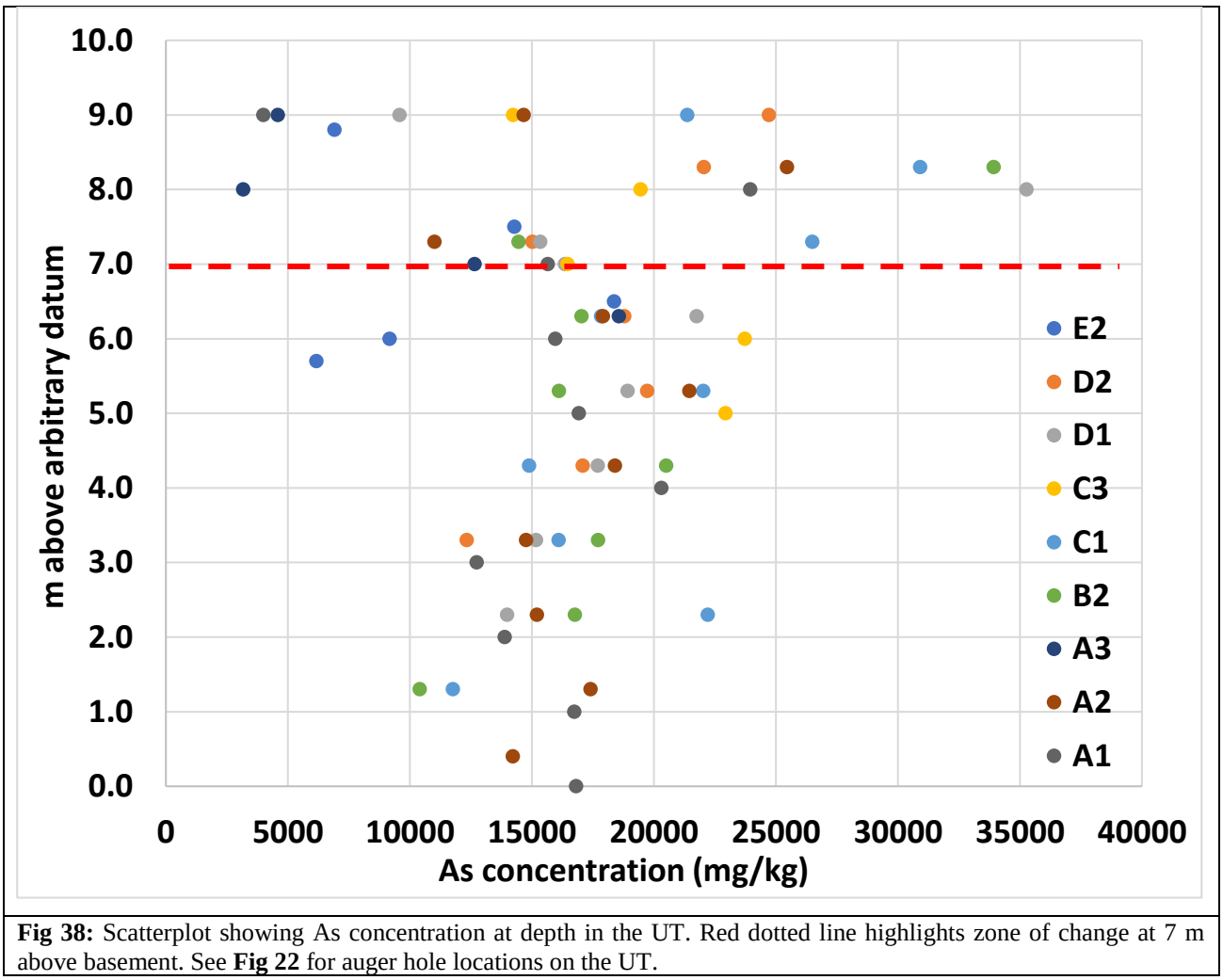

Fig 38: Scatterplot showing As concentration at depth in the UT. Red dotted line highlights zone of change at 7 m above basement. See **Fig 22** for auger hole locations on the UT.

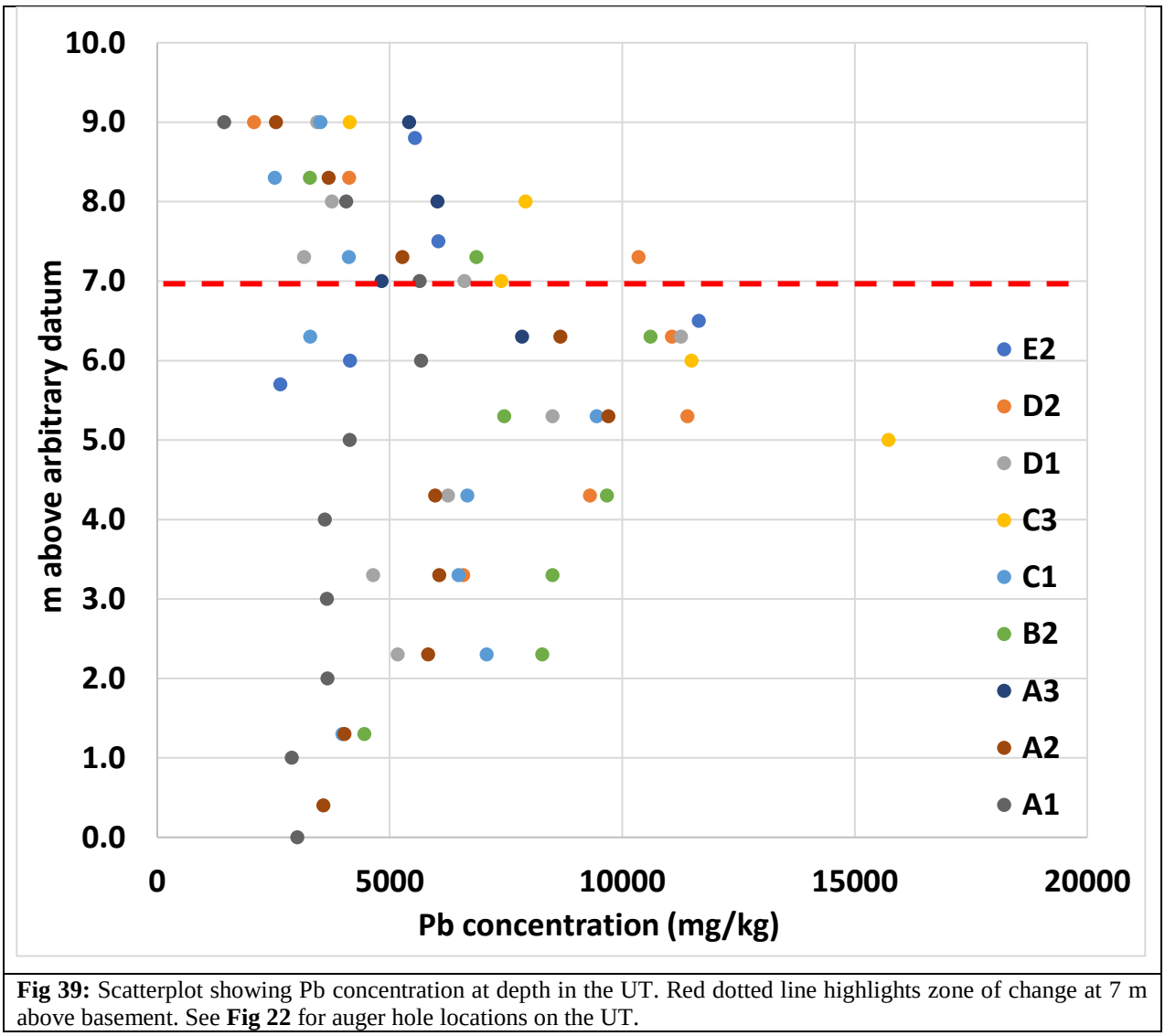

Fig 39: Scatterplot showing Pb concentration at depth in the UT. Red dotted line highlights zone of change at 7 m above basement. See **Fig 22** for auger hole locations on the UT.

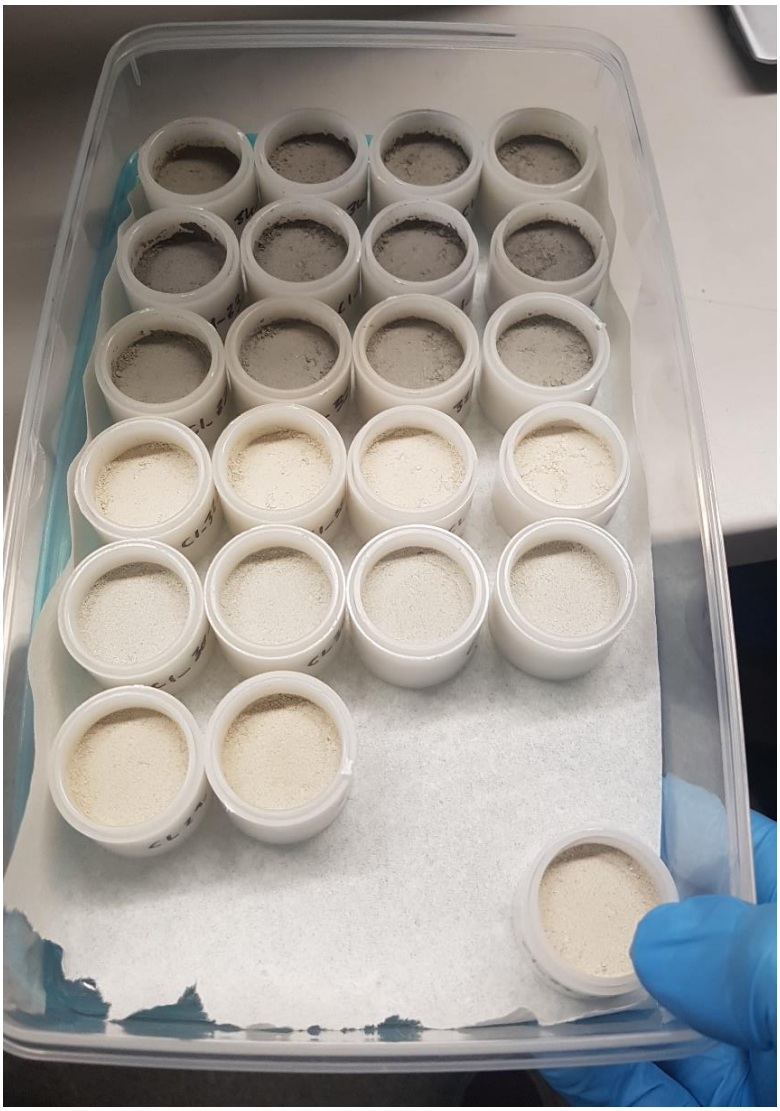

Fig 40: Samples prepared for XRF analysis showing distinct colour change within one auger profile. Shallower samples (white) are to the bottom of the image.

5.4 Tailings mineralogy

Two samples from each auger in the UT underwent mineralogical analysis, producing a diverse range of metal(loid) bearing minerals (**Table 5**). Cu is found in Beudantite and Chenevixite, Zn is found in Franklinite and Sphalerite, and Pb is found in Anglesite, Beudantite, and Segnitite. As was found in a larger number of minerals, namely Arsenopyrite, Beudantite, Chenevixite, Claudetite, Scorodite, and Segnitite.

Table 5: Summary of minerals found in mine waste samples (n = 18) from the UT (individual samples in **Appendix 2**).

Mineral name	Chemical formula	Database code
Anglesite	$PbSO_4$	ICSD 98-004-5230
Arsenopyrite	$As_{0.01}FeS_{0.99}$	ICDD 01-075-6906
Beudantite	$(Fe,Cu)_3Pb((As,S)O_4)_2(OH,H_2O)_6$	ICDD 00-061-0751
Birnessite	$K_{0.27}(Mn_{0.96}O_2)(H_2O)_{0.69}$	ICDD 01-073-7867
Chenevixite	$Cu^{2+}_2Fe^{2+}_3(AsO_4)_2(OH)_4 \cdot H_2O$	ICDD 00-014-0068
Claudetite	As_2O_3	ICDD 00-030-0103
Franklinite	$(Zn_{0.922}Fe_{0.078})(Fe_{1.943}Zn_{0.047})O_4$	ICDD 01-070-3383
Glauconite	$(K,Na)(Fe,Al,Mg)_2(Si,Al)_4O_{10}(OH)_2$	ICDD 00-058-2023
Hydroniumjarosite	$(K_{0.2}(H_3O)_{0.81})Fe_3(SO_4)_2(OH)_6$	ICDD 01-075-9730
Illite	$(K,H_3O)Al_2Si_3AlO_{10}(OH)_2$	ICDD 00-026-0911
Magnetite	Fe_3O_4	ICSD 98-004-1424
Muscovite	$H_2KAl_3(SiO_4)_3$	ICDD 00-001-1098
Orthoclase	$K(Al,Fe)Si_2O_8$	ICDD 00-008-0048
Phengite	$H_2Al_{1.85}K_{0.97}Mg_{0.56}O_{12}Si_{3.59}$	ICSD 98-005-8671
Pyrite	$Fe_{0.987}S_2$	ICDD 01-074-8366
Quartz	SiO_2	ICDD 01-089-8936
Scorodite	$FeAsO_4 \cdot 2H_2O$	ICDD 00-018-0654
Segnitite	$PbFe_3(AsO_4)_2(OH)_5(H_2O)$	ICDD 01-088-1944
Sphalerite	$Zn_{0.66}Fe_{0.34}S$	ICDD 01-073-6560
Zeolite	$H_{6.8}Al_{12}Cs_{1.1}N_{1.7}O_{96}Si_{36}Sr_{4.6}$	ICSD 98-003-5465

Figure 41 shows a diffractogram typical of those collected from UT samples. Samples consisted mostly of quartz according to the semi-quantitative analysis produced by the High Score Plus software, with metal(loid) bearing minerals making up a small percentage of the sample.

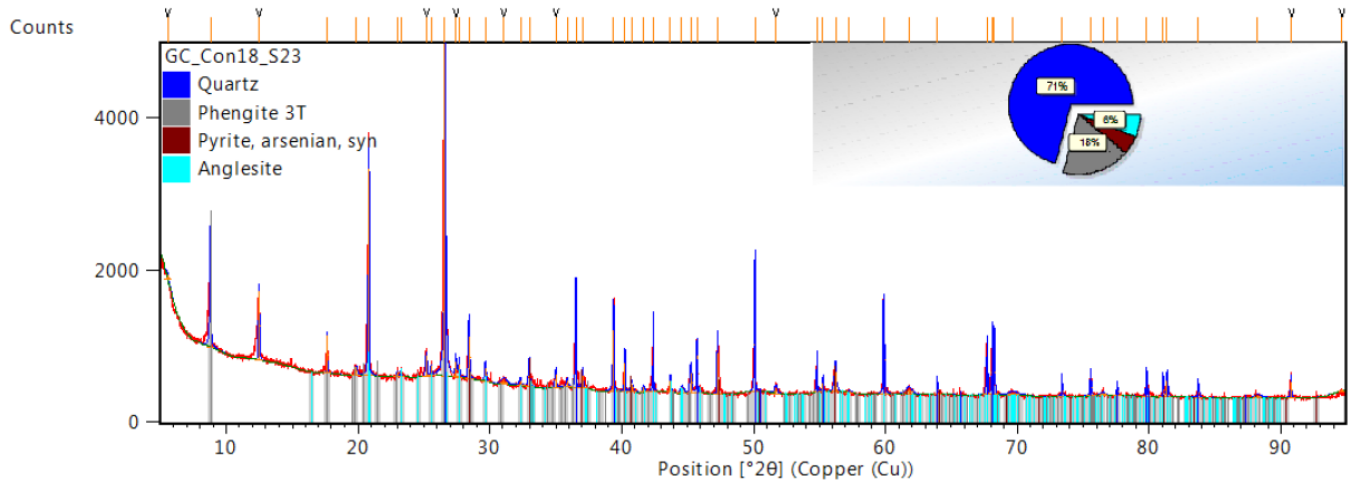

Fig 41: Diffractogram of a typical sample from the upper tailings. Pie chart shows semi-quantitative analysis of minerals identified in the sample. The y-axis is shown to 5000 counts maximum, which has truncated the 100 % quartz peak at 26.6° 2θ.

5.5 Salt mineralogy

Salt efflorescences measured on mine wastes (n = 13), around the King Conrad processing/smelting area (**Fig 2**) produced a highly diverse range of metal(loid) bearing minerals (**Table 6**). Arsenic is found in the hydrated minerals haidingerite and picropharmacolite while As and Cu are found in the sulfide mineral colusite (**Table 6**). Pb is bound in the lead sulfate anglesite and Zn in the zinc sulfide sphalerite ferrous. This complex and diverse assemblage of metal(loid) bearing sulfides, oxides and hydrated minerals indicates the presence of a chemically concentrated material, and a mixture of different waste products in the smelter/processing area.

Table 6: Summary of the diversity of mining waste mineralogy surrounding the King Conrad smelting/processing area (individual samples in **Appendix 3**).

Mineral name	**Chemical Formula**	**Database code**
Albite	$Al_{1.02}Ca_{0.02}Na_{0.98}O_8Si_{2.98}$	ICSD 98-005-6885
Alum-(K)	$KAl(SO_4)_2 \cdot 12H_2O$	ICDD 00-007-0017
Anglesite	$Pb(SO_4)$	ICDD 01-089-7356
Anhydrite	$Ca(SO_4)$	ICDD 01-086-2270
Brushite	$CaPO_3(OH) \cdot 2H_2O$	ICDD 00-011-0293
Colusite	$As_{3.6}Cu_{25.84}S_{32}Sb_{0.6}Sn_{1.8}V_2$	ICSD 98-007-5855
Gibbsite	$Al(OH)_3$	ICDD 00-029-0041
Glauconite	$(K,Na)(Fe,Al,Mg)_2(Si,Al)_4O_{10}(OH)_2$	ICDD 00-058-2024
Gypsum	$CaSO_4 \cdot 2H_2O$	ICDD 00-006-0046
Haidingerite	$CaH(AsO_4)H_2O$	ICDD 01-070-1581
Heulandite	$C_{8.16}H_{70.5}Al_{8.7}N_{8.16}Na_{0.52}O_{82.77}Si_{27.3}$	ICSD 98-010-2457
Jarosite	$(K_{0.86}(H_3O)_{0.14})Fe_3(SO_4)_2(OH)_6$	ICDD 01-075-9735
Microcline	$Al_1K_{0.96}Na_{0.04}O_8Si_3$	ICSD 98-004-5647
Moorhouseite	$CoSO_4(H_2O)_6$	ICDD 01-073-1446
Muscovite	$H_2Al_3K_1O_12Si_3$	ICSD 98-000-5503
Picropharmacolite	$H_{24}As_4Ca_4Mg_1O_{27}$	ICSD 98-004-6085
Pyracmonite	$(NH_4)_3Fe(SO_4)_3$	ICDD 00-003-0043
Quartz	SiO_2	ICSD 98-001-2469
Sphalerite	$Fe_{0.215}S_1Zn_{0.785}$	ICSD 98-004-9032
Wupatkiite	$(Co,Mg,Ni)Al_2(SO_4)_4 \cdot 22H_2O$	ICDD 00-048-1884

5.6 Water quality

Standing waters on site and surface waters of Borah Creek and Maids Creek (**Fig 42**) were measured for oxidation-reduction potential (ORP), hydrogen ion concentration (pH) and electrical conductivity (n = 31).

The slightly acidic pH of 6 for Borah Creek in Site 1 and Maids Creek is normal for native bushland in northeastern NSW with heightened background mineralisation (**Fig 42**) (Geoscience Australia 2010). On the transition between the undisturbed Site 1 and disturbed Site 2, pH drops to the lowest recorded value of 2.0, ORP rises to the highest recorded value of 530 mV and conductivity rises to the highest recorded value of 2800 µS/cm (**Fig 42**). Adjacent to the discharge point of Allwell shaft, 500 m downstream of Conrad Shaft input, a tributary buffers the acidity and reduces ORP and conductivity, however the contribution from the King Conrad processing area runoff after 1500 m channel length again degrades surface water quality (**Fig 42**). This accounts for the increased in channel mineral precipitation near Allwell shaft yet limited precipitation below the lower processing area input. All three water quality parameters return to near-reference values by Copeton Reservoir (**Fig 42**).

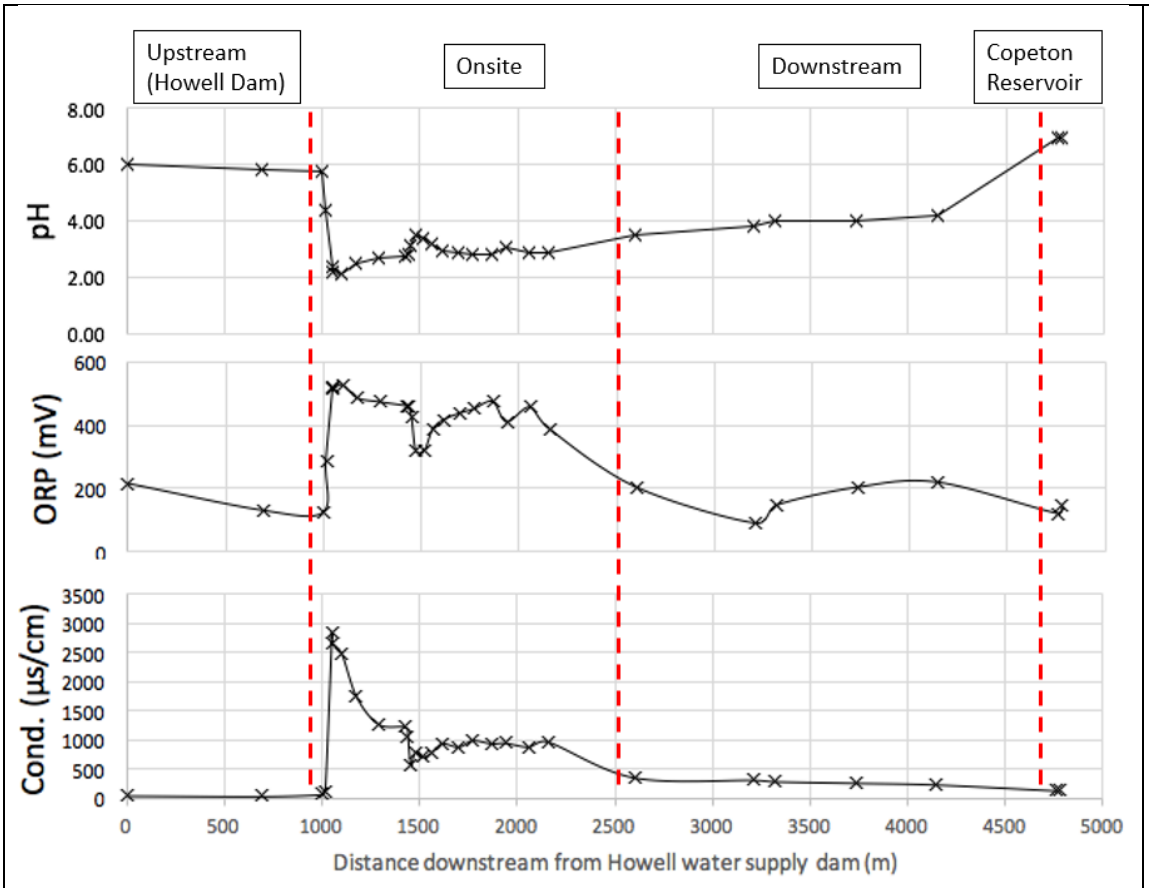

Fig 42: Water quality parameters pH, ORP and conductivity from Howell Dam to Copeton Reservoir.

5.7 Water Chemistry

Water was sampled at 24 locations across the site during two periods of fieldwork. The first was during an above average period of rainfall in March 2017, while the second was during a below average period of rainfall in October 2018 (**Table 7**). The March 2017 fieldwork found the creeks flowing and UT leaking into the sediment trap below, while the October 2018 fieldwork found the site in a much drier state, with almost no water onsite. Due to these differences, water chemistry data has been differentiated between the two trips.

Table 7: Comparison of rainfall for Inverell, showing above and below average figures for 2017 and 2018 respectively. Full year (Jan – Dec) figures not available for 2018 at the time of writing. Data from Weatherzone (2018).

Year	Recorded rainfall (mm)	Long-term average rainfall (mm)	% of long-term average
2017 (Jan – Dec)	1063.6	705	132
2018 (Jan – Nov)	405.2	805.2	57.5

Table 8 shows almost all onsite and downstream locations exceeding ANZECC species survival limits for Cu, Zn, As, and Pb. The exception is Copeton Reservoir, however the large volume of water held in the reservoir would dilute any metal(loid)-rich mine water being received. The two 2017 reference sites situated upstream in Maids Creek do exceed ANZECC guidelines for some elements. However, the exceedances are minimal compared to non-reference sites, and can likely be attributed to the heightened background mineralisation of the area (**Section 2.1**). The 2018 reference site far exceeds ANZECC guidelines for Cu, Zn, and Pb. The sample was taken from an isolated pool in the dry creek bed that had undergone significant evaporation, leading to evaporative concentration.

Table 8: Water chemistry and relevance to ANZECC guidelines. Values in **orange** exceed the threshold for 95 % species survival, and values in **red** exceed 80 % species survival (ANZECC/ARMCANZ 2018). Flow rate only measured in certain locations.

Location	Cu (mg/L)	Zn (mg/L)	As (mg/L)	Pb (mg/L)	Flow Rate (mL/s)
2017 samples, during wetter period					
Sediment trap below the UT	**0.097**	**160**	**12.2**	**0.079**	
Borah Ck. Downstream of UT drainage entry; adjacent to Conrad shaft	**3.39**	**144**	**0.202**	**0.037**	
Borah Creek. Adjacent to Allwell adit and shaft	**0.475**	**15.6**	**1.69**	**0.221**	
Borah Creek. Upstream of slag heap	**0.765**	**16.8**	**0.149**	**0.169**	
Runoff channel from slag heap	**1.07**	**10.8**	0.022	**0.101**	
Borah Creek. Immediately downstream of the LT	**0.933**	**14.6**	**0.064**	**0.153**	

Drainage from the LT	**7.80**	**10.33**	**0.199**	**0.204**	
Below confluence of Maids and Borah creeks	**1.52**	**8.61**	**0.119**	**0.143**	
Maids Creek, midway between mine and reservoir	**1.40**	**7.67**	**0.126**	**0.202**	
Copeton Reservoir	<0.005	<0.005	0.014	<0.005	
2017 Reference sites					
Maids Ck, ~100 m upstream of confluence with Borah Ck	**0.015**	**0.013**	**0.027**	<0.005	
Maids Ck, ~500 m upstream of confluence with Borah Ck	<0.005	<0.005	**0.037**	<0.005	
Howell Dam, upstream of mine	0.005	<0.005	0.022	<0.005	
2018 samples, during drier period					
Borah Creek. Isolated pond ~80 m downstream of Conrad shaft	**10.5**	**123**	**0.393**	**1.05**	
Borah Creek. Pool ~150 m downstream of Conrad shaft. Conspicuous return flow from jointing in granite bedrock filling pool.	**15.6**	**70.4**	0.006	**1.75**	~10
Borah Creek. Pool ~100 m downstream of Allwell shaft and adit. Possibly being filled by joint flow.	**0.285**	**13.5**	**0.131**	**0.134**	~5
Adit leaking above the slag heap	**1.83**	**20.1**	<0.005	**5.99**	
Leaking capped drill hole	**0.007**	**10.7**	**2.54**	**0.075**	~3
Water exfiltrating from below the slag heap	**1.11**	**11.5**	0.009	**0.143**	~3
Lower tailings (recently capped) drainage	**28.4**	**32.1**	0.022	**0.047**	~10
Borah Creek. ~30 m upstream of the lower tailings	**0.824**	**11.1**	**0.027**	**0.099**	
Dam ~150 m downstream of the lower tailings. Blue/green in colour	**6.66**	**15.9**	**0.092**	**0.040**	
Maids Creek. ~100 m downstream of the confluence with Borah Creek	**1.77**	**10.8**	0.017	**0.365**	
2018 Reference site					
Small and isolated puddle in Maids Creek, ~50 m upstream of the confluence with Borah Creek	**5.16**	**16.6**	0.004	**0.125**	

Discharge point sources of metal(loid) contamination from the site have been identified (**Figs 43, 44**). Three potential sources are identified: the UT, the LT, and the slag heap. The UT is of particular concern, as pooled runoff contains the highest As and Zn levels found onsite, at 12.2 mg/L and 160 mg/L respectively. This places Zn at 5160 times the 80 % ANZECC species survival limit, and As at 34 times.

Zn and As levels rise sharply downstream of where drainage from the UT intersects Borah Creek (**Fig 44)**, despite the capping and sediment trap constructed at the base of the structure (**Figs 10, 11, 12**).

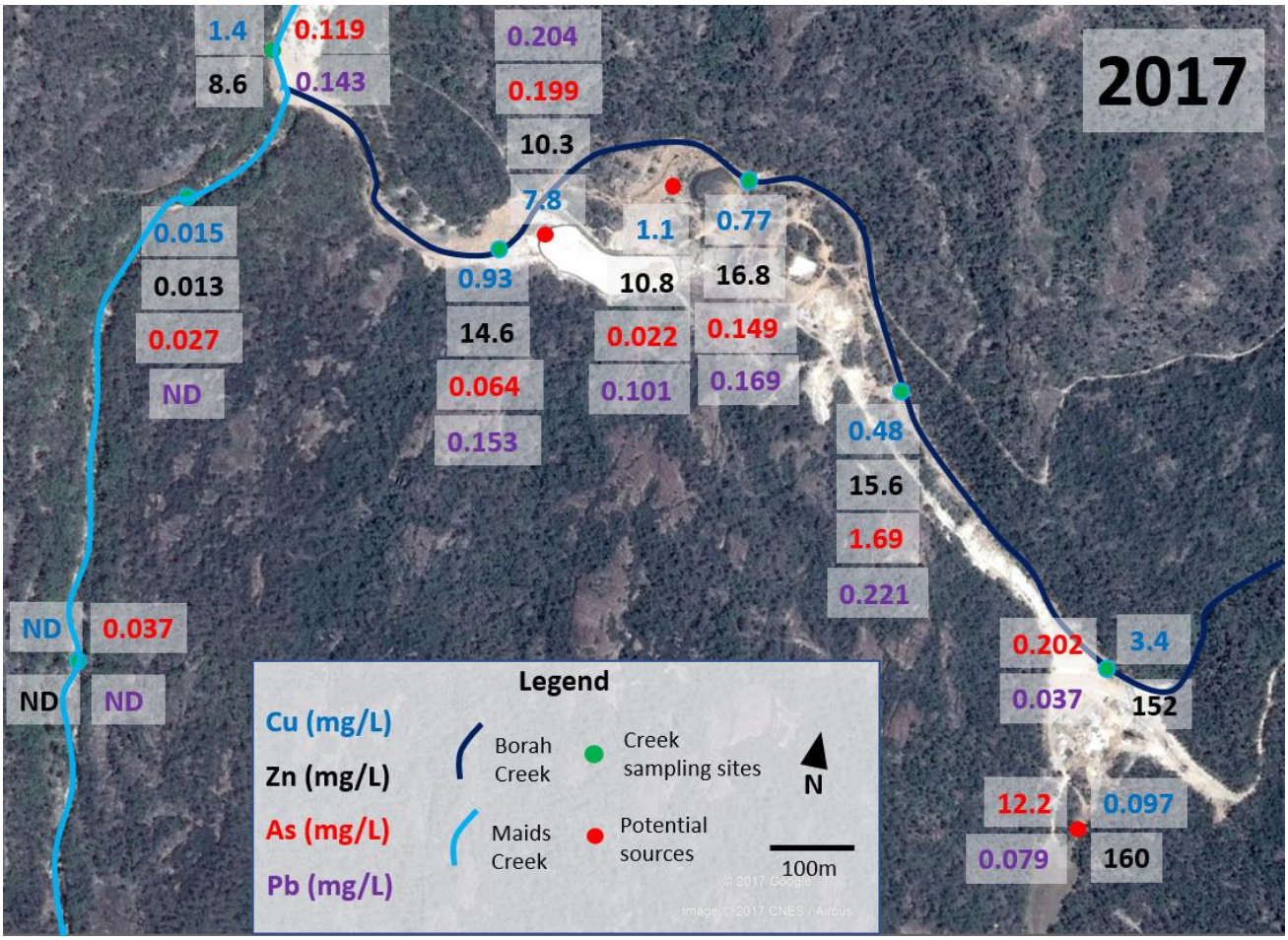

Fig 43: Metal(loid) concentrations in water along Borah and Maids creeks, and potential point sources of contamination. Samples from the wetter 2017 fieldwork. (Image: Google Earth 2015).

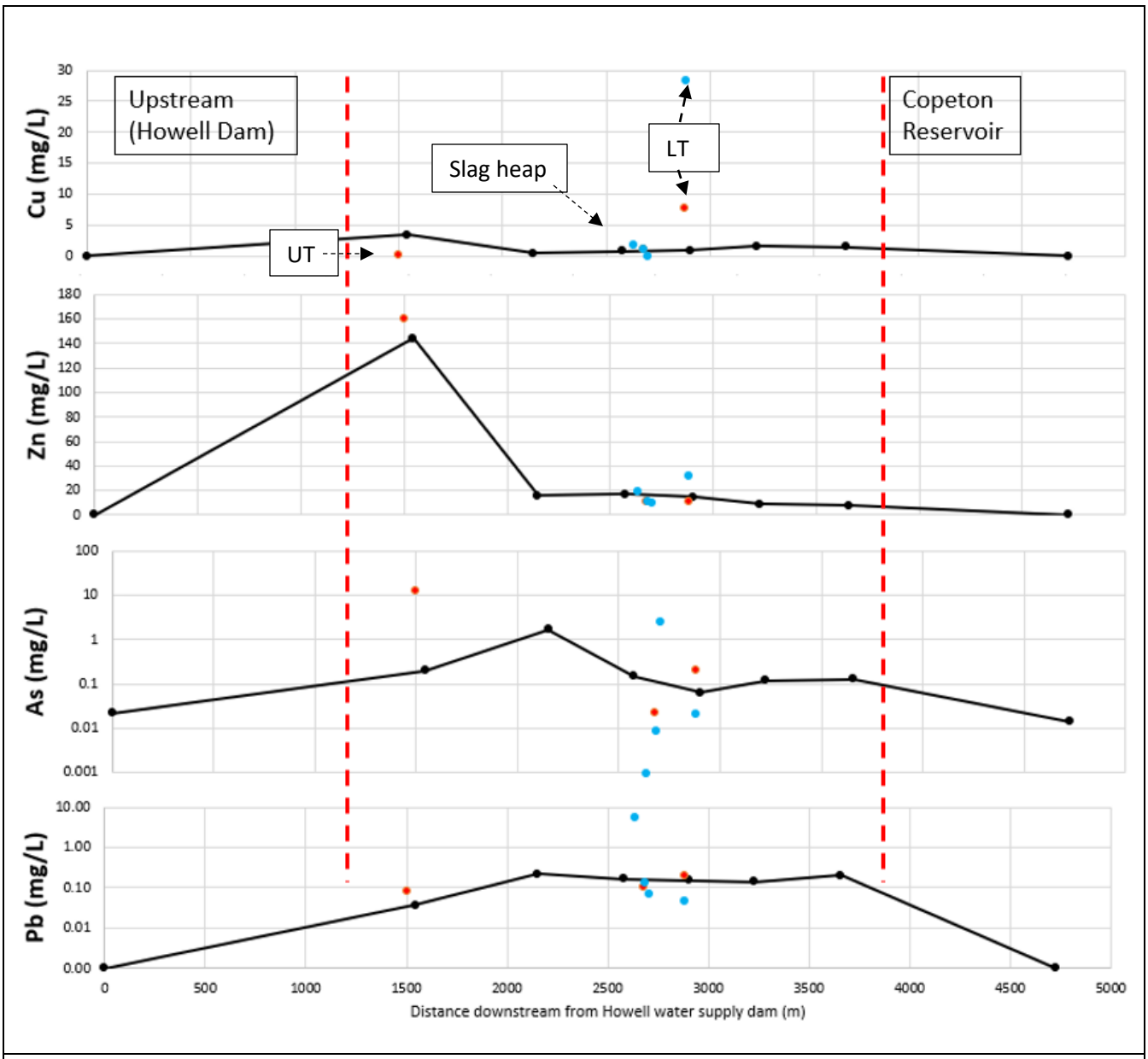

Fig 44: Metal(loid) concentrations along Borah and Maids creeks from the Howell water supply dam to Copeton Reservoir. Red and blue markers indicate point sources of contamination. Red for the wetter 2017 fieldwork, and blue for the drier 2018 fieldwork. Note the log scale for As and Pb.

During the drier sampling in 2018, perennial sources of aqueous contamination were able to be observed. The adit above the slag heap, and water exiting from below the slag heap and LT had Cu, Zn, and Pb levels above the 80 % ANZECC species survival limit (**Table 8, Fig 45)**. A leaking, capped drill hole to the west of the slag heap exceeded the 80 % ANZECC species survival limit for Cu, Zn, Pb, and particularly As, at 2.54 mg/L (**Fig 45**). Two pools of return flow from the jointed granite bedrock were observed and measured in Borah Creek. These joints were producing water exceeding the 80 % ANZECC species survival limit for Cu, Zn, and particularly Pb, at 1.75 mg/L (**Table 8**, **Fig 45**). This was the highest

Pb concentration found onsite. These two locations were flowing at an approximate rate of 5 and 10 mL/s (**Table 8**), producing enough water to fill small pools despite evaporative loss (**Fig 46**).

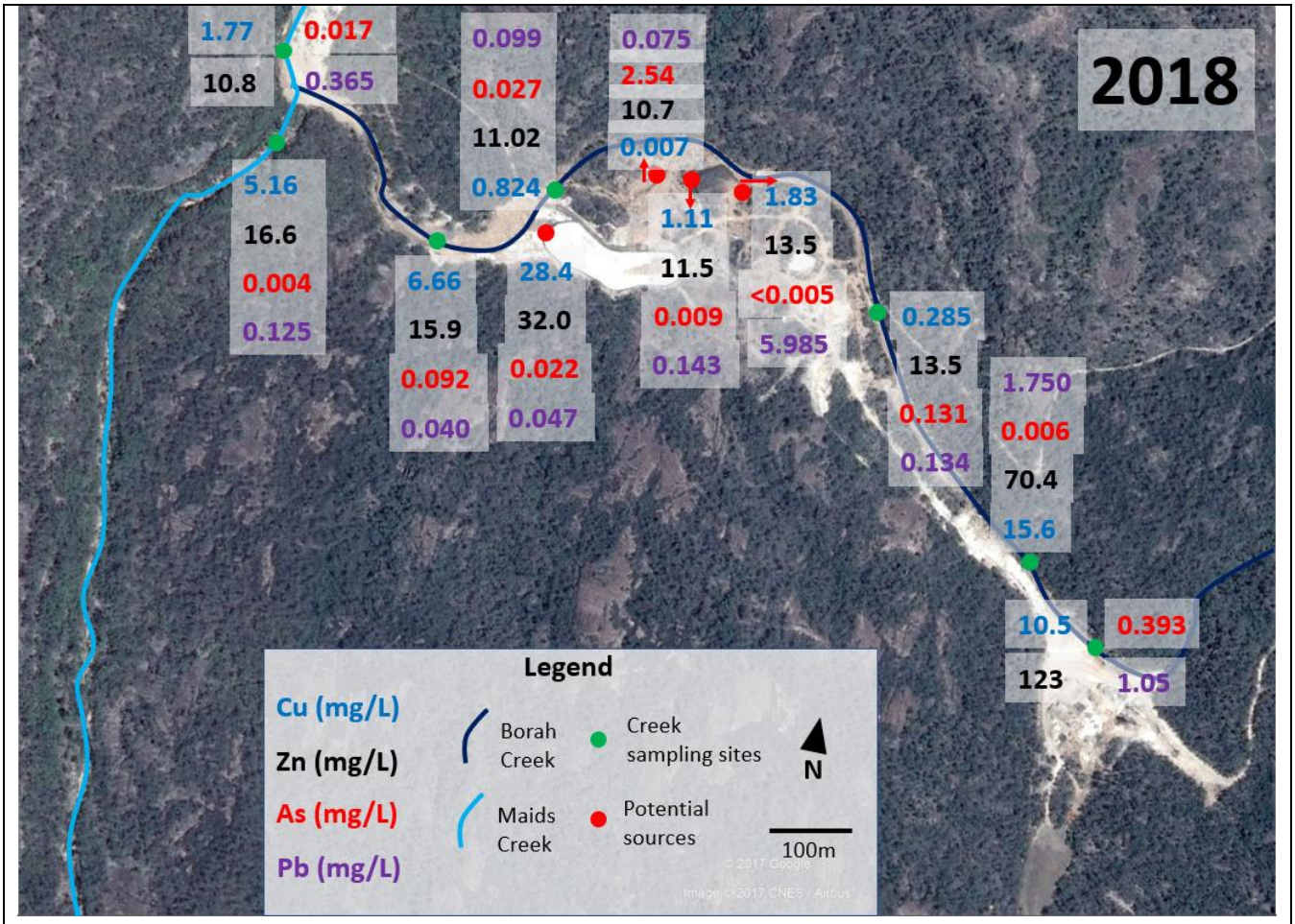

Fig 45: Metal(loid) concentrations in water along Borah and Maids creeks, and potential point sources of contamination. Samples from the drier 2018 fieldwork. (Image: Google Earth 2015).

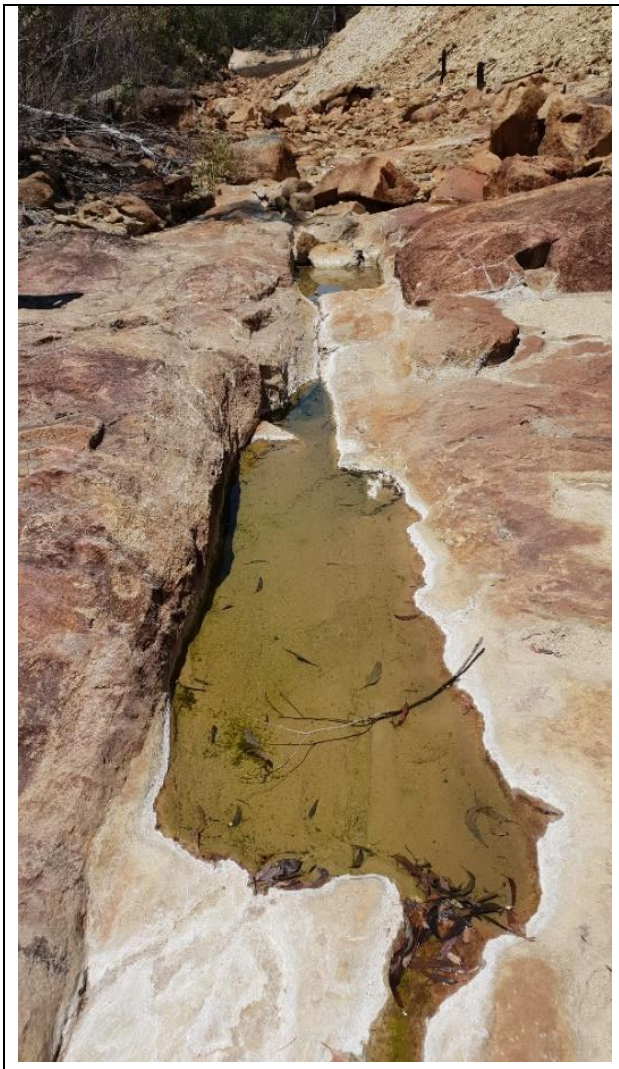

Fig 46: Image of a pool in Borah Creek sustained by exfiltrating joint flow in an otherwise dry creek bed. View looking upstream from (29°57'18.08'' S 151°1'28.63'' E).

5.8 Leachate Extraction

Leachate extraction from bulk samples of UT mine waste resulted in leachates with very high metal(loid) concentrations (**Table 9**). Compared to water sampled directly onsite, Cu and Pb levels are higher in the leachate (**Table 9**), while Zn and As are lower (**Table 8**).

Table 9: Elemental composition of leachates extracted from UT bulk samples. Sample codes refer to hole identifications shown in **Fig 24**.

Sample	Cu (mg/L)	Zn (mg/L)	As (mg/L)	Pb (mg/L)
Control	0.002	0.009	<0.005	<0.005
E2	6.27	178	10.3	3.28
D1	0.617	84.8	5.90	5.45
D2	0.699	77.3	8.22	3.77
C1	1.96	123	9.83	6.53
C3	0.435	57.3	6.98	3.29
B2	0.664	87.1	7.63	3.67
A1	0.487	94.0	8.78	4.83
A2	0.648	62.8	7.89	2.14
A3	2.25	71.1	7.95	3.60

5.9 Hydraulic conductivity

Hydraulic conductivity measurements were taken of the different layers in the capping of the UT. The compacted clay layer, there for hydraulic isolation, had an average K_{sat} of 8.6 x 10^{-9} m/s (0.070 cm/day); while the tailings were much more hydraulically conductive, with an average K_{sat} of 7.5 x 10^{-7} m/s (6.51 cm/day) (**Fig 47**). One measurement of the gravel capillary break was taken, returning a K_{sat} of 4.8 x 10^{-7} m/s (0.041 cm/day), which is even slower than the compacted clay. This is due to the infilling of pore spaces between the gravels with fine sediment (**Fig 47**).

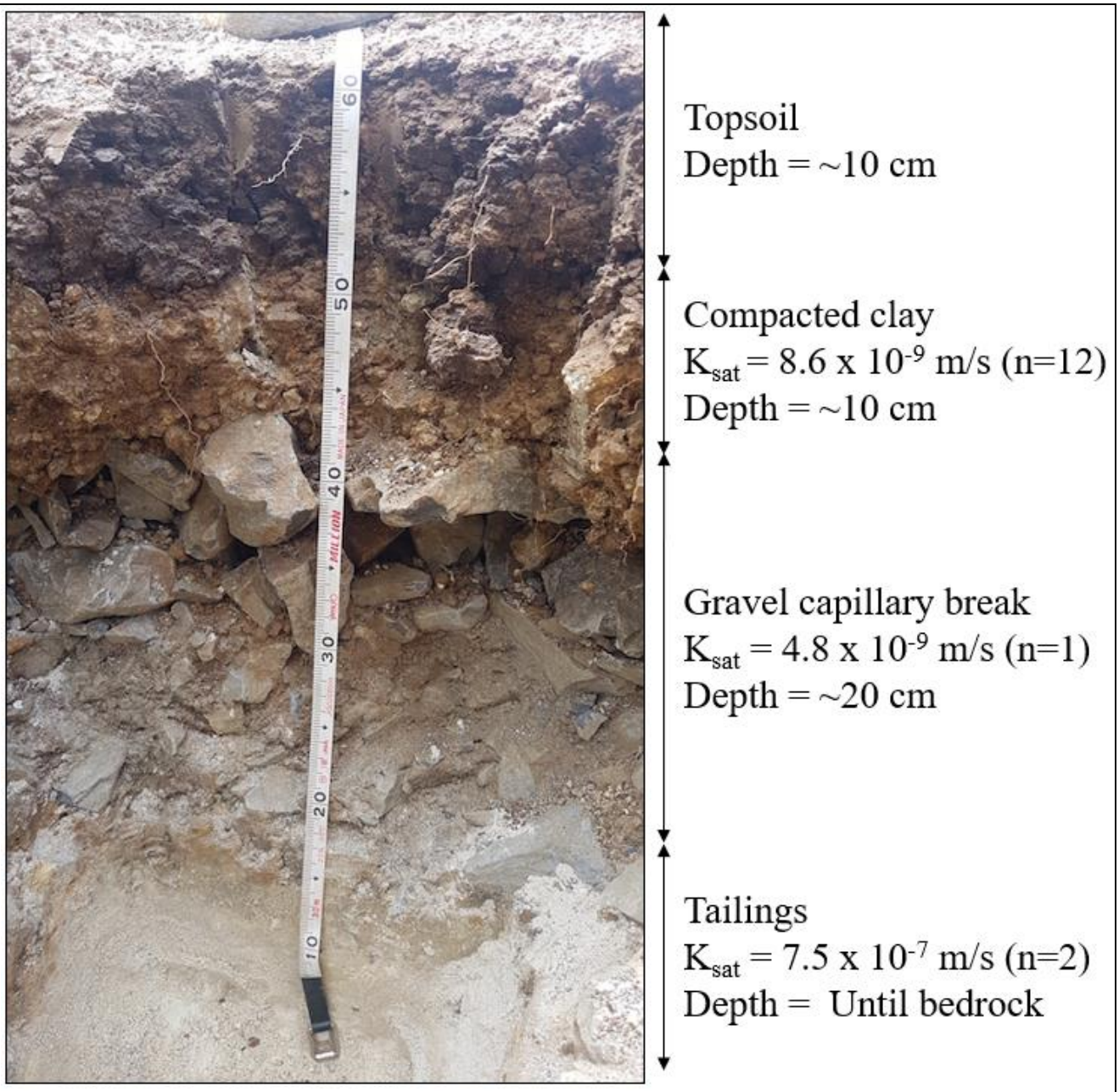

Fig 47: Vertical profile of the UT capping, with K_{sat} figures from measured layers. K_{sat} is given as the geometric mean of all measurements taken for that layer. Note the significant infilling of pore spaces in the capillary break.

5.10 Topographical Survey

One longitudinal and five lateral transects were measured over the UT (**Fig 48**), to capture the dimensions of the structure and allow volume estimations. Two volume estimations are offered: a minimal estimate and a maximal estimate. The conservative estimate uses only the known auger depths and surface shape, while the realistic estimate also factors in the likely shape of the valley wall beneath the eastern side of the tailings (**Fig 49**). **Table 10** calculates the minimal estimate at 17,650 m^3, and the maximal estimate at 18,880 m^3, a difference of 1,230 m^3, representing a measurement uncertainty of ~7 %.

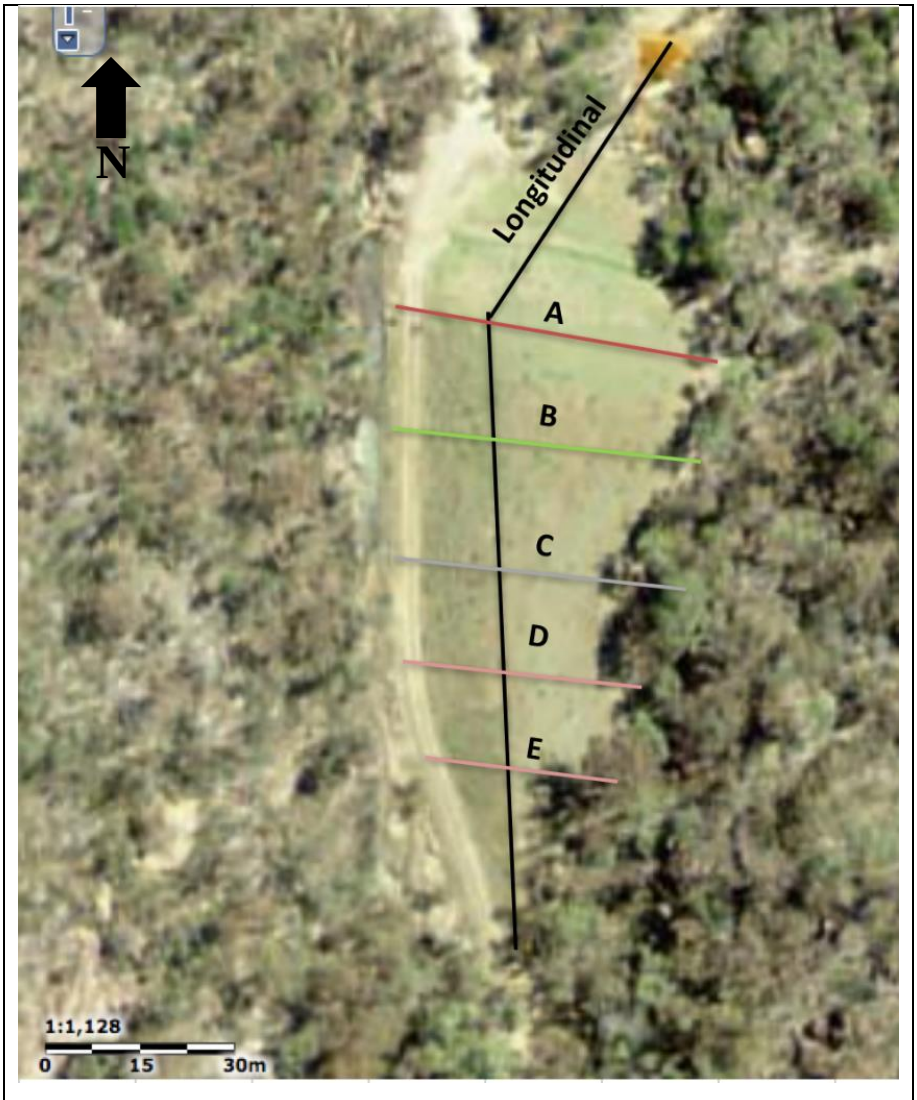

Fig 48: Top-down view of where the one longitudinal (north-south) and five lateral (east-west) transects were surveyed.

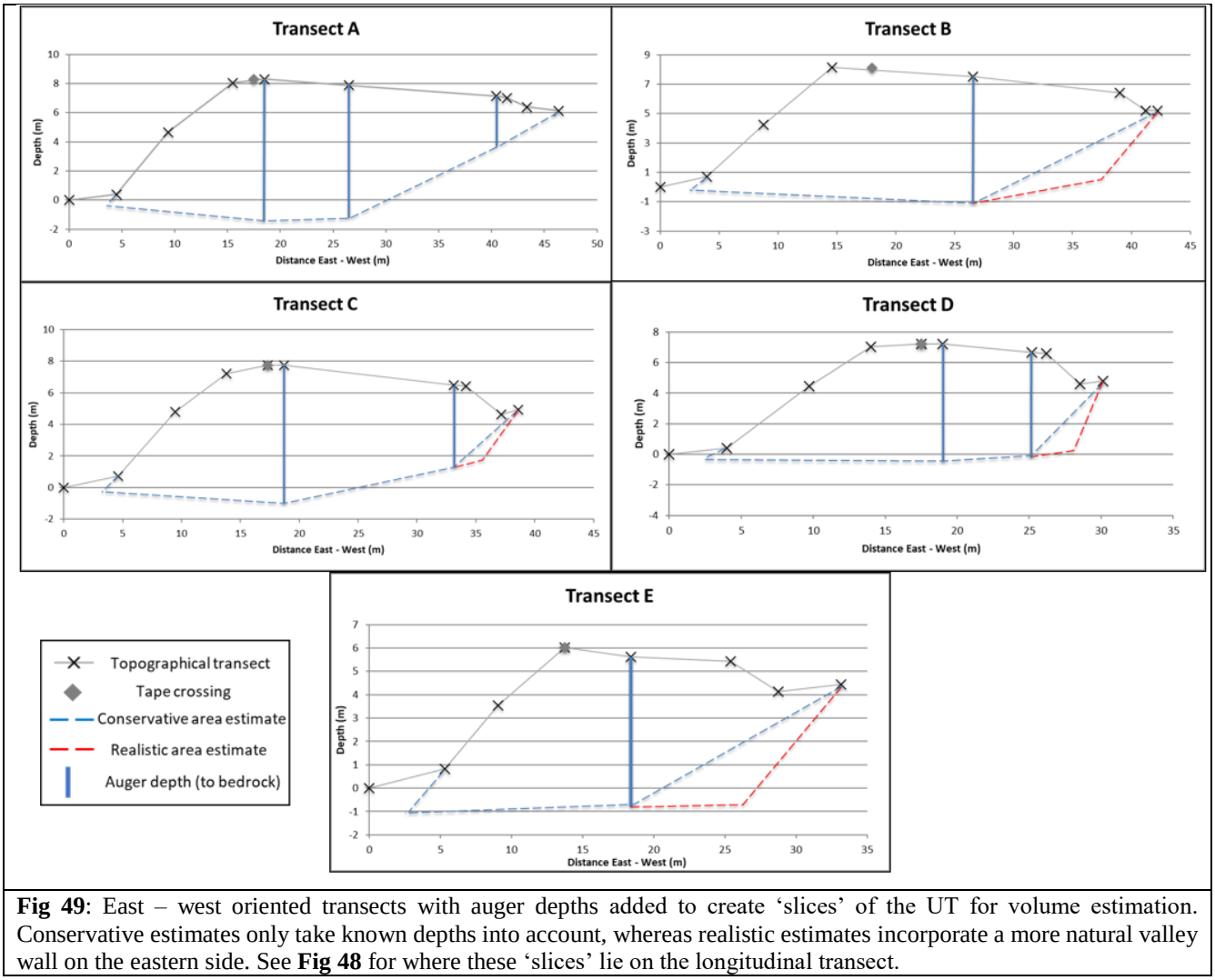

Fig 49: East – west oriented transects with auger depths added to create 'slices' of the UT for volume estimation. Conservative estimates only take known depths into account, whereas realistic estimates incorporate a more natural valley wall on the eastern side. See **Fig 48** for where these 'slices' lie on the longitudinal transect.

Table 10: Volume estimates based on the longitudinal transect length (**Fig 49**) and lateral transect 'slice' areas (**Fig 50**).

Transect	**Length (m)**	**Cross-sectional area – minimal (m^2)**	**Cross-sectional area – maximal (m^2)**	**Volume– minimal (m^3)**	**Volume – maximal (m^3)**
North batter slope	30.0	120	120	3,600	3,600
A	11.0	263	263	2,900	2,900
B	11.0	214	240	2,350	2,640
C	16.5	190	197	3,140	3,250
D	20.8	138	147	2,870	3,070
E	38.7	72	88.4	2,790	3,420
Sum	128.0	997	1056	**17,650**	**18,880**

5.11 Macroinvertebrate ecotoxicology

Macroinvertebrates were sampled at seven locations across the site (**Fig 26**). These can be grouped into two reference locations, two onsite locations, two downstream locations, and Copeton Reservoir (**Fig 50**). These groupings are arranged by family richness and SIGNAL 2 (Stream Invertebrate Grade Number - Average Level) score, with water quality quadrants defined as per Chessman (2003).

The SIGNAL 2 scoring system uses macroinvertebrate family sensitivity and abundance to measure water quality (Chessman 2003). Reference locations fell into quadrant 1, indicating good water quality; Copeton Reservoir fell into quadrant 2, indicating fair water quality; while onsite and downstream locations fell into quadrant 4, indicating significant water quality problems affecting organisms.

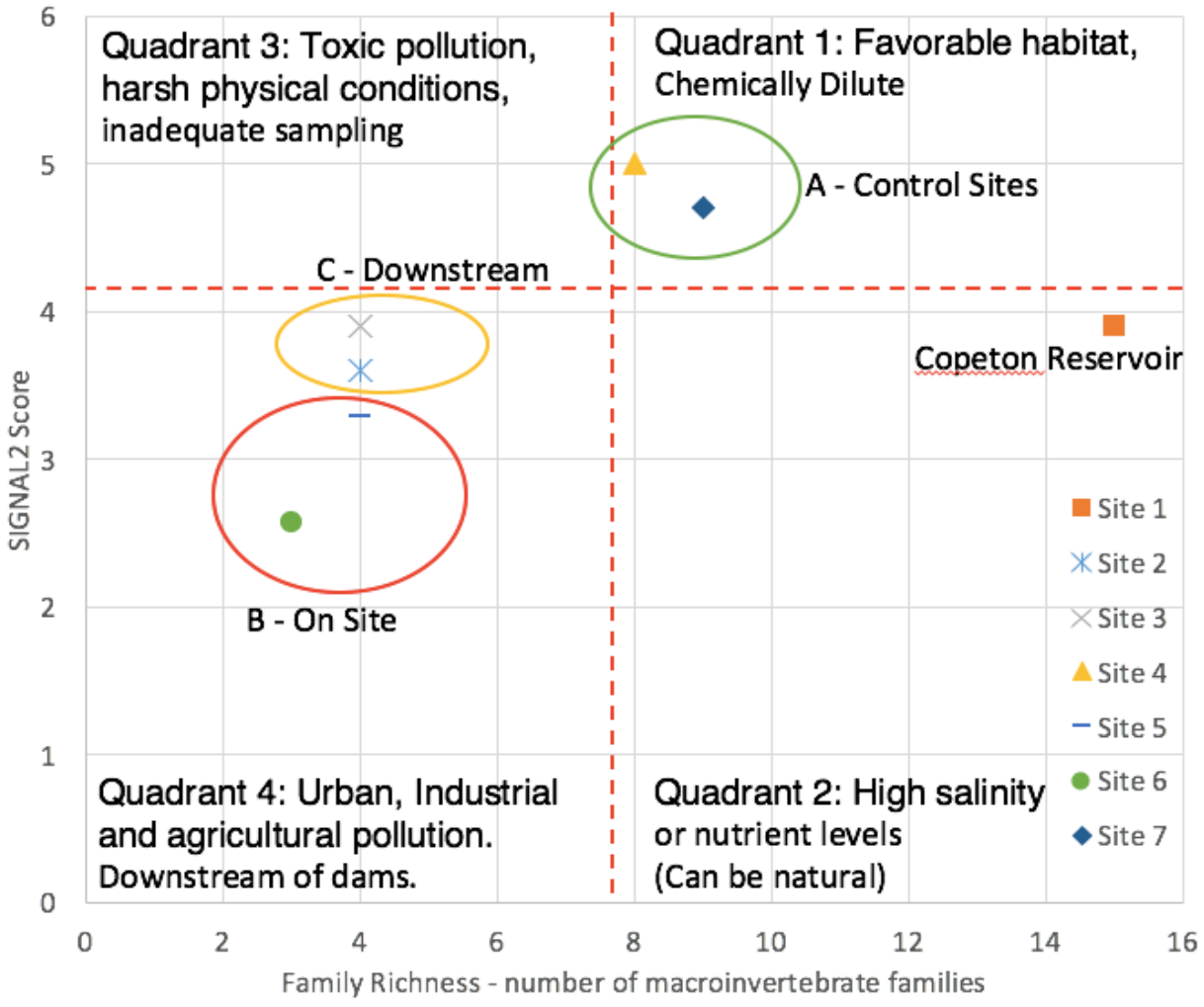

Fig 50: Family quadrant diagram of SIGNAL 2 score and richness (produced in accordance with Chessman, 2003). See **Fig 26** for site locations. Declines in species richness for sites B and C are due to loss of invertebrate families *Philorheithridae* and *Leptophlebiidae*.

High macroinvertebrate family diversity at Howell Dam and Copeton Reservoir were recorded (**Fig 51**). All sampled locations onsite and directly downstream of the mine show decreased species richness (**Fig 51**). SIGNAL 2 scores remain high except for the sampling location on Borah Creek 300 m downstream of Conrad Shaft, its associated processing infrastructure, and the UT (**Fig 51**). This location also provided the lowest SIGNAL 2 score.

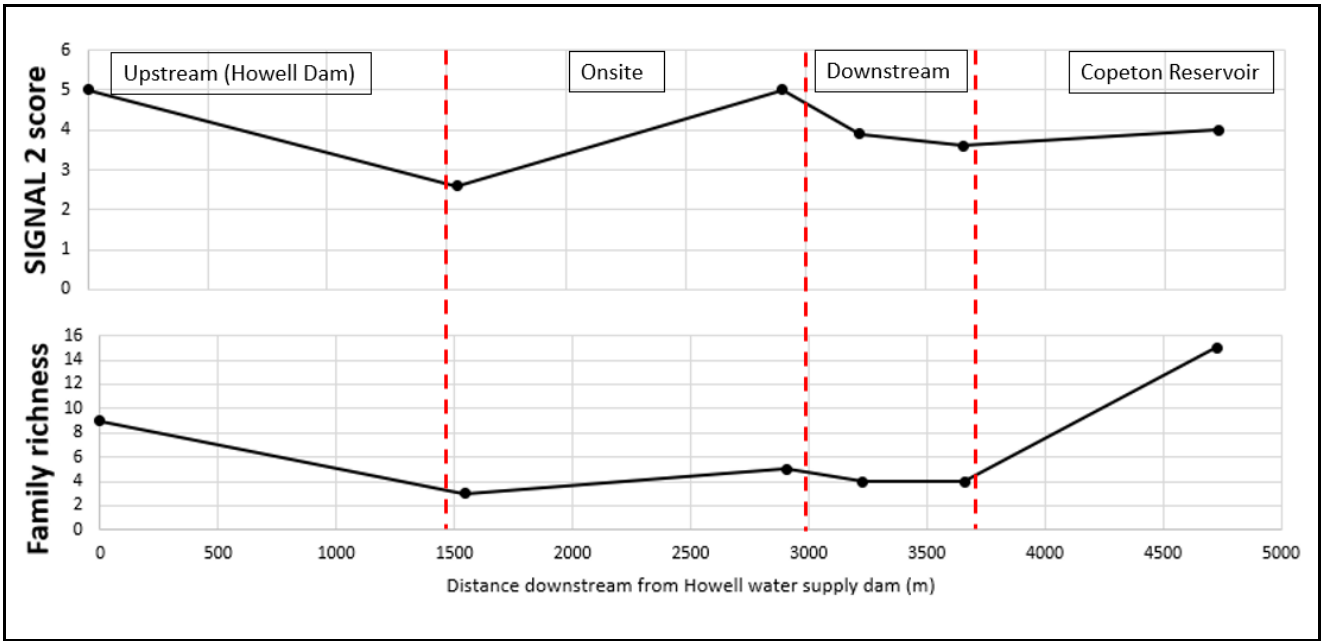

Fig 51: Downstream trends of family richness and SIGNAL 2 score.

6. Discussion

While rehabilitation works have been conducted at Conrad, the site still represents a substantial environmental liability. Residual contamination from mine workings is a source of contamination; however other liabilities have been created by, or are continuing despite, the rehabilitation works (Gore et al. 2007). Several point sources were identified, including the UT, LT, slag heap, and various piles of mine wastes (**Figs 27-34, 43, 45**). Of these sources, the UT poses the greatest environmental threat. The UT is producing leachate water heavily polluted with Zn and As (**Table 8, Figs 43, 44)**, which follows drainage lines downstream (**Fig 13**) from the sediment trap (**Fig 11**) and is received by Borah Creek, and ultimately reaching Inverell's water supply (**Fig 44**). As only one sample of UT leachate was able to be collected onsite, laboratory-based leachate extractions from UT material were used to confirm the metal(loid) concentrations of leachate from the UT (**Table 9**). Aqueous contamination from Conrad is having a negative effect on the downstream environment, significantly impacting aquatic macroinvertebrate family richness and SIGNAL 2 score (**Fig 50**). The lowest of these figures were

recorded immediately downstream of where drainage from the UT is received by Borah Creek (**Fig 51**). This leakage of contamination continues despite capping works undertaken to limit water movement into and out of the tailings. This research suggests that this capping has (at least partly) failed in its intended function, and the significant environmental liability posed by waste within the UT has remained. Therefore, further rehabilitation is required.

Determining the source of the water entering the UT is necessary to ensure future rehabilitation works to remedy the correct problem. There are three possible avenues of entry for water into the UT (**Fig 52**). The first and most simple option is that rainfall is infiltrating through the capping and into the tailings. This would imply that the clay capping, which was intended to hydraulically isolate the tailings, is of insufficient thickness or quality. The hydraulic conductivity results (**Fig 47)** do not confirm this theory, showing the capping had a geometric mean K_{sat} value of 8.6 x 10^{9} m/s (0.070 cm/day). Bear (2013) categorises this as an impervious clay, and Oosterbaan and Nijland (1986) as a dense clay with no cracks or pores, indicating that the hydraulic isolation of the capping is likely sufficient. The second and third options (**Fig 52**) involve water infiltrating and exfiltrating though jointed bedrock observed in the valley where the UT lies. **Figs 49** and **52** show the eastern side of the tailings lying against the jointed valley wall, where there is no protection from infiltration/exfiltration. Observations in **Table 8** and **Fig 46** demonstrate that joint flow occurs elsewhere onsite. Given these observations and the effective capping currently in place, it is likely that water is infiltrating into the UT through joint flow from the eastern valley wall or from the valley bottom. To confirm either of these scenarios, groundwater modelling within the UT is required. This was attempted as part of this thesis, with three groundwater dataloggers installed in the augered holes in the UT. However, with the region receiving only 57.5 % of the long-term average rainfall in 2018 (**Table 7**), no water was recorded in the UT from January to mid-November 2018.

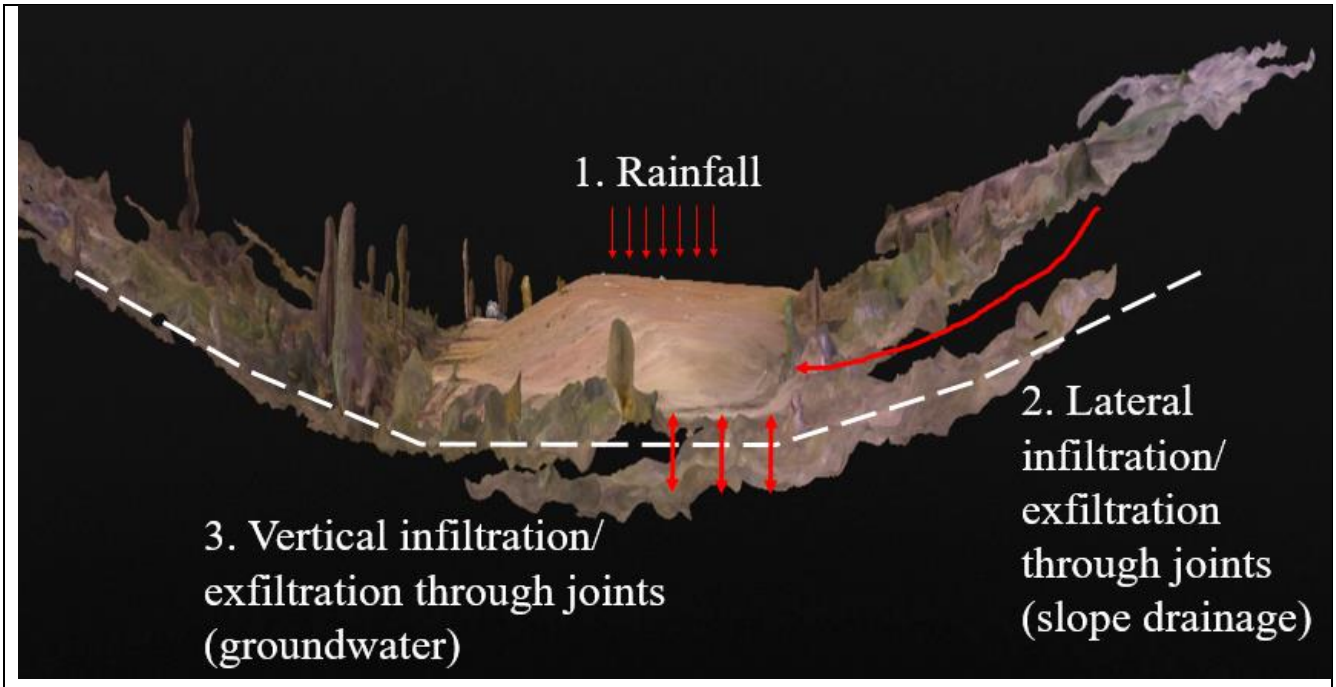

Fig 52: Three potential sources of water entering the UT. Image courtesy of the NSW Department of Planning and Environment, Legacy Mines Program.

Once the source of the water entering the UT is identified, further remediation options can be explored (**Fig 53**).

1) If the hydraulic conductivity results of this thesis are underestimated, due to hole sealing or insufficient measurement replication, and it is revealed that the capping is ineffective, a replacement capping design could be constructed on top of the current structure. The recently capped LT could be used as a guide if found to be effective, which incorporated a thicker clay layer of 1 m and geofabric to stop the infilling of capillary break pore spaces (**Fig 47**).
2) If water is found to be entering the UT through the eastern valley wall, a vertical barrier could be installed to divert water before it enters the UT.
3) If groundwater infiltration through joints in the valley floor are providing water to the UT, cement stabilisation of the pile would significantly reduce infiltration (Johnson & Hallberg 2005).
4) Transport pathway treatments are an alternative to the hydraulic isolation techniques of options 1, 2, and 3. Treatment options include intercepting and treating the leachate using Permeable Reactive Barriers (PRB) where it exits the UT, or treating it within the sediment trap. These techniques could be used regardless of how water is entering the UT.

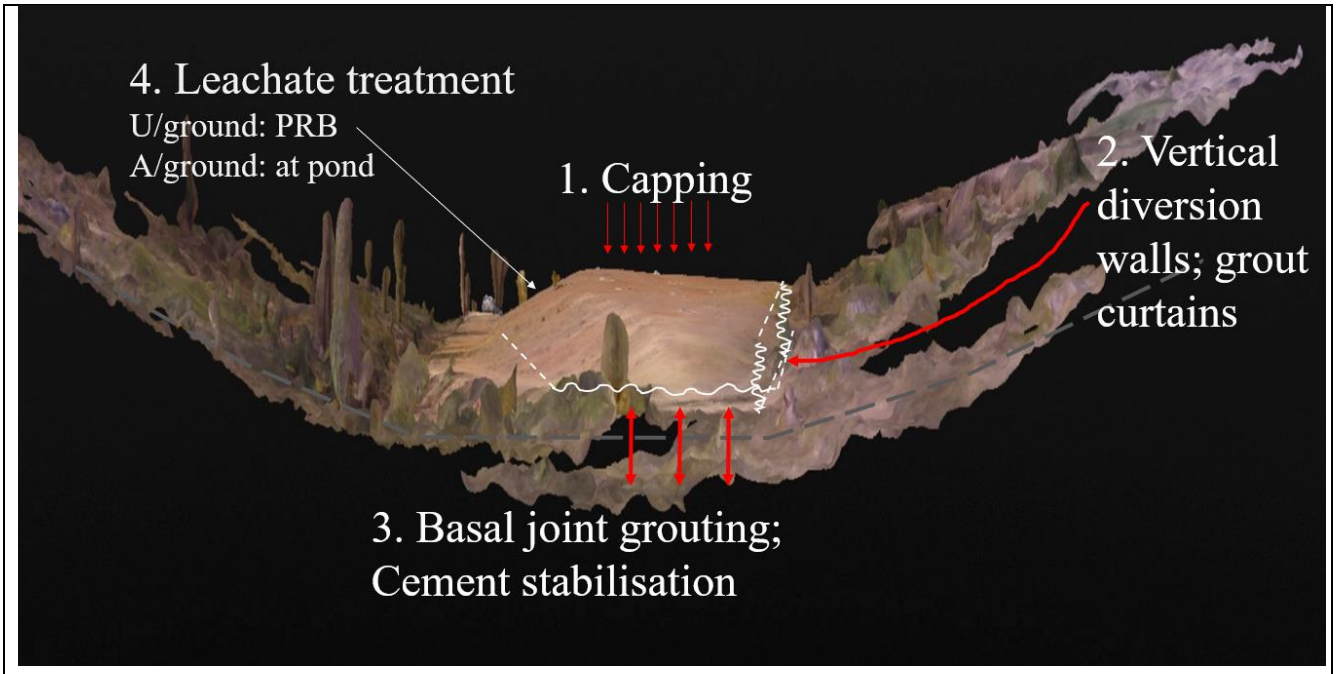

Fig 53: Four potential remediation options for the UT. Image courtesy of the NSW Department of Planning and Environment, Legacy Mines Program.

7. Recommendations

Further work should confirm these findings, particularly through monitoring of groundwater in the UT. This should be a priority for the site, as the LT has recently undergone similar capping (**Fig 17**). Results finding the UT water infiltration pathway could be used to inform future rehabilitation projects at legacy mines. This research indicates the LT and the slag heap as potential sources (**Figs 43, 45**), but are a lower priority for rehabilitation. With the LT having recently had more waste added, and changing the structure from gabion containment to clay capping, the nature of the contamination may also have been altered.

The use of mine waste as part of the materials for the diversion and battering of Borah Creek (**Fig 9**) as well as contour banking around the mine (**Fig 8**), has created a new source of contaminated material for fluvial transport (Gore et al. 2007). Much of the fine material used in this work has been eroded and transported, choking downstream sections of Borah Creek with contaminated sediment (**Fig 20, 21**). Some of this sediment has been transported through to Copeton Reservoir, where it exceeds the ANZECC guidelines (**Fig 35**). Further use of potentially contaminated mine waste material in rehabilitation works should be halted. Elemental analyses should also be conducted on any potentially contaminated material before use in rehabilitation works.

Future analytical work should;

1) Continue the UT groundwater infiltration monitoring during periods of significant rainfall.

2) Repeat and confirm the solid and aqueous phase chemistry, as well as macroinvertebrate ecotoxicology, using the same methods employed in this research.
3) Complete a battery of acute toxicity tests using UT leachate.
4) Monitor water exiting the LT to ensure that recent capping is effective.

8. Conclusions

This study examined sources of offsite contamination originating from Conrad Mine. Soil measurements revealed a variety of mine wastes left exposed around the site, including waste rock used for creek diversion and road building as part of rehabilitation efforts. Of the 207 measurement locations, 91 exceeded the NEPM HIL-D values for As and 136 for Pb. Downstream sediment chemistry in Borah and Maids Creeks showed As and Pb levels remaining well above the NEPM ISQG High guidelines until reaching Copeton Reservoir. Water quality and chemistry measurements showed decreased water quality and elemental concentrations exceeding ANZECC guidelines onsite and downstream of the mine. The UT, LT, and slag heap were identified as point sources for aqueous metal(loid) contamination. Of these, the UT contributed the most. Water sampling during a drier period found joint flow originating from fractured granite bedrock, revealing a possible pathway for water infiltration into the UT. Elemental analysis of UT samples revealed a metal(loid) rich material of, on average, 0.048 wt% Cu, 0.40 wt% Zn, 1.58 wt% As, and 0.544 wt% Pb. The volume of the tailings was estimated at 18,880 m^3. Hydraulic conductivity measurements showed that the clay capping was effective, suggesting rainfall infiltration through the capping structure was not the cause of leachate production in the UT. This further suggests that water is entering the UT through jointed granite bedrock on the valley floor or wall. Groundwater dataloggers were installed in the UT to determine the source of water, but did not record any water as the Inverell area received only 57.5 % of long-term average rainfall while data collection occurred. This inhibited the effectiveness of the study, as definitive rehabilitation options for the UT cannot be offered without knowing the source of water infiltration. Therefore, four potential options for future rehabilitation efforts of the UT were offered, covering each possible infiltration scenario. Future research should focus on reinstalling groundwater monitoring equipment so that the UT, the worst source of offsite contamination from Conrad, can be properly rehabilitated.

9. References

ANZECC/ARMCANZ 2018. Australian and New Zealand guidelines for fresh and marine water quality. National water quality management strategy: Australian and New Zealand Conservation Council & Agriculture, and Resource Management Council of Australia and New Zealand. Available: http://www.waterquality.gov.au/anz-guidelines/guideline-values/default [Accessed 19 Nov 2018].

Ashley, P.M., Lottermoser, B.G., Collins, A.J. & Grant, C.D. 2004. Environmental geochemistry of the derelict Webbs Consols mine, New South Wales, Australia. Environmental Geology 46(5), 591-604.

ASTM. 2018. Standard Specification for Reagent Water D1193–06. West Conshohocken, PA, USA.

Bear, J. 2013. Dynamics of Fluids in Porous Media. Courier Corporation, MA, USA

Brooks, K. A. & Mcilveen, G. R. 1988. The Impact of a Derelict Base Metal Mine on the Aquatic Environment. In: The Third International Mine Water Congress.

Brown, R. E. & Stroud, W. J. 1997. Metallogenic Study and Mineral Deposit Data Sheets: Inverell data sheets. SH/56-5, 1:250,000. Sydney: Geological Survey of New South Wales.

Burke, H. 2000. An historical archaeological assessment of the Conrad Mine, Inverell, NSW. Department of Land and Water Conservation. Sydney. Unpublished report obtained from the Legacy Mines Program, Department of Planning and Environment, Maitland NSW. November 2018.

Cato, N. & Mahmud, S. 2003. Abandoned mine site characterization and cleanup handbook. Diane Publishing Company, Seattle.

Chessman B. 2003. SIGNAL 2 – A Scoring System for Macro-invertebrate ('Water Bugs') in Australian Rivers. Department of the Environment and Heritage, Canberra.

Department of the Environment. 2016. *Homoranthus prolixus* in species profile and threats database. Department of the Environment, Canberra. Available: http://www.environment.gov.au/sprat. [Accessed 19 Nov 2018].

DIN 38414-S4. 1984. German Standard Procedure for Water, Wastewater and Sediment Testing (Group S), Determination of Leachability by Water, Institutfür Normung, Berlín, Alemania.

DMR 1954. Application for Advance for Battery - E.C. Walker and Sons, Conrad Mine, Howell. NSW MR 0150 - Department of Mineral Resources, Sydney, Australia, 28pp. Unpublished report obtained from the Legacy Mines Program, Department of Planning and Environment, Maitland NSW. November 2018.

Donnelly, M. 2011. Review of Environmental Factors. Conrad Project, NSW, ML 6040, EPL 1050. Malachite Resources Limited, Lindfield, NSW, Australia. Unpublished report obtained from the Legacy Mines Program, Department of Planning and Environment, Maitland NSW. November 2018.

Ecotone Ecological Consultants Pty, Ltd. 2002. Bat survey and assessment for proposed rehabilitation work, Conrad Mine, Howell near Inverell, NSW. Unpublished report obtained from the Legacy Mines Program, Department of Planning and Environment, Maitland NSW. November 2018.

EPA 1995. Contaminated Sites Sampling Design Guidelines. In: Department of Environment and Heritage (ed.). Sydney, NSW: EPA.

ESRI 2017. ArcGIS Desktop: Release 10.5. Redlands, CA: Environmental Systems Research Institute.

Gore, D.B., Preston, N.J. & Fryirs, K.A. 2007. Post-rehabilitation environmental hazard of Cu, Zn, As and Pb at the derelict Conrad Mine, eastern Australia. Environmental Pollution 148, 491-500.

Grant, C.D., Campbell, C.J. & Charnock, N.R. 2002. Selection of Species Suitable for Derelict Mine Site Rehabilitation in New South Wales, Australia. Water, Air, and Soil Pollution 139, 215-235.

Hawes, W. & Eade, A. 1998 Vegetation assessment of the Conrad Mine Site, Unpublished.

Johnson, D.B. & Hallberg, K.B. 2005. Acid mine drainage remediation options: a review. Science of the Total Environment, 338(1), 3-14.

Kolkert, H. 2015. Ecological assessment: site assessment and remediation scoping Conrad mine, Howell NSW. Dubbo, NSW: NSW Trade and Investment - Guyra Local Government Area. Unpublished report obtained from the Legacy Mines Program, Department of Planning and Environment, Maitland NSW. November 2018.

Ledin, M. & Pedersen, K., 1996. The environmental impact of mine wastes – Roles of microorganisms and their significance in treatment of mine wastes. Earth-Science Reviews, 41(1), 67-108.

Legacy Mines Program. 2018. Funding Guidelines. NSW Department of Planning and Environment, Sydney, Australia. Available: https://resourcesandgeoscience.nsw.gov.au/__data/assets/pdf_file/0009/594198/POL16-7-Derelict-Mines-Program-Funding-Priority-Guidelines.pdf. [Accessed 19 Nov 2018].

Lewin, K. 1996. Leaching tests for waste compliance and characterisation: recent practical experiences. Science of the total environment, 178, 85-94.

Lottermoser, B. 2010. Mine Wastes: Characterization, Treatment and Environmental Impacts. Springer Berlin Heidelberg.

Menzies, I. A. 1967. The Conrad Mines, Howell. Report GS1967/077. NSW Department of Mineral Resources, Sydney, Australia, 6 pp. Unpublished report obtained from the Legacy Mines Program, Department of Planning and Environment, Maitland NSW. November 2018.

NEPM 2013. Schedule B 1 - Guideline on Investigation Levels for Soil and Groundwater. Environmental Protection Authority. Available: https://www.scu.edu.au/media/scueduau/commercial-services/eal/NEPM-guideline-on-investigation-levels-for-soils-and-groundwater046a.pdf. [Accessed 19 Nov 2018].

Oosterbaan, R. & Nijland, H. 1986. Determining the Saturated Hydraulic Conductivity. Drainage Principles and Applications. International Institute for Land Reclamation and Improvement. Wageningen, The Netherlands

Pearson, M. & Mcgowan, B. 2000. Mining Heritage Places Assessment Manual. Australian Council of National Trusts - Australian Heritage Commission.

Pietrass-Wong, B., Meares, R. & Bannerman, C. 2012. Final Report for the Year Ended 15 July 2012 Howell Project, NSW - EL7176. Malachite Resources Limited, Lindfield, NSW, Australia. Unpublished report obtained from the Legacy Mines Program, Department of Planning and Environment, Maitland NSW. November 2018.

Qld DNRM (Queensland, Department of Natural Resources and Mines). 2001. Queensland Australian River Assessment System (AusRivAS) Sampling and Processing Manual. Available: https://ausrivas.ewater.org.au/index.php/resources2/category/16-manuals?download=22:qld-sampling-and-processing-manual-063mb. [Accessed 19 Nov 2018].

Rashed, M.N. 2010. Monitoring of contaminated toxic and heavy metals, from mine tailings through age accumulation, in soil and some wild plants at Southeast Egypt. Journal of Hazardous Materials, 178(1), 739-746.

SIX-MAPS. 2017. NSW Map. NSW Government. Available: https://maps.six.nsw.gov.au/ [Accessed 19 Nov 2018].

Talsma, T. & Hallam, P.M. 1980. Hydraulic conductivity measurement of forest catchments. Soil Research, 18(2), 139-148.

US EPA SESDPROC-300-R3. 2014. SESD Operating Procedure: Soil Sampling. Science and Ecosystems Support Division. Athens, Georgia, USA.

US EPA. 2007. Test Method 6200: Field Portable X-Ray Fluorescence Spectrometry for the Determination of Elemental Concentrations in Soil and Sediment.

Weatherzone. 2018. Inverell Rainfall Reports. Fairfax Media Network. Available: http://www.weatherzone.com.au/station.jsp?lt=site&lc=56018&list=rb. [Accessed 19 Nov 2018].

Williams, M. 2001. Arsenic in mine waters: an international study Environmental Geology, 40(3), 267-298.

10. Appendices

Appendix 1: Data from the experiment justifying the method described in **Section 4.1.1**.

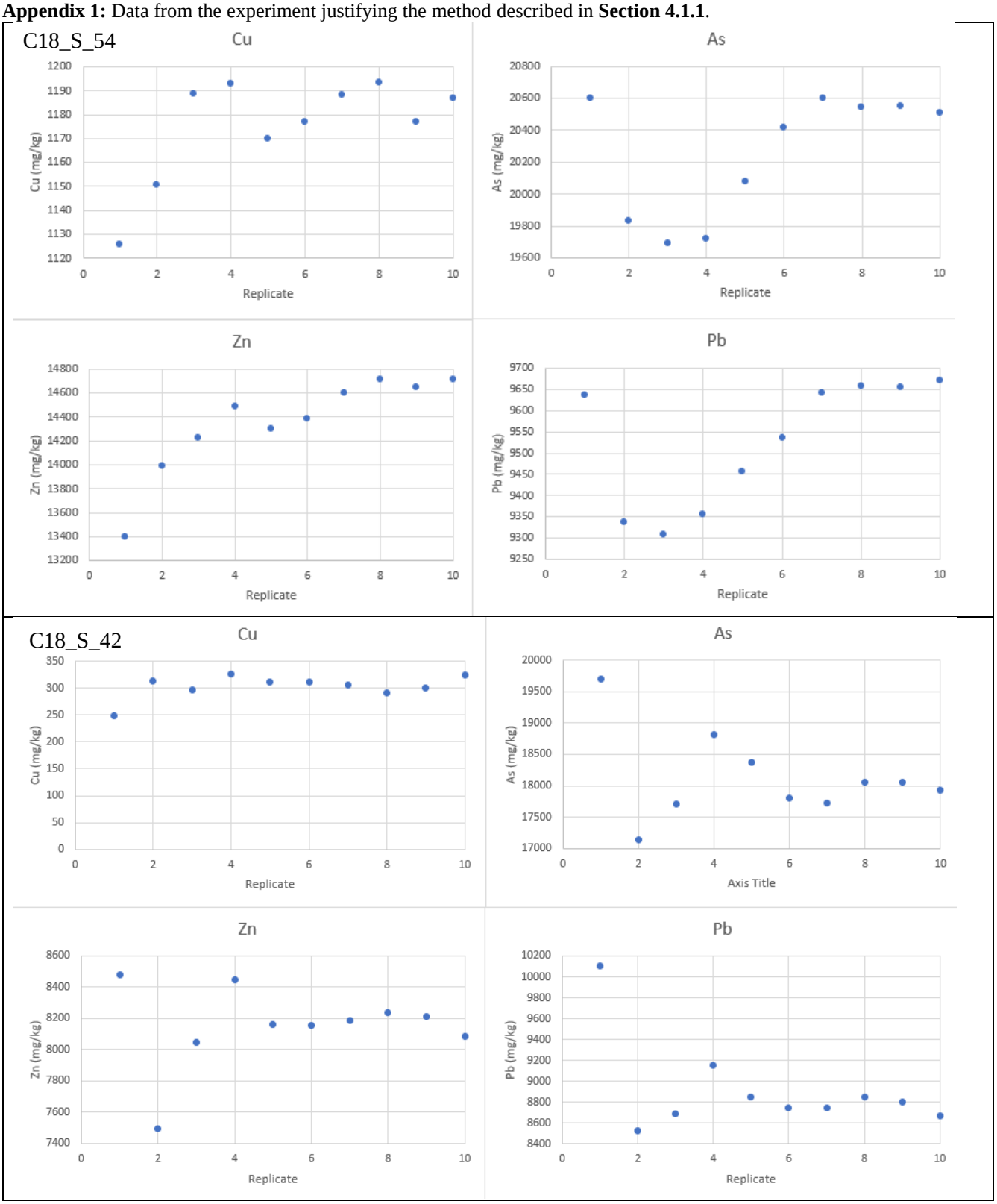

C18_S_81

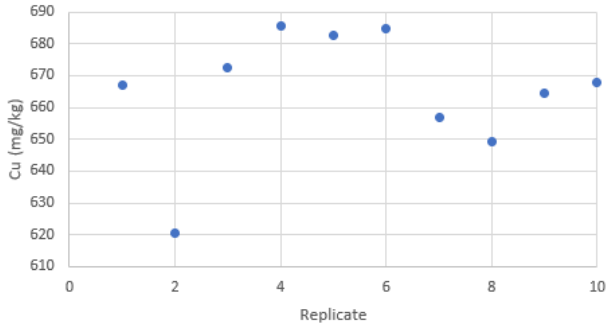

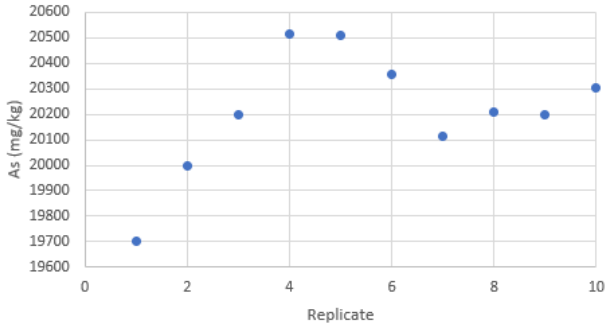

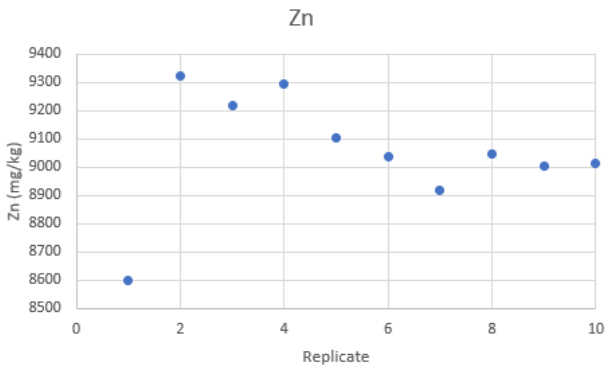

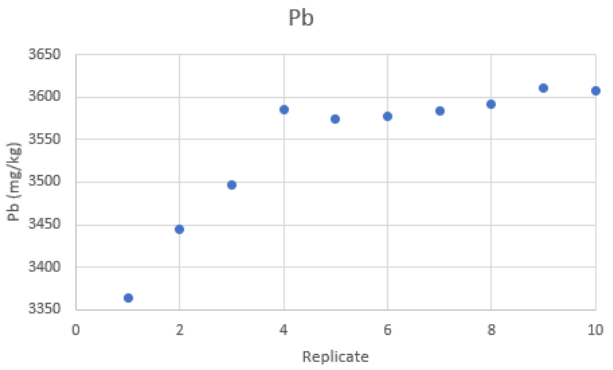

C18_S_85

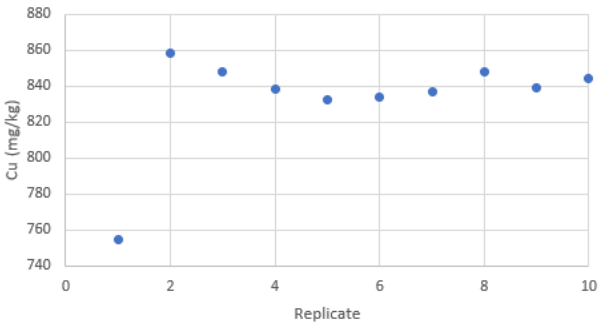

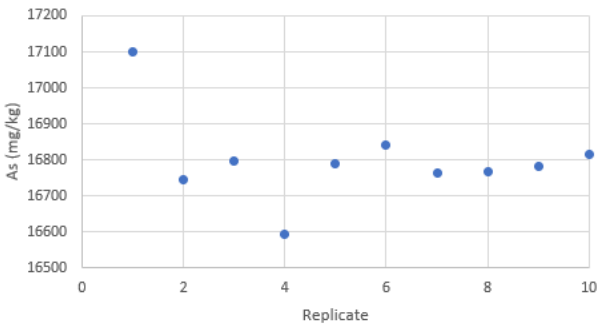

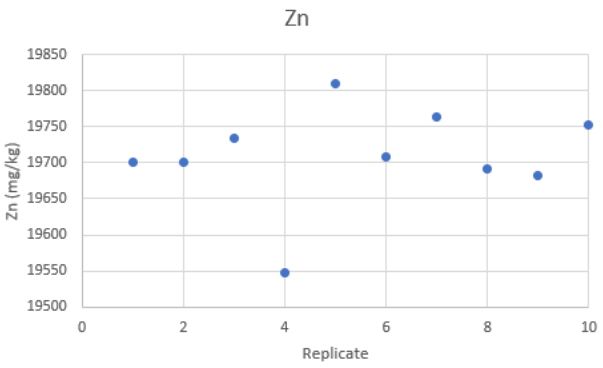

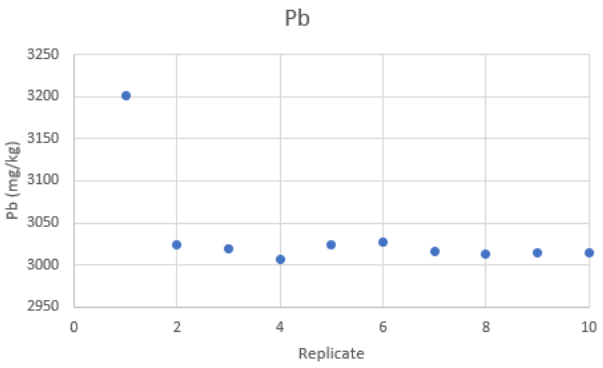

C18_S_57

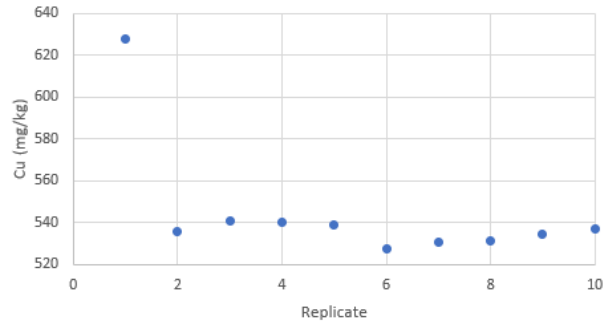

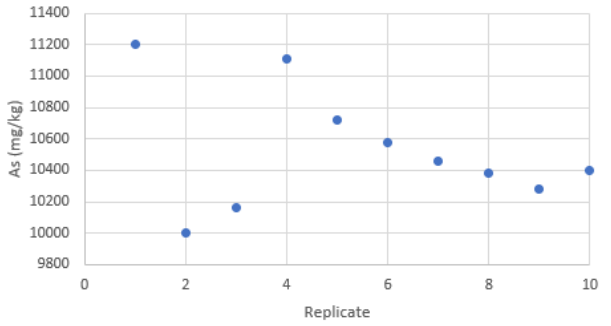

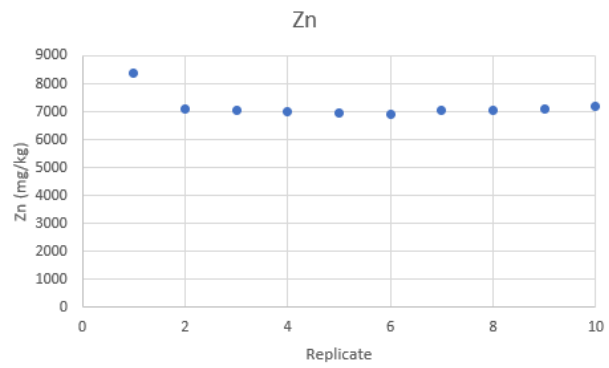

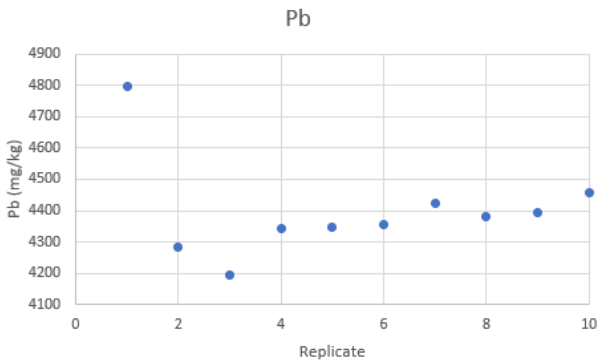

C18_S_24

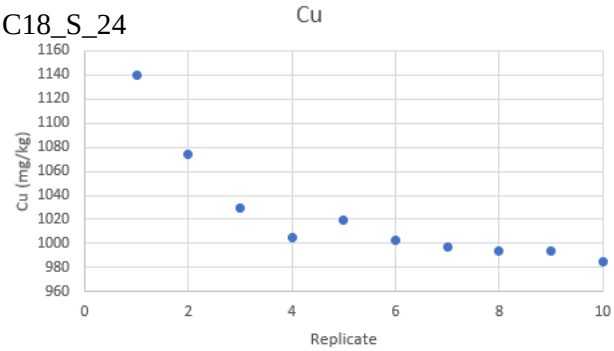

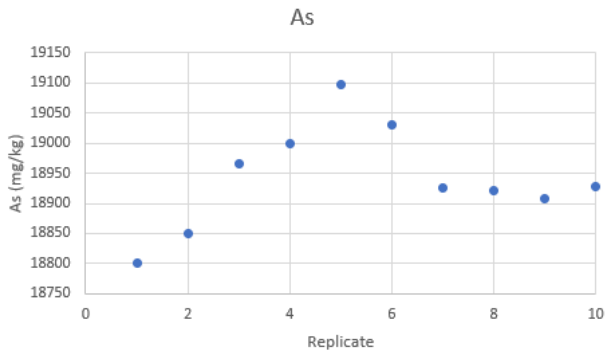

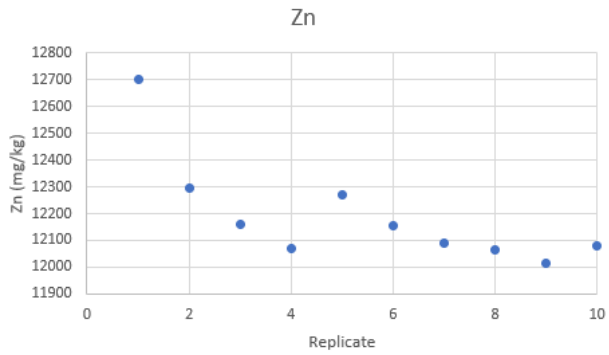

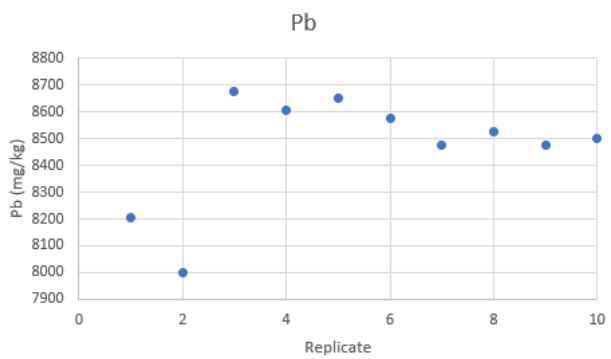

C18_S_90

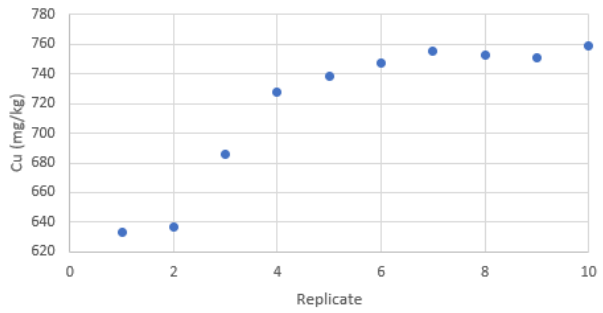

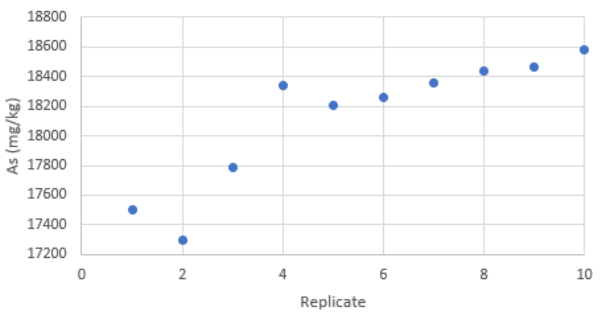

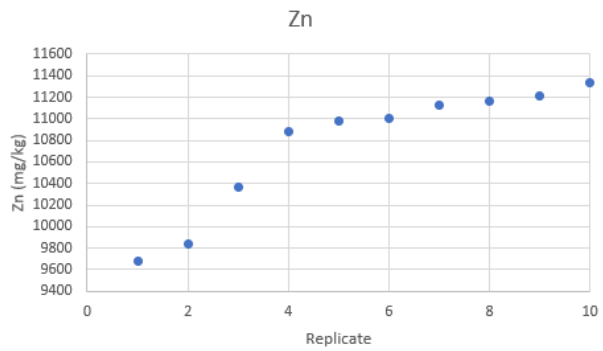

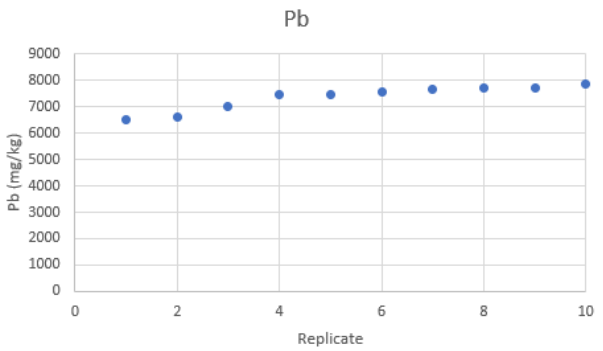

C18_S_62

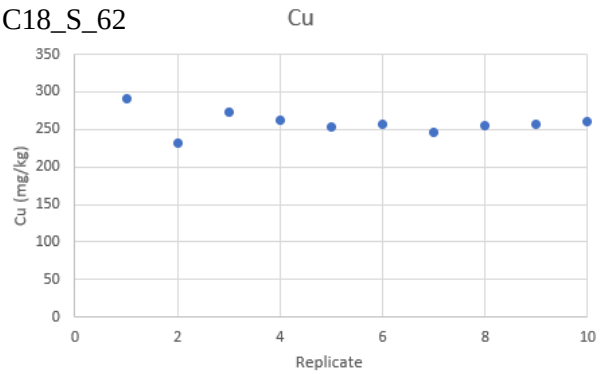

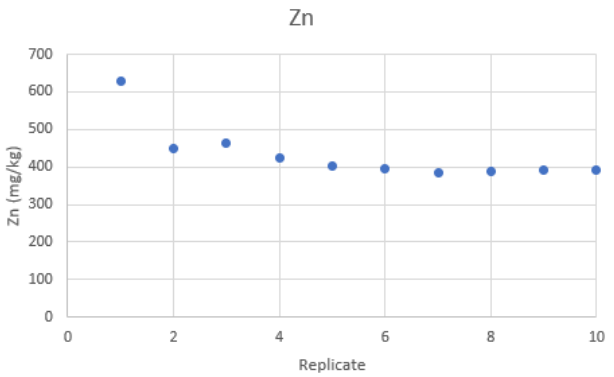

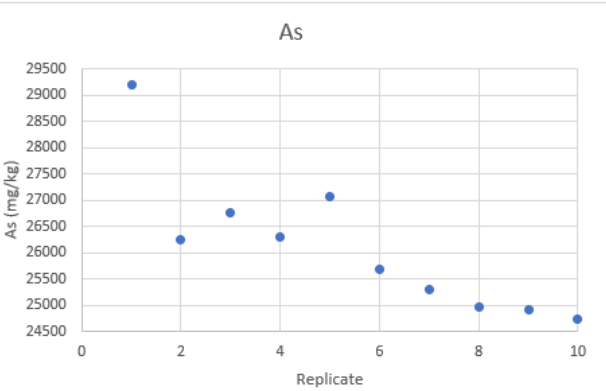

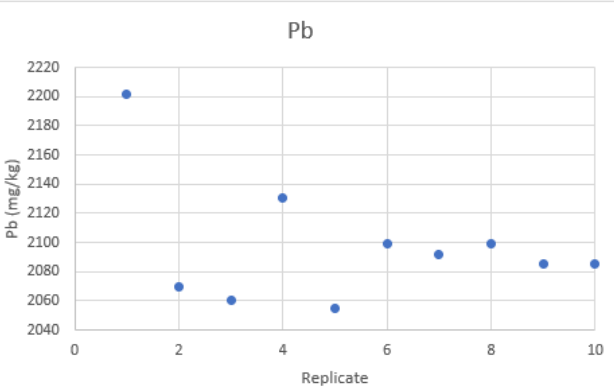

C18_S_36

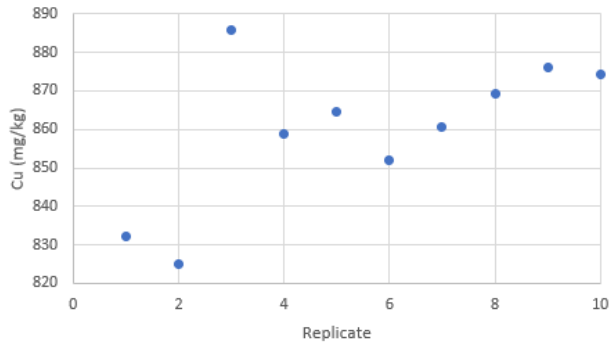

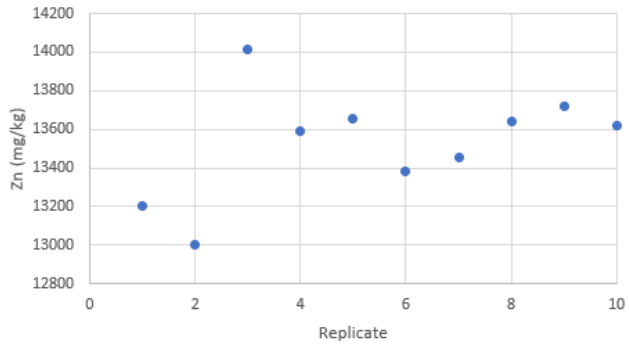

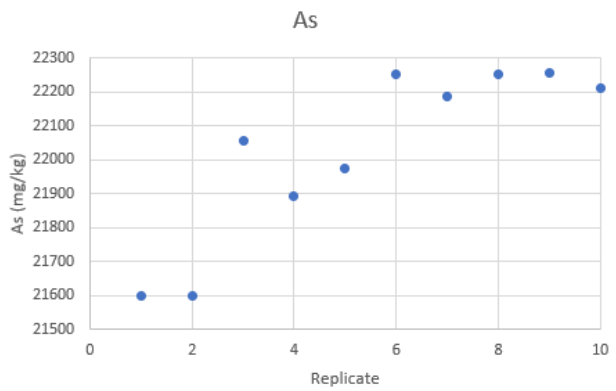

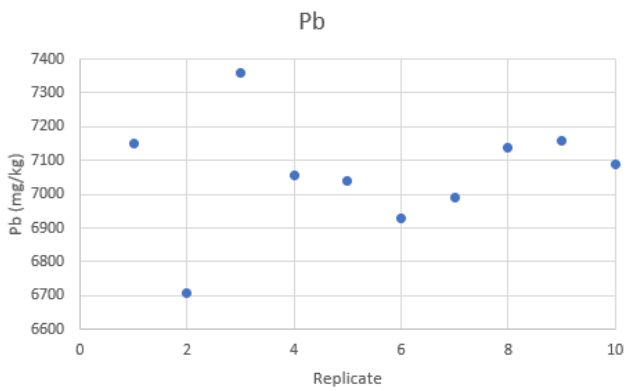

C18_S_73

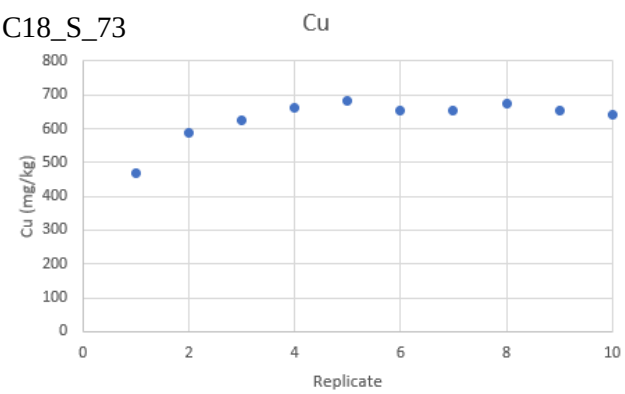

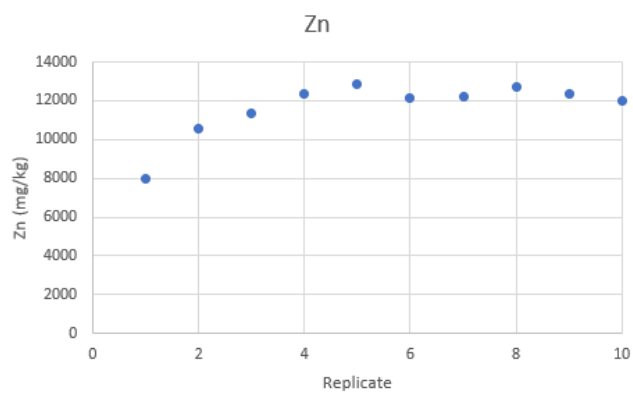

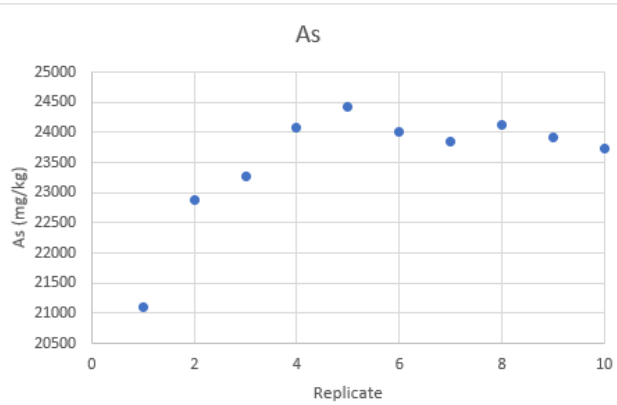

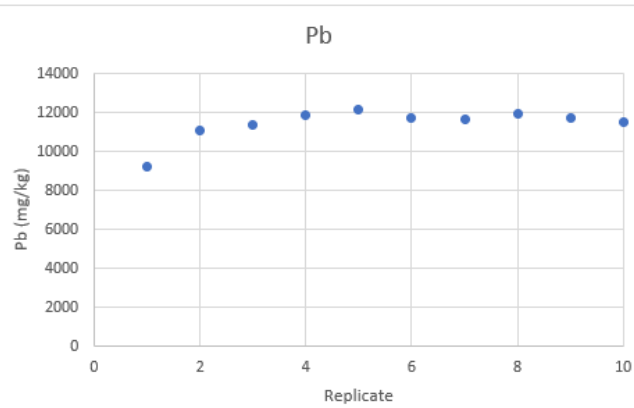

Appendix 2: Mineralogy of samples from the upper tailings.

Sample	Mineral name	Chemical formula	Database code
Con18_S13	Quartz	SiO_2	ICDD 01-089-8936
	Glauconite	$(K,Na)(Fe,Al,Mg)_2(Si,Al)_4O_{10}(OH)_2$	ICDD 00-058-2023
	Arsenopyrite	$As_{0.01}FeS_{0.99}$	ICDD 01-075-6906
	Quartz low	SiO_2	ICSD 98-004-6012
	Claudetite	As_2O_3	ICDD 00-030-0103
	Birnessite	$K_{0.27}(Mn_{0.96}O_2)(H_2O)_{0.69}$	ICDD 01-073-7867
Con18_S15	Quartz	SiO_2	ICDD 01-089-8936
	Glauconite	$(K,Na)(Fe,Al,Mg)_2$ (Si,Al)4O10$(OH)_2$	ICDD 00-058-2024
	Muscovite	$H_2KAl_3(SiO_4)_3$	ICDD 00-001-1098
	Birnessite	$Na_{0.58}Mn_2O_4(H_2O)_{1.5}$	ICDD 01-072-7297
	Beudantite	$(Fe,Cu)_3Pb((As,S)O_4)_2$ $(OH,H_2O)_6$	ICDD 00-061-0751
Con18_S20	Quartz low	SiO_2	ICSD 98-003-4023
	Scorodite	$FeAsO_4{\cdot}2H_2O$	ICDD 00-018-0654
	Glauconite	$(K,Na)(Fe,Al,Mg)_2(Si,Al)_4O_{10}(OH)_2$	ICDD 00-058-2023
Con18_S23	Quartz	SiO_2	ICSD 98-010-7204
	Phengite	$H_2Al_{1.85}K_{0.97}Mg_{0.56}O_{12}Si_{3.59}$	ICSD 98-005-8671
	Arsenopyrite	$As_{0.02}FeS_{1.98}$	ICDD 01-075-6906
	Anglesite	$PbSO_4$	ICSD 98-004-5230
Con18_S29	Quartz	SiO_2	ICDD 01-075-8322
	Scorodite	H_4AsFeO_6	ICSD 98-000-5760
	Phengite	$H_2Al_{1.848}KMg_{0.58}O_{12}Si_{3.572}$	ICSD 98-003-8753
	Orthoclase	$K(Al,Fe)Si_2O_8$	ICDD 00-008-0048
Con18_S33	Quartz	SiO_2	ICDD 01-075-8322
	Sphalerite	$Zn_{0.66}Fe_{0.34}S$	ICDD 01-073-6560
	Birnessite	$K_{0.46}(Mn_2O_4)(H_2O)_{1.55}$	ICDD 01-075-8312
	Franklinite	$(Zn_{0.922}Fe_{0.078})(Fe_{1.943}Zn_{0.047})O_4$	ICDD 01-070-3383
Con18_S40	Quartz low	SiO_2	ICSD 98-005-4678
	Scorodite	$FeAsO_4{\cdot}2H_2O$	ICDD 00-037-0468
	Zeolite	$H_{6.8}Al_{12}Cs_{1.1}N_{1.7}O_{96}Si_{36}Sr_{4.6}$	ICSD 98-003-5465
Con18_S47	Quartz	SiO_2	ICDD 01-070-3755
	Sphalerite	$(Fe_{0.2}Mn_{0.05}Zn_{0.75})S$	ICDD 01-071-8294
	Birnessite	$K_{0.296}Mn_{0.926}O_2(H_2O)_{0.42}$	ICDD 01-074-7885
Con18_S50	Quartz	SiO_2	ICDD 01-075-8322
	Scorodite	H_4AsFeO_6	ICSD 98-000-5760
	Phengite	$H_2Al_{1.848}KMg_{0.58}O_{12}Si_{3.572}$	ICSD 98-003-8753
Con18_S54	Quartz	SiO_2	ICDD 01-089-8936
	Sphalerite	$(Cd_{0.04}Fe_{0.24}Zn_{0.72})S$	ICDD 01-071-4135
	Segnitite	$PbFe_3(AsO_4)_2$ $(OH)_5(H_2O)$	ICDD 01-088-1944
	Birnessite	$K_{0.296}Mn_{0.926}O_2(H_2O)_{0.42}$	ICDD 01-074-7885
Con18_S68	Quartz	SiO_2	ICDD 01-075-8320
	Beudantite	$(Fe,Cu)_3Pb((As,S)O_4)_2(OH,H_2O)_6$	ICDD 00-061-0751
	Sphalerite	$Zn_{0.66}Fe_{0.34}S$	ICDD 01-073-6560

	Illite	$(K,H_3O)Al_2Si_3AlO_{10}(OH)_2$	ICDD 00-026-0911
Con18_S74	Quartz	SiO_2	ICDD 01-075-8321
	Zeolite	$H_{6.8}Al_{12}Cs_{1.1}N_{1.7}O_{96}Si_{36}Sr_{4.6}$	ICSD 98-003-5465
	Sphalerite	$Fe_{0.1989}Mn_{0.0453}Zn_{0.7558}S$	ICDD 03-065-9970
	Franklinite	$(Zn_{0.906}Fe_{0.094})(Fe_{1.927}Zn_{0.063})O_4$	ICDD 01-070-3384
	Chenevixite	$Cu^{2+}{}_2Fe^{2+}{}_3(AsO_4)_2(OH)_4\cdot H_2O$	ICDD 00-014-0068
Con18_S62	Quartz low	SiO_2	ICSD 98-003-4023
	Scorodite	$FeAsO_4\cdot 2H_2O$	ICDD 00-026-0778
	Zeolite	$Al_{12}Cs_{1.1}O_{96}Si_{36}Sr_4$	ICSD 98-002-8769
Con18_S70	Quartz low	SiO_2	ICSD 98-003-4023
	Hydroniumjarosite	$(K_{0.2}(H_3O)_{0.81})Fe_3(SO_4)_2(OH)_6$	ICDD 01-075-9730
	Zeolite	$Al_{12}Cs_{1.1}O_{96}Si_{36}Sr_4$	ICSD 98-002-8769
Con18_S77	Quartz low	SiO_2	ICSD 98-003-4023
	Scorodite	$FeAsO_4\cdot 2H_2O$	ICDD 00-018-0654
	Zeolite	$Al_{12}Cs_{1.1}O_{96}Si_{36}Sr_4$	ICSD 98-002-8769
Con18_S85	Quartz	SiO_2	ICDD 01-075-8322
	Sphalerite	$Fe_{0.1989}Mn_{0.0453}Zn_{0.7558}S$	ICDD 03-065-9970
	Birnessite	$H_{0.84}K_{0.296}Mn_{0.926}O_{2.42}$	ICSD 98-010-3056
	Glauconite	$(K,Na)(Fe,Al,Mg)_2(Si,Al)_4O_{10}(OH)_2$	ICDD 00-058-2024
	Pyrite	$Fe_{0.987}S_2$	ICDD 01-074-8366
Con18_S88	Quartz	SiO_2	ICDD 01-070-3755
	Beudantite	$(Fe,Cu)_3Pb((As,S)O_4)_2(OH,H_2O)^6$	ICDD 00-061-0751
	Muscovite	$(K,Na)(Al,Mg,Fe)_2(Si_{3.1}Al_{0.9})O_{10}(OH)_2$	ICDD 00-007-0042
Con18_S90	Quartz	SiO_2	ICDD 01-075-8321
	Sphalerite	$Zn_{0.628}Fe_{0.372}S$	ICDD 01-089-3700
	Magnetite	Fe_3O_4	ICSD 98-004-1424

Appendix 3: Mineralogy of salt samples from various mine wastes around the King Conrad smelter/processing area. (Samples from within 50 m of 29°57'2.01'' S 151°1'7.72'' E).

Sample	**Mineral name**	**Chemical formula**	**Database code**
Con17_016	Wupatkiite	$(Co,Mg,Ni)Al_2(SO_4)_4\cdot 22H_2O$	ICDD 00-048-1884
Con17_017	Brushite	$CaPO_3(OH)\cdot 2H_2O$	ICDD 00-011-0293
	Glauconite, glycolated	$(K,Na)(Fe,Al,Mg)_2(Si,Al)_4O_{10}(OH)_2$	ICDD 00-058-2024
Con17_018	Wupatkiite	$(Co,Mg,Ni)Al_2(SO_4)_4\cdot 22H_2O$	ICDD 00-048-1884
	Sphalerite ferrous	$Fe_{0.215}SZn_{0.785}$	ICSD 98-004-9032
	Gypsum	$CaSO_4\cdot 2H_2O$	ICDD 00-006-0046
	Heulandite	$C_{8.16}H_{70.5}Al_{8.7}N_{8.16}Na_{0.52}O_{82.77}Si_{27.3}$	ICSD 98-010-2457
	Gibbsite	$Al(OH)_3$	ICDD 00-029-0041
	Quartz	SiO_2	ICSD 98-001-2469
Con17_019	Alum-(K)	$KAl(SO_4)_2\cdot 12H_2O$	ICDD 00-007-0017
	Quartz	SiO_2	ICDD 01-087-2096

	Muscovite 3T	$H_2Al_3KO_{12}Si_3$	ICSD 98-000-5503
	Anhydrite	$Ca(SO_4)$	ICDD 01-086-2270
Con17_020	Quartz	SiO_2	ICDD 01-075-6051
	Jarosite, hydronian,	$K_{0.86}(H_3O)_{0.14})Fe_3(SO_4)_2(OH)_6$	ICDD 01-075-9735
	Anglesite	$PbSO_4$	ICDD 01-089-7356
Con17_021	Quartz low	SiO_2	ICDD 01-087-2096
Con17_022	Quartz	SiO_2	ICDD 01-085-0796
	Microcline	$AlK_{0.96}Na_{0.04}O_8Si_3$	ICSD 98-004-5647
	Albite	$Al_{1.02}Ca_{0.02}Na_{0.98}O_8Si^{2.98}$	ICSD 98-005-6885
	Jarosite, hydronian	$K_{0.86}(H_3O)_{0.14}Fe_3(SO_4)_2(OH)_6$	ICDD01-075-9735
Con17_038	Quartz	SiO_2	ICDD 01-085-0796
	Gypsum	$CaSO_4.2H_2O$	ICSD 98-010-2494
	Microcline	$AlKO_8Si_3$	ICSD 98-001-7340
Con17_039	Gypsum	$CaSO_4.2H_2O$	ICDD 01-074-1433
	Quartz low	SiO_2	ICDD 01-087-2096
Con17_040	Gypsum	$CaSO_4.2H_2O$	ICSD 98-010-2494
Con17_041	Gypsum	$CaSO_4.2H_2O$	ICDD 01-076-8724
	Quartz	SiO_2	ICDD 01-085-050
Con17_042	Gypsum	$CaSO_4.2H_2O$	ICSD 98-001-1992
	Haidingerite	$CaH(AsO_4)H_2O$	ICDD 01-070-1581
	Quartz low	SiO_2	ICSD 98-009-0450